NTIS

SOLID POLYMER ELECTROLYTE WATER ELECTROLYSIS TECHNOLOGY DEVELOPMENT FOR LARGE-SCALE HYDROGEN PRODUCTION. FINAL REPORT, OCTOBER 1977-NOVEMBER 1981

GENERAL ELECTRIC CO., WILMINGTON, MA.
AIRCRAFT EQUIPMENT DIV

1981

REPORT

SOLID POLYMER ELECTROLYTE WATER ELECTROLYSIS TECHNOLOGY DEVELOPMENT FOR LARGE-SCALE HYDROGEN PRODUCTION

FINAL REPORT
FOR THE PERIOD
OCTOBER 1977—NOVEMBER 1981

GENERAL ELECTRIC COMPANY
AEROSPACE INSTRUMENTS DEPARTMENT
DIRECT ENERGY CONVERSION PROGRAMS
50 FORDHAM ROAD
WILMINGTON, MA 01887—2190

PREPARED FOR THE

U.S. DEPARTMENT OF ENERGY
ASSISTANT SECRETARY FOR ENERGY STORAGE SYSTEMS
OFFICE OF ENERGY TECHNOLOGY

UNDER CONTRACT DE—AC—02—78ET 26202

DIRECT ENERGY CONVERSION PROGRAMS

50 FORDHAM ROAD
WILMINGTON, MASSACHUSETTS 01887

GENERAL ⊕ ELECTRIC

DISCLAIMER

ABSTRACT

This final report covers those portions of the General Electric Electrolyte Bulk Hydrogen Water Electrolysis Development Program which was sponsored by the Department of Energy from October 1977 through December 1981 under Contract No. DE-AC02-78ET26202.

The major DOE-sponsored tasks involved the design and development of 2.5 ft^2 cell-size electrolysis modules and the design and development of prototype 50 kW and 200 kW systems.

The results of the performance evaluations of forty-six modules including sealing and operation within and outside the normal operating envelope is discussed.

Early process development of cells with 10 ft^2 active area is described.

The results of a techno/economic study of the sensitivity of the cost of generated hydrogen to various design and operational parameters is presented.

The overall development program is continuing under other sponsorship.

TABLE OF CONTENTS

i
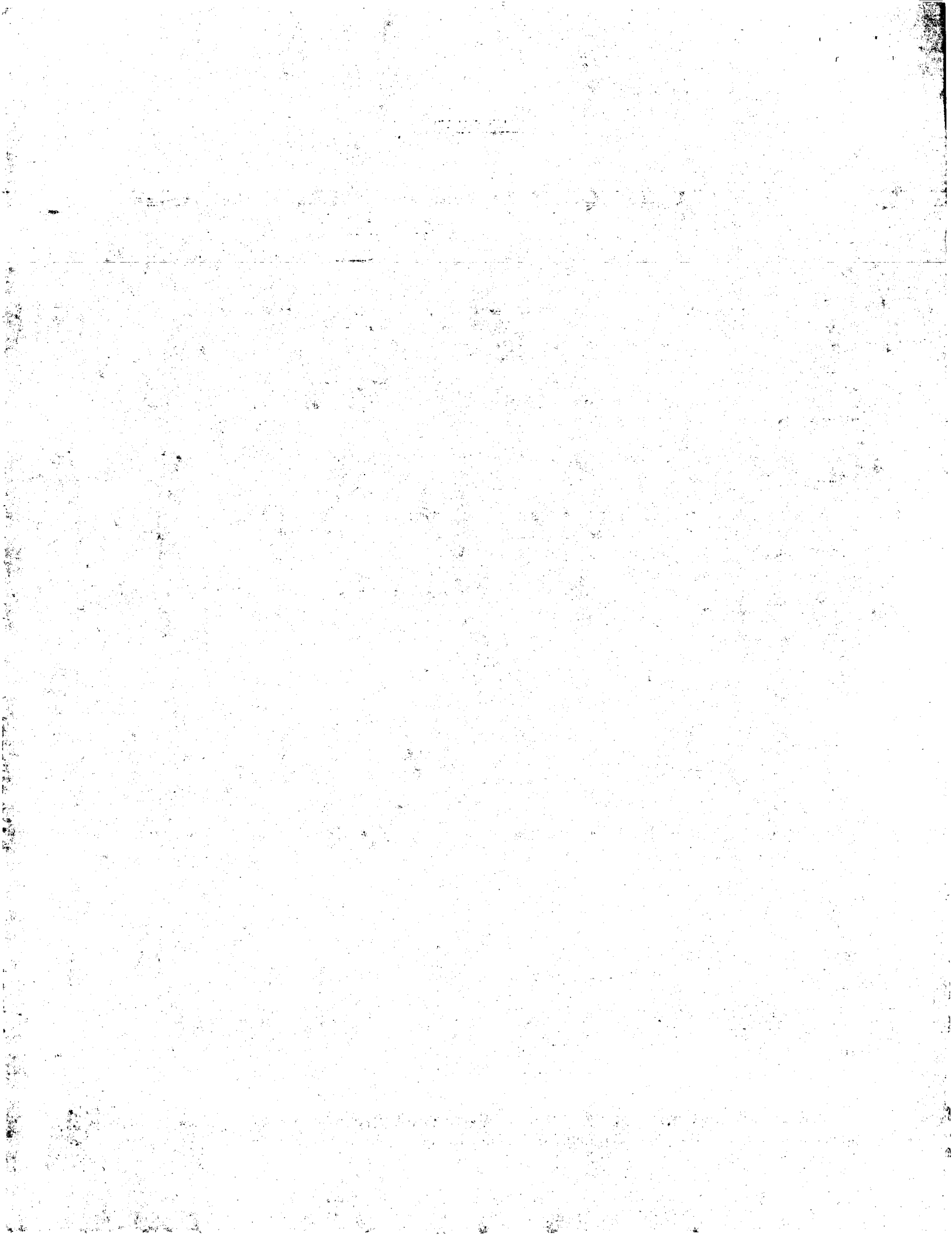
LIST OF FIGURES

ii

LIST OF FIGURES (Cont'd.)

iii

LIST OF TABLES

1.0 INTRODUCTION

This is the final report of a 4-year U.S. Department of Energy (DOE)-sponsored effort aimed at the development of the solid polymer electrolyte water electrolysis technology for large scale hydrogen production. This effort, encompassing Government Fiscal Years 1978, 1979, 1980 and 1981, was performed by the General Electric Co., Direct Energy Conversion Programs (GE/DECP) under B/N No. DE-AC02-78ET 26202 (Formerly Contract No. ET-78-C-02-4689).

This effort formed a portion of a continuing joint government, utility and General Electric Company funded program which had started in 1975. Other sponsors included the Niagara Mohawk Power Corporation (NMPC), the Empire State Electric Energy Research Corporation (ESEERCO), the New York State Energy Research and Development Authority (NYSERDA), and the Gas Research Institute (GRI).

1.1 Background

During the early 1970's, the General Electric Company had developed a unique water electrolysis technology based on the use of a solid polymer electrolyte. This technology was then applied toward the generation of hydrogen in commercial units sized for use in laboratories and the generation of oxygen for spacecraft and submarine life support.

In a 1975 GE/DECP study for Brookhaven National Laboratory (Contract 350400S), feasibility of developing the SPE technology for large scale hydrogen generation was established, specifically in conjunction with large (58 MW) peak shaving facilities.

As a result of this study, a joint program was initiated with the following goals:

- High overall system efficiency: 85-90%
- Low capital cost: $100/kW, 1975 dollars (approximately $170/kW, 1981 dollars), based on large plants of approximately 58 MW capacity.
- Long life: 40,000 hours for cells, 20 years for the system.
- Preliminary scale-up to 2.5 Ft^2 cell size and demonstrate in 200 kW (approximately 2000 SCFH) module.
- Further scale-up to 10 Ft^2 cell size and demonstrate in 2 to 5 MW module.

1

Initial support was received in June 1975 in the form of a 27-month DOE (then ERDA) contract covering front end technology development and initial scale-up activities.

Niagara Mohawk Power Corporation (NMPC) joined the program in 1976, and the Empire State Electric Energy Research Corporation (ESEERCO) became a co-sponsor in 1977. Support from both organizations has continued through the present time. Added support from the New York State Energy Research and Development Authority (NYSERDA) was received during 1978 and from the Gas Research Institute in 1979 and 1980.

In October of 1977 (the start of GFY 78) DOE support took the form of an extended contract - the subject of this report.

Figure 1 is a milestone chart of the overall program. DOE support during GFY 78 through GFY 81 has been primarily associated with hardware scale-up and demonstrations (tasks 2 and 3) plus the associated test facilities (task 7).

At the end of February 1981, a stop work order on the hardware scale-up effort was received from DOE as a result of federal budget rescissions. The limited effort since then includes a techno-economic study, participation in DOE contractor reviews, and International Energy Agency (IEA) meetings, and preparation of this report continued through December 1981.

1.2   Scope of Report

As shown in Figure 1, this final report covers the DOE-sponsored tasks which form a portion of the total planned program.

The major DOE-sponsored effort was applied to the 2.5 ft^2 scale-up which included manufacturing and fabrication of facilities for testing. A second major task was the development of a 200 kW Engineering Model System which involved design of the system, procurement of components, and operational evaluation of scaled-up modules to assess system operation. The third area of effort was the scale-up of the 2.5 ft^2 technology to 10 ft^2 size including module design, manufacturing process development and equipment procurement.

Although the contracted effort was applied to discrete tasks as outlined in the milestone chart (Figure 1), the Discussion of Results (Section 4.0) is structured not by tasks, but chronologically to provide a more coherent presentation.

The techno-economic study, which was performed concurrently with preparation of this final report, will be published under separate cover.

MAJOR MILESTONE CHART
BULK HYDROGEN GENERATION DEVELOPMENT PLAN

1985 1984 1983

WORK EFFORT
COVERED BY
THIS REPORT

TBD

50 kW   200 kW

DECISION ON 10 ft² DEV

1.0 Technology Development Program
1.1 Low Cost Current Collector
1.2 High Temperature Operation
1.3 Catalytic Electrode Development
1.4 Low Cost Polymer Development
1.5 Cell and SPE Optimization
1.6 Performance Improvement

2.0 Electrolysis Module Design & Development
2.1 Cell Assembly Design (2.5 ft²)
2.2 Stack Assembly Design (2.5 ft²)
2.3 Manufacturing Processes Development
2.4 Material Procurement & Fab. of Cells (2.5 ft²)
2.5 Assembly & Test of Cells & 6 Cell Module (2.5 ft²)
2.7 Manufacturing Development of Cells (10 ft²)
2.8 Assembly & Test of Cells & 12-Cell Module (10 ft²)

3.0 Engineering Model 200 kW System
3.1 System Analysis and Definition
3.2 Procure System Components
3.3 Fabricate Cells (2.5 ft²) & Stack Hdw.
3.4 Assemble Module & System Components
3.5 Performance Test 200 kW System
3.6 Refurbish Elec. Modules to Up-Date Technology
3.7 Performance Test 200 kW System
3.8 Performance Test 250 kW Module

4.0 Prototype 250 kW System (2.5 ft² Cells)
4.1 System Analysis and Definition
4.2 Procure System Components
4.3 Fabricate Cells & Module
4.4 Assemble System
4.5 Performance Test System
4.6 Deliver System to Customer Site
4.7 Field Installation and Check Out
4.8 Field Engineering and Design Support

5.0 Demonstration of Improvements (1 ft²)
5.1 Fab. 1 ft² Modules w/Optimized Collectors
5.2 Endurance Test Modules w/Optimized Collectors
5.3 Fab. & Test Thin SPE Module
5.4 Fab. & Test 1982 Improvements

6.0 Prototype 2 MW System (10 ft² Cells)
6.1 System Design and Specification
6.2 Procure System Components
6.3 Cell and Stack Design Modifications
6.4 Fabricate Cell and Stack Hardware
6.5 Assemble System at Customer Site
6.6 Performance and Check-Out Tests
6.7 Field Application Evaluations

7.0 Development & Installation of Facilities
7.1 Test Facilities for 2.5 ft² Cell to 500 kW Unit
7.2 Test Facilities for 10 ft² Cell to 500 kW Unit
7.3 Check-Out Facilities for 2 MW System
7.4 Production Manufacturing Facilities
7.5 Production Test Facilities
7.6 Production Release

Techno-Economic Study

Final Report

Figure 1

3

DIRECT ENERGY CONVERSION PROGRAMS

2.0 CONTRACT OBJECTIVES

The major objectives of this DOE contract were:

a) Electrolysis module design and development at the 2.5 ft^2 cell size including

    1) Completion of the stack assembly design.

    2) Cell and module process development.

    3) Design and construction of a 50 kW test bed system.

    4) Operational evaluation of 2.5 ft^2 cells in single and multi-cell modules.

b) Development of a 200 kW Engineering Model System including

    1) Design and fabrication of a 200 kW system.

    2) Fabrication of a 60-cell, 200 kW module.

    3) Operational demonstration of the 200 kW module in the 200 kW system.

This effort was a part of the U.S. contribution to the International Energy Agency (IEA) Annex IV.

c) Development of the 10 ft^2 cell and module including

    1) Process development of the 10 ft^2 M&E. (Note: The design of the 10 ft^2 cell and module was accomplished under GRI sponsorship.)

    2) Procurement of components for a 200 kW system for operating 10 ft^2 modules.

d) Perform a techno-economic analysis to quantify the cost of generated hydrogen as a function of operational parameters such as current density, operating temperature, and gas generation pressure, and design parameters such as module production cost and module performance capability.

4

3.0 SUMMARY OF ACCOMPLISHMENTS

3.1 Hardware Scale-up

The membrane and electrode assembly was successfully scaled to 2.5 ft^2, and processes were developed to reduce both resistance and contamination during processing.

- The molded carbon current collector process was scaled up to 2.5 ft^2 with improved sealing achieved through the incorporation of sealing ridges. An implemented change from phenolic binder to a fluoropolymer binder reduced cell contamination during operations.

- A 2.5 ft^2 porous titanium anode support was developed to replace the original perforated titanium foil which did not have sufficient strength to prevent deformation into the H_2O/O_2 flowfield.

- The concept of pneumatically-loaded endplates was successfully implemented in the 2.5 ft^2 size along with terminal plate modifications to improve flexibility and producibility.

3.2 2.5 ft^2 Module Testing

A 500 SCFH system developed for evaluating 2.5 ft^2 modules, ranging from single cells to 12 cells, was operated for over 5,750 hours. Significant results from testing in this system were:

- Demonstrated effective cell sealing of 2.5 ft^2 modules up to 300 psig.

- Demonstrated the feasibility of reduced thickness membrane (7 mils dry vs. the standard 10 mils dry).

- Demonstrated the feasibility of greatly reduced catalyst loadings and identified performance variations as a function of catalyst loading.

3.3 200 kW System Development

A 2000 SCFH system was designed, fabricated and operated for a total of 3,100 hours with 2.5 ft^2 modules ranging from 6 to 60 cells. Significant results of this phase of the program were:

- A 60-cell (200 kW) module was operated for over 700 hours at 100 psi hydrogen generation pressure and 205°F average operating temperature. Cell performance was 1.90 VDC at 1000 ASF.

- An improved deionizer configuration was developed to prevent contamination of the module from amines eluted from the mixed deionizer bed.

- A water purge system was developed to prevent dry-out of the module in the event of a high temperature shutdown.

3.4 Performance Improvement

- The steady improvement in cell performance which has been demonstrated as a result of this development program is shown in Figure 2.

- Based on the current development status, performance in the 1.7 VDC range at 240°F is projected as shown in Figure 3.

3.5 Cost Improvement

- The electrolyzer mature production cost reduction which has resulted from the overall development program is shown in Figure 4.

3.6 Miscellaneous

- This development effort was a significant U.S. contribution to the International Energy Agency (IEA) hydrogen program (Annex IV). Papers covering this effort were presented at annual IEA workshops and reports as required were prepared.

- A techno-economic study was performed which quantified the cost of hydrogen as a function of operational and design parameters and established the sensitivity of the hydrogen cost to the various parameters.

Figure 2. 2.5 Ft² Cell Performance History at 1000 ASF, 180°F

DIRECT ENERGY CONVERSION PROGRAMS
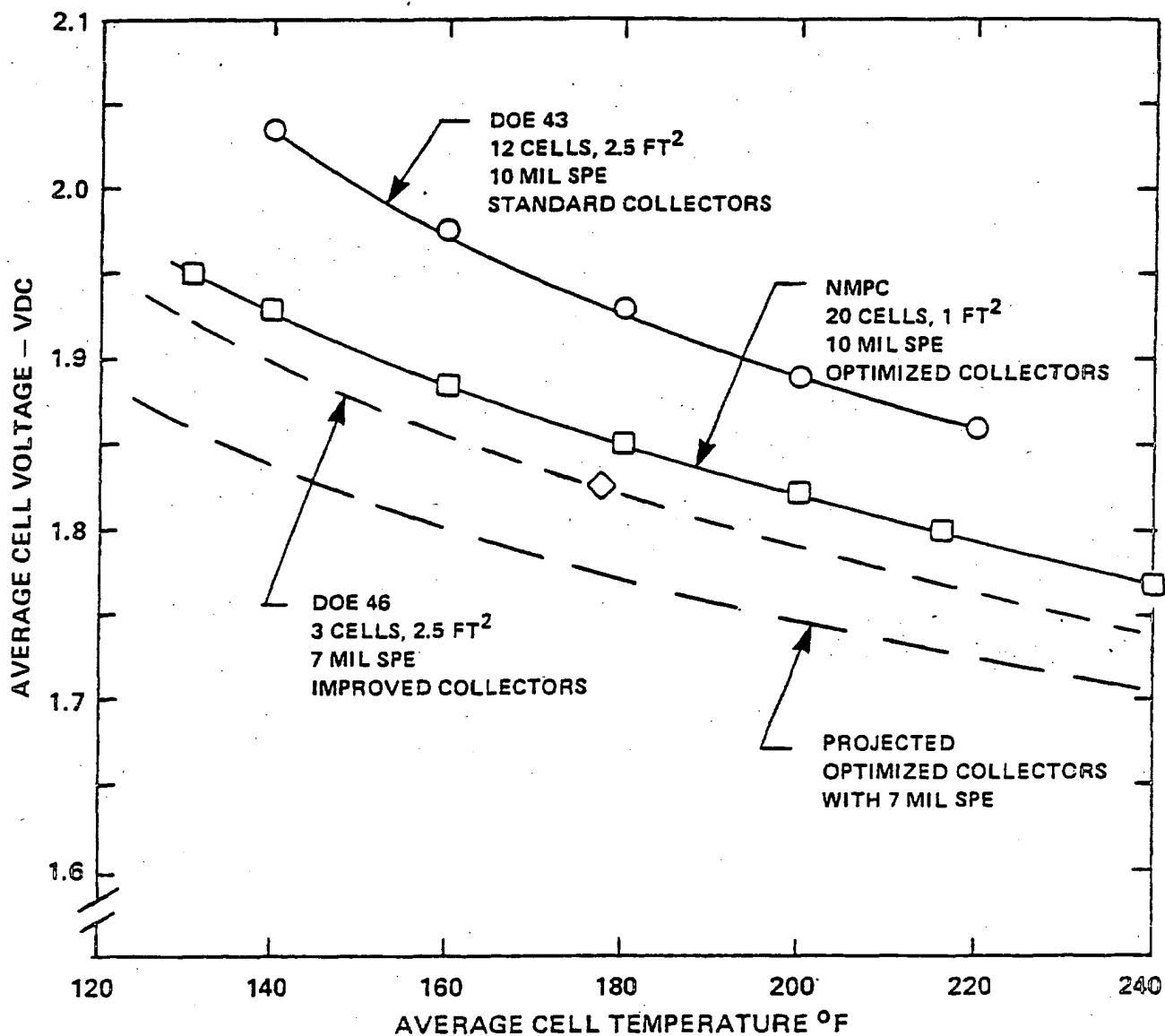
Figure 3.   Cell Performance vs. Temperature - 1000 ASF
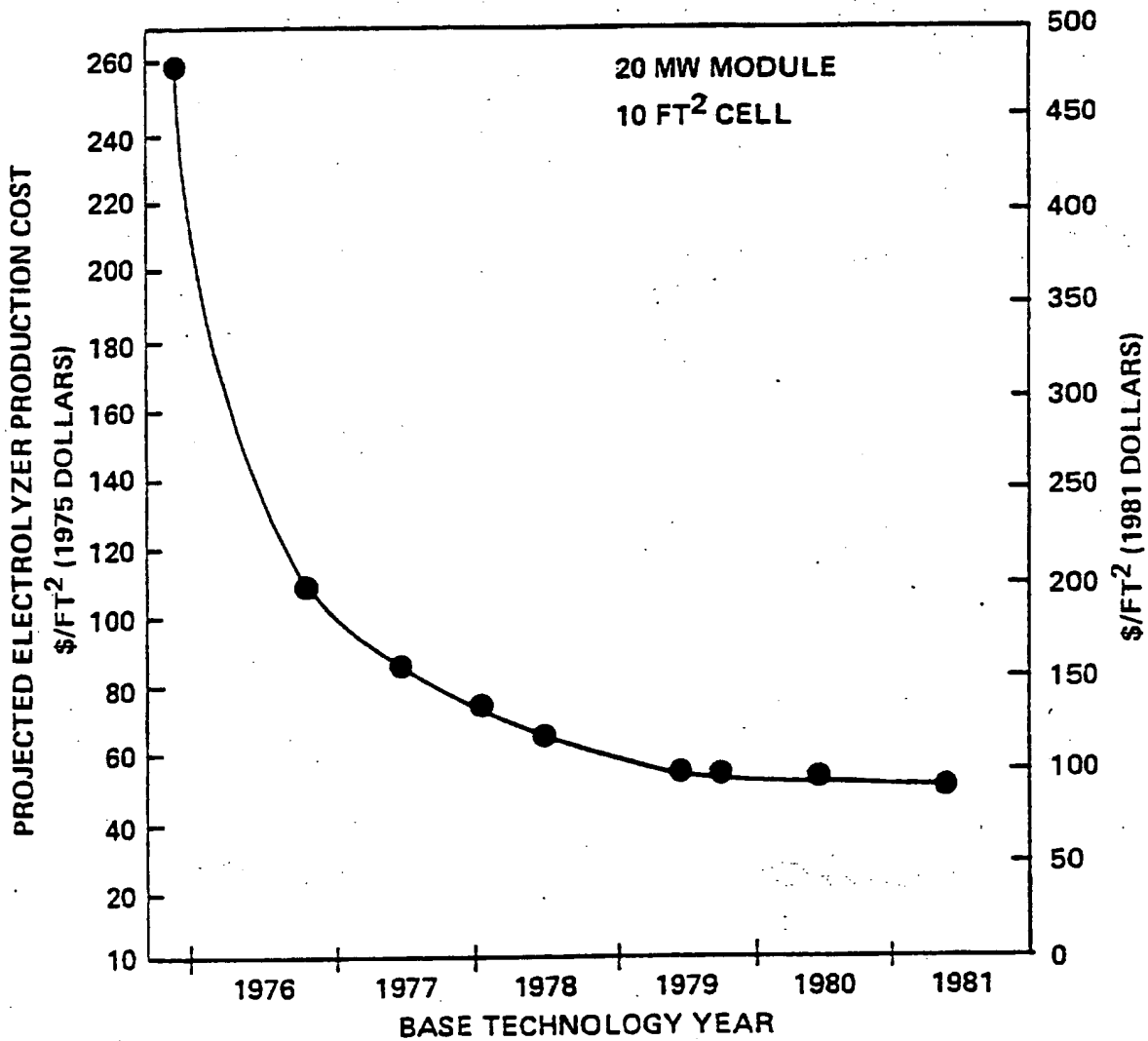
Figure 4.   Projected Electrolyzer Production Cost

DIRECT ENERGY CONVERSION PROGRAMS

4.0   DISCUSSION OF RESULTS

4.1   2.5 Ft^2 Cell and Module Development

4.1.1   Module Design

        Under a previous DOE contract, the design of the 2.5 ft^2 stack hardware was complete and is shown in Figure 5. The bipolar design incorporated dynamic pneumatic endplates and is shown in detail in Figure 6. This provides uniform stack component loading which facilitates cell sealing and better electrical current distribution. Fluid plates for providing process water and removal of gases are positioned on either side of a center negative buss so the system piping is at ground potential.

        The cell components had been developed in laboratory-size hardware and designed in 2.5 ft^2 size.

        The membrane and electrode assembly (M&E), a sheet of solid polymer electrolyte with anode and cathode catalyst applied to opposite sides, was scaled up to 2.5 ft^2 size. The membrane border area acts as a seal for both external porting and overboard sealing.

        Earlier development had shown that a support for the M&E was required on both the anode and cathode side to prevent creep of the membrane into flow areas. The anode support was a thin titanium foil with many small holes etched through to provide for transport of water to the catalyst from the flowfield and outflow of the oxygen gas. As shown in Figure 7, the scale-up to 2.5 ft^2 size of the anode support was nearly completed at the beginning of this contract. The cathode support was a commercially available carbon fiber paper.

        The current collector-bipolar separator provides for internal manifolding cell to cell, active area gas-water distribution, and the through stack current path. The collector is compression molded from a mixture of carbon and binder. The carbon material is stable in hydrogen, but on the oxygen side must be protected from corrosion by in-situ attachment of a titanium foil. The collector design was completed prior to this contract, and construction of the 2.5 ft^2 mold was started.

        A cross-section of the stack cell components is shown in Figure 8.

4.1.2   Module Hardware Development

        Stack Hardware

        Detailed design and drafting of 12-cell stack assembly components was completed early in GFY 78. The titanium fluid

10

CELL STACKS

FLUID PLATE

FLUID PLATE

PNEUMATIC END PLATE (+)

PNEUMATIC END PLATE (+)

CENTER BUS PLATE
(NEGATIVE GROUND)
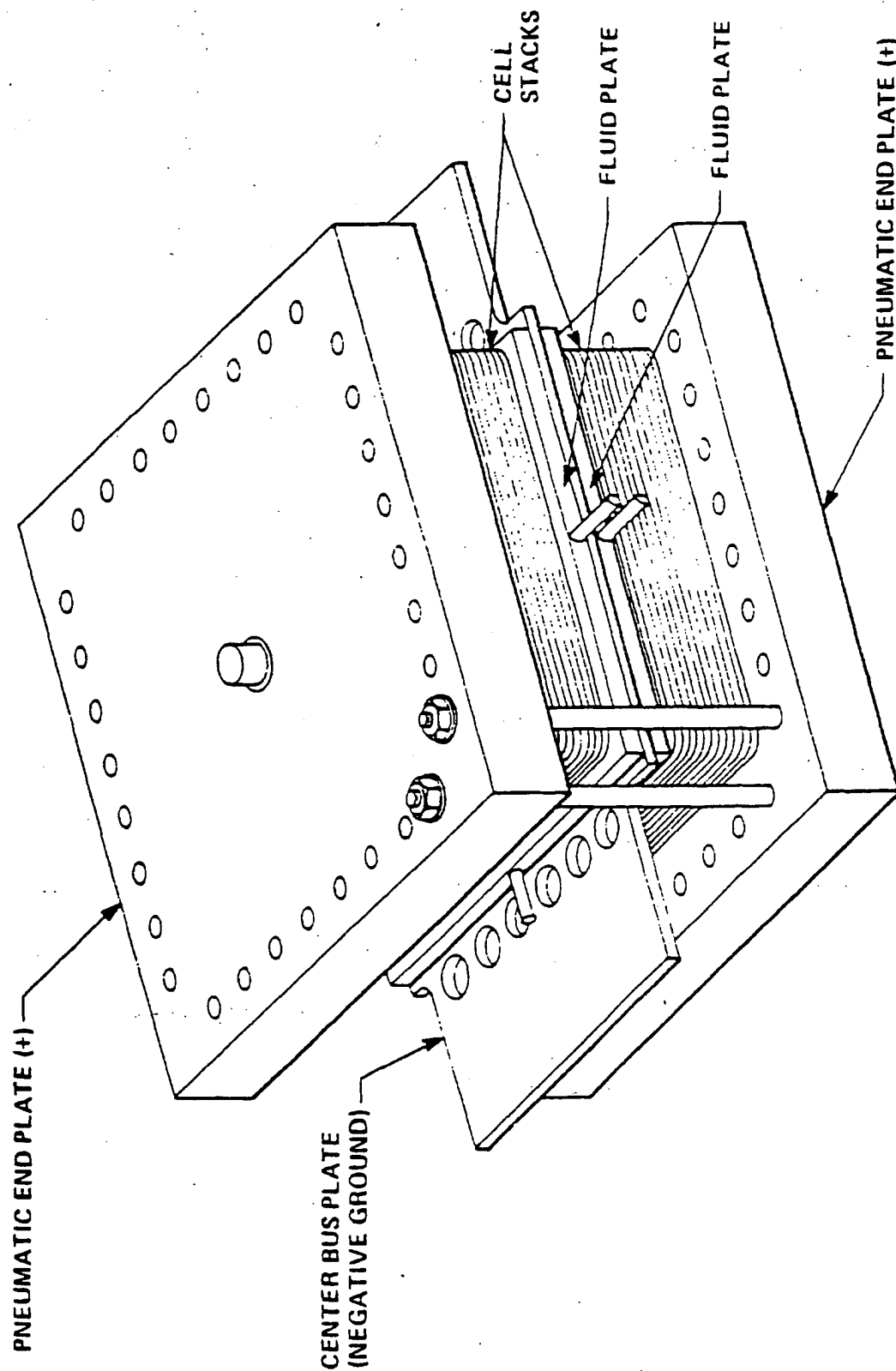
Figure 5.   Water Electrolysis Stack

11
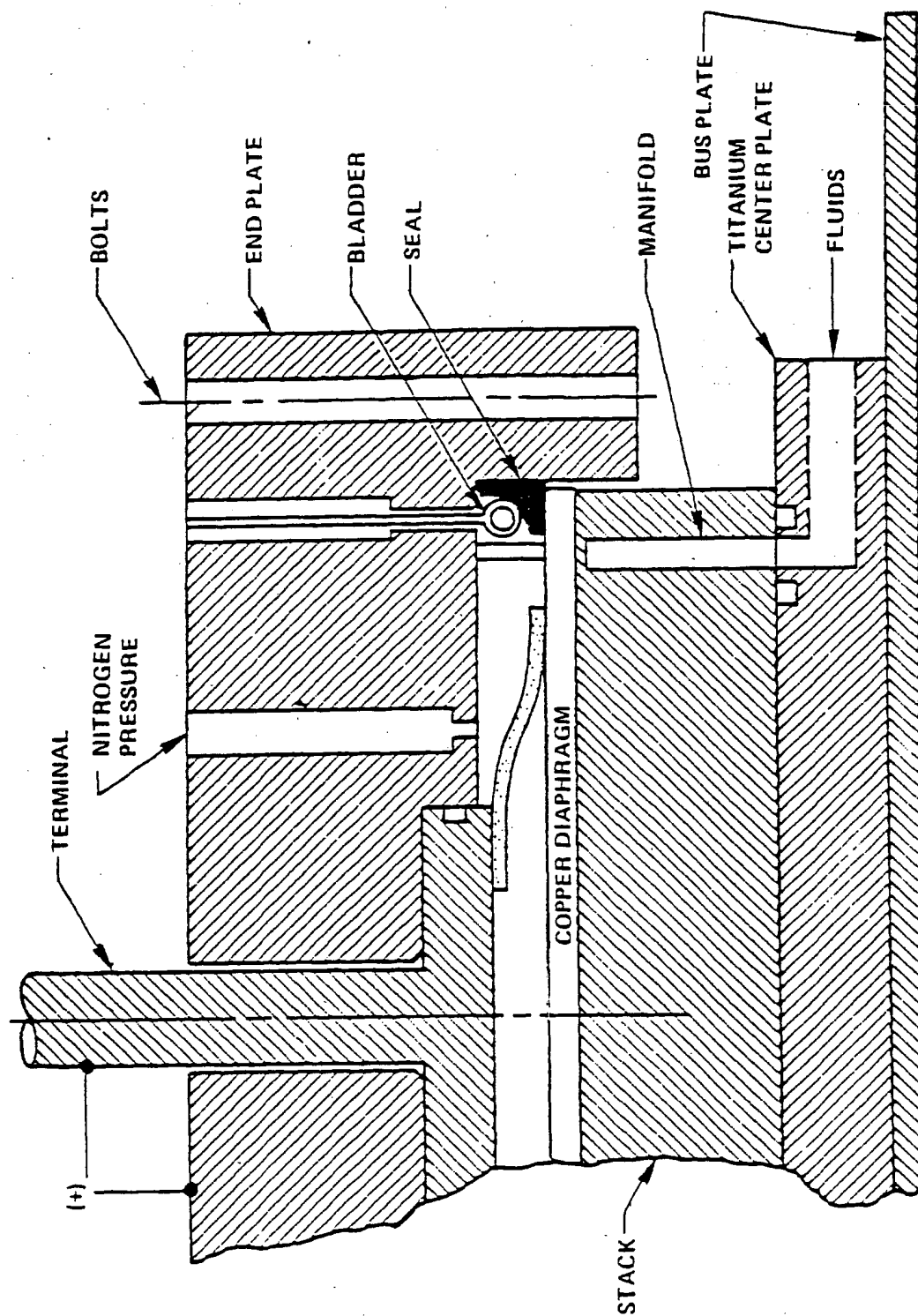
Figure 6. Stack Containment Concept – Design IV

BOLTS

END PLATE

BLADDER

SEAL

MANIFOLD

BUS PLATE

TITANIUM CENTER PLATE

FLUIDS

TERMINAL

NITROGEN PRESSURE

COPPER DIAPHRAGM

(+)

STACK

OUTLINE OF
ANODE FLOW FIELD

ANODE SUPPORT

MEMBRANE &
ELECTRODE

CATHODE SUPPORT

COPPER DIAPHRAGM
(ELECTRIC BUS)

PNEUMATIC SEAL

CENTER BUS PLATE

MANIFOLD
COVER
PLATE

FLUID MANIFOLD

FLUID MANIFOLD

STACK

PNEUMATIC END PLATE
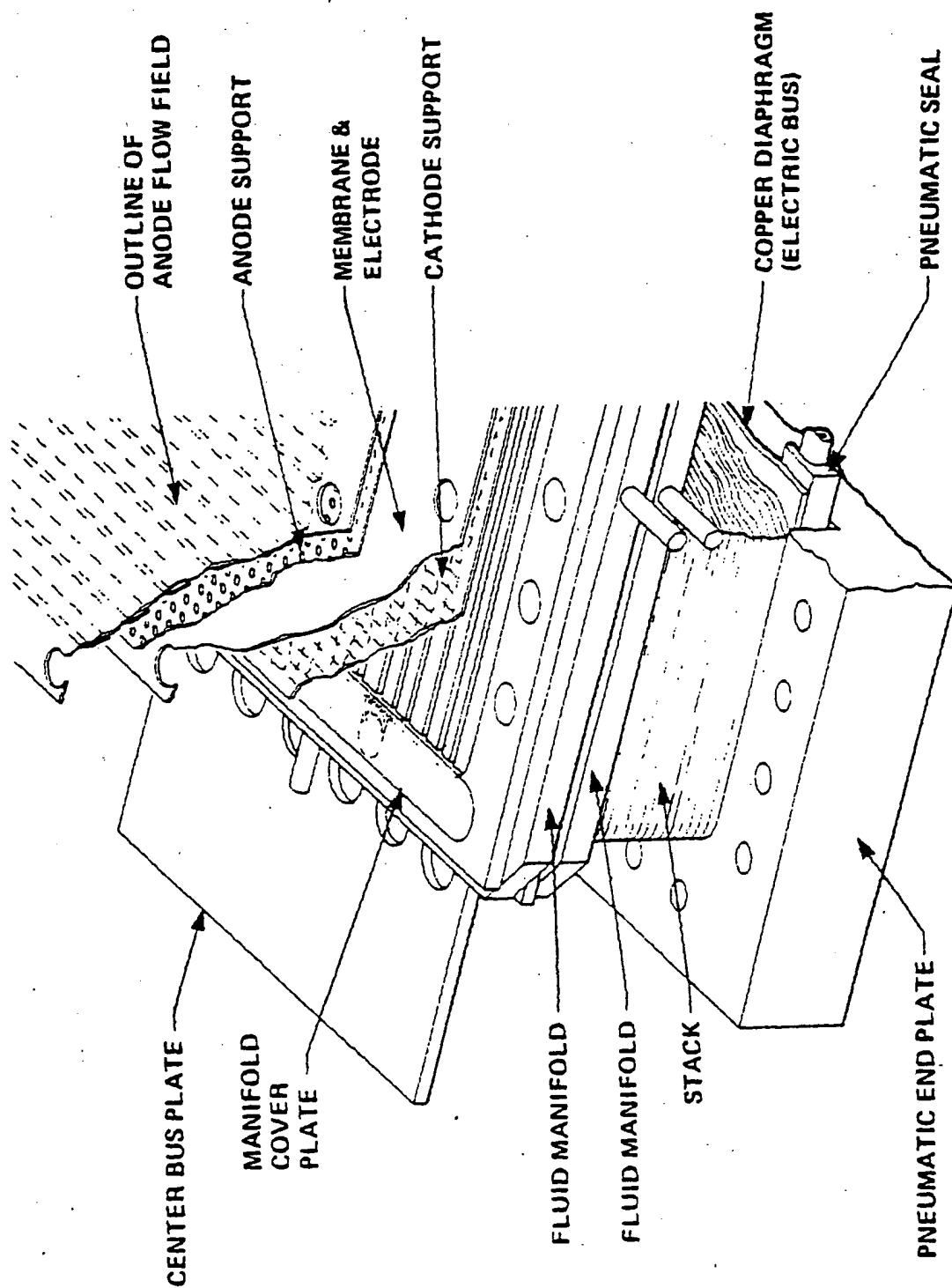
Figure 7. Single Cell Detail

13

Metal Foil

Collector → Carbon

H₂/H₂O   H₂/H₂O

Cathode Catalyst
Electrode → ◁ △ ◁ ▷ ▽ △ △ ◁ ▽ ▽ △ △▽ ← Cathode Support

Solid Polymer Electrolyte

Anode Catalyst
Electrode → ▽ ▷ △ △ ▷ △ △ ← Anode Support

O₂/H₂O   O₂/H₂O   O₂

Collector → Carbon
Collector
Oxidation
Shield

H₂/H₂O   H₂/H₂O

▽ ▽ △ ▽ △ ▽ ▷ △ △ ◁ △ ▽ △ △

Solid Polymer Electrolyte

▽△ △ ▷ △ ▷ △ ▽ △ ▷ △ △

O₂/H₂O   O₂/H₂O   O₂

Carbon

Ribbed Carbon Collector with Support
for Solid Polymer Electrolyte and Electrodes

Figure 8. Schematic of Bipolar Molded Carbon Collector Cell

14

plates were fabricated and plated. The diaphragm assemblies were brazed. The fabrication of the endplates and the center bus plate was completed. The remaining stack components (i.e., supports, brackets, simulated stacks, insulators, etc.) were completed and received by the end of January, 1978. The pneumatic diaphragm seals were received and inspected.

Test fixtures for the endplate pneumatic-seal checkout were designed and fabricated. The full-scale hardware was tested for the pneumatic diaphragm seal concept verification, before releasing the endplates for plating.

The diaphragm assemblies, titanium plates and center bus plates are gold-plated (electroless nickel pre-plate) for high current transfer at interfaces. Arrangements were made for selective gold plating (brush type) of the endplates at the high current electrical contact interface surfaces.

All materials necessary for construction of 2.5 ft^2 stacks were procured and processed.

Membrane and Electrode Assembly

Development of 2 1/2 Ft^2 M&E manufacturing techniques were completed. A fixture was designed and built for the catalyst transfer process, which rolls the membrane onto a catalyst decal with minimal catalyst movements. Electrodes made with the new improved rolling technique were used for initial tests.

Anode Support

A die was used for cutting the anode perforated titanium foil supports to the proper size for assembly. Full-sized sheets of single seam perforated Ti foil were to be received.

Six perforated anode support foils with two overlap laser weld seams joining four smaller perforated sheets were fabricated. The support foils were fabricated with two overlap laser weld seams instead of a single overlap laser weld joining two larger sheets because of difficulty in maintaining proper hole distribution size in the two joining sheets.

The support foils were successfully coated in a new facility for low-contact resistance platinum plating.

Collector Mold

Manufacture and assembly of the 2 1/2 ft^2 collector mold took place at the J.G. Tilp Company. Pre-chrome inspection of the mold by GE/DECP and the mold maker was completed in January 1978, with delivery to the molder during February 1978.

15

A second set of modified inlet/exit manifold inserts were made by the molder for a second generation of collectors. These collectors are to be made with improved corrosion-resistant borders. First tooling proof molding trial runs took place in March 1978.

Density and visual appearance of molded non-foiled collectors were acceptable. In-situ molding of collectors with titanium foil on the oxygen side resulted in splitting of the foil in flow channels and poor adhesion of the foil to the collector surface.

Corrective action included annealing of the foil to improve its ductility and lowering of molding temperature and increasing in-mold dwell time to allow gaseous molding by-products to escape.

Two more 2 1/2 ft^2 collector molding runs were completed at the vendor's plant during 1978. As a result of this experience:

a) a molding cycle was developed which includes a 50°F cool-down prior to part removal, producing good foil adhesion.

b) foil splitting in the flowfield was eliminated by the use of properly annealed Ti foil.

c) A thickness runout of approximately .006" was achieved.

Several areas required further work:

a) some degree of wrinkling of the foil at the corners of the sealing area tends to form external leak paths and

b) machinery requirements (in addition to the cool-down molding cycle) tend to produce a high manufacturing cost.

Improvements in the collector design and manufacturing processes were pursued to correct these problems. Sufficient collectors of adequate quality for initial cell testing were fabricated.

The next batch of collectors had the foil cut back to the active area, avoiding the corner wrinkling problem.

Further collector improvements were made during the program and are included in sections of 2.5 Ft^2 Cells with Updated Technology for the 200 kW System and Assembly and Test of 2.5 Ft^2 Cell Stacks.

16

4.2   50 kW System

Prior to the start of this contract, the test facilities for operational evaluation of 2.5 ft^2 modules up to a capacity of 50 kW were designed, and most of the components procured.

The facility was designed for remote control of a 2.5 ft^2 active area electrolysis module operating at approximately 50 kW equivalent hydrogen output at 300°F and 600 psia. Automatic control of water feed, thermal control, and automatic shutdown were incorporated. The anode water was recirculated with gas/water separation at pressure. The cathode water and gas were separated at low pressure.

Procurement and fabrication of ancillaries continued early in this contract. Component installation was initiated along with fabrication of control panels. A satisfactory checkout of the power supply was accomplished. The basic test facility construction was completed.

The design incorporates flexible connectors to compensate for thermal expansion and shunts for measuring current into each of the two cell stacks. Bus bars are designed to carry 10,000 amp at 60°C rise. A portable scissor-type lift table for the module assembly and test was used as a bed plate to support the stack for development tests. The power supply, satisfactorily checked out for 10,000 amps output capability, was moved into its permanent location in the test cell mezzanine.

Procurement and fabrication of ancillaries was completed along with installation of components, sub-system plumbing and fabrication of the fluid and pressure control panels. In addition, installation of components into the electrical control console and instrumentation console was completed. Figures 9, 10 and 11 show the installation.

The power conditioner interfacing bus bars and bus assemblies were fabricated, plated and received. The interfacing flexible connectors assemblies were designed, fabricated and plated.

A dummy stack was constructed and was installed in its final position on the test bed. The stack was removed for leak tests in another area while the final installation of components (and verification and calibration tests) were completed in the test facility.

The ultrasonic level sensors (which control the makeup water entering the system) shown to be unreliable were subsequently replaced with more dependable capacitive-type level sensors.

17
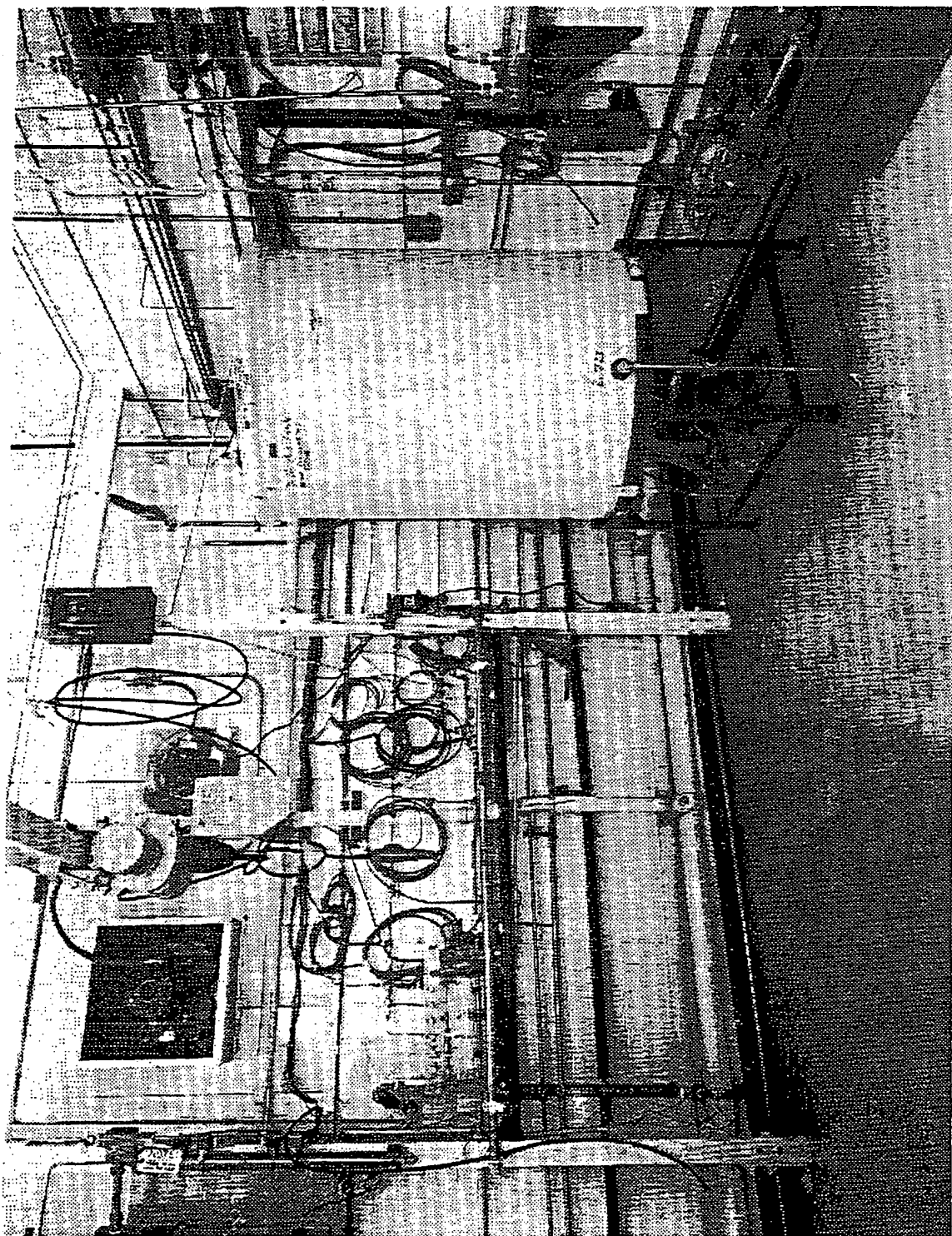
Figure 9. 50 kW Test Facility – Facing Southeast (in Process of Assembly)
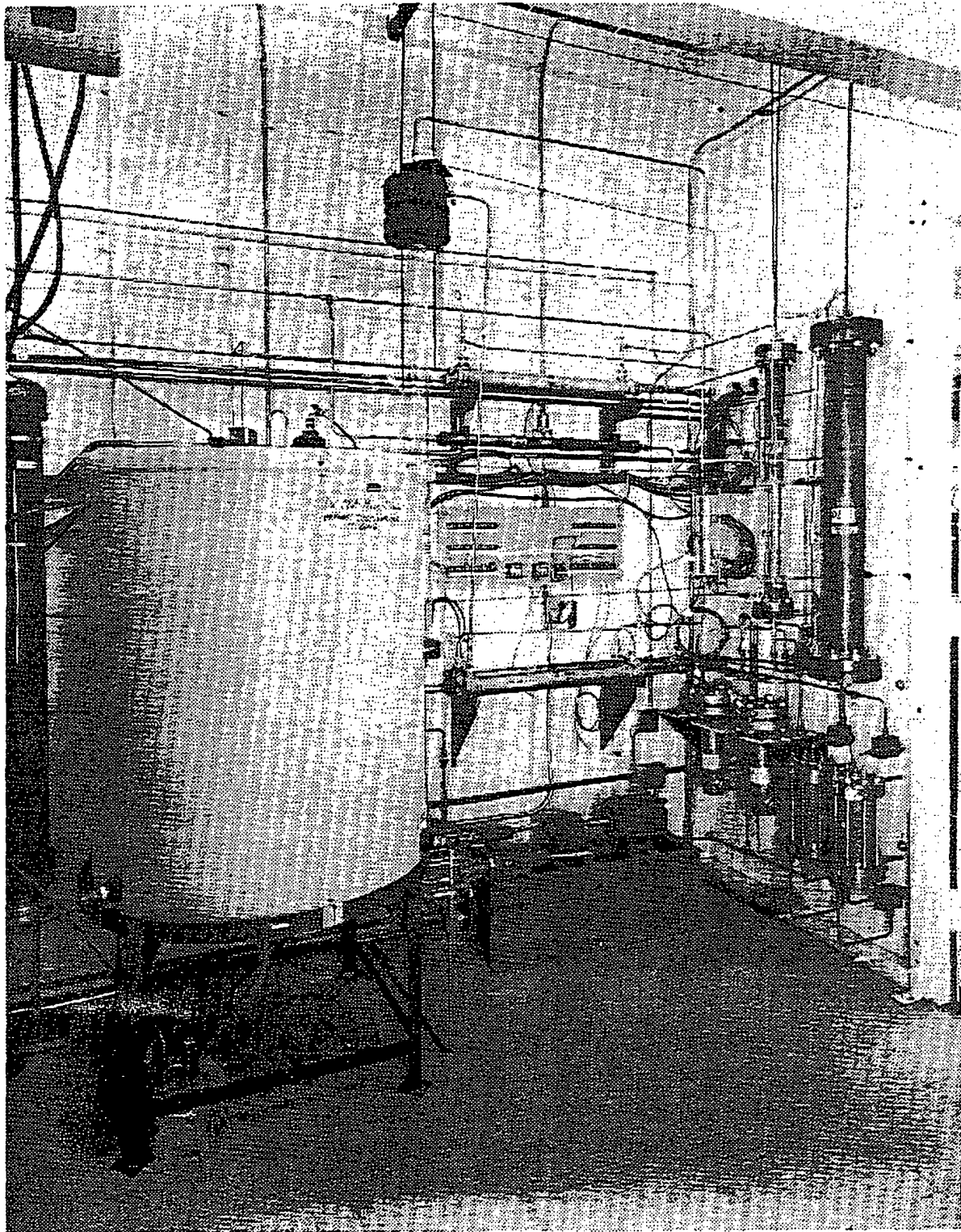
Figure 10.   50 kW Test Facility - Facing Southwest
(in Process of Assembly)

DIRECT ENERGY CONVERSION PROGRAMS
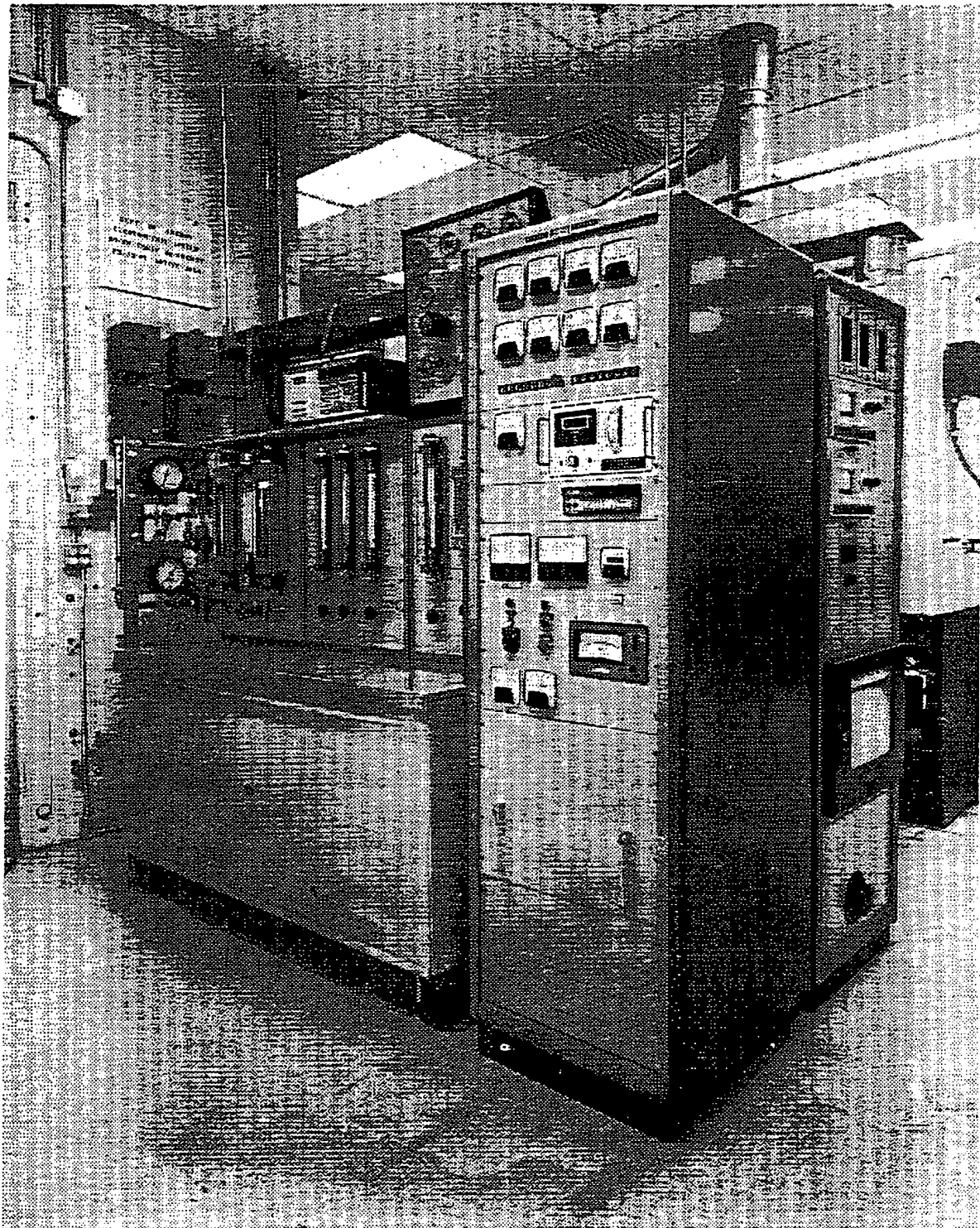
Figure 11. 50 kW Test Facility Fluid and Electrical
Controls and Instrumentation

Figures 12 and 13 show views of the completed test area. An operational manual covering operation of this facility was prepared.

The 50 kW system became operational in August 1978, and since that time 24 modules have been operated in it for a total of over 5,775 hours. These modules are listed in Table 1.

TABLE 1

MODULES TESTED IN DOE 50 kW TEST FACILITY

Module Number	Number of Cells	Hours of Operation
DOE-5	1	19
8	3	125
11	1	130
12	1	46
13	1	137
14	1	18
15	1	114
16	1	18
17	6	451
18	12	113
19	1	137
20	1	462
22	1	80
23	1	19
24	1	607
26	1	51
27	1	297
28	1	70
29	12	53
30	12	132
34	12	1013
41	1	998
44	3	611
46	3	78
		5779

Over the course of the program, the 50 kW facility has been modified as follows:

- Installation of a new circulating pump with a 50 psi head to match more closely the final flow-pressure drop requirements of the 2 1/2 ft^2 cells.

DIRECT ENERGY CONVERSION PROGRAMS
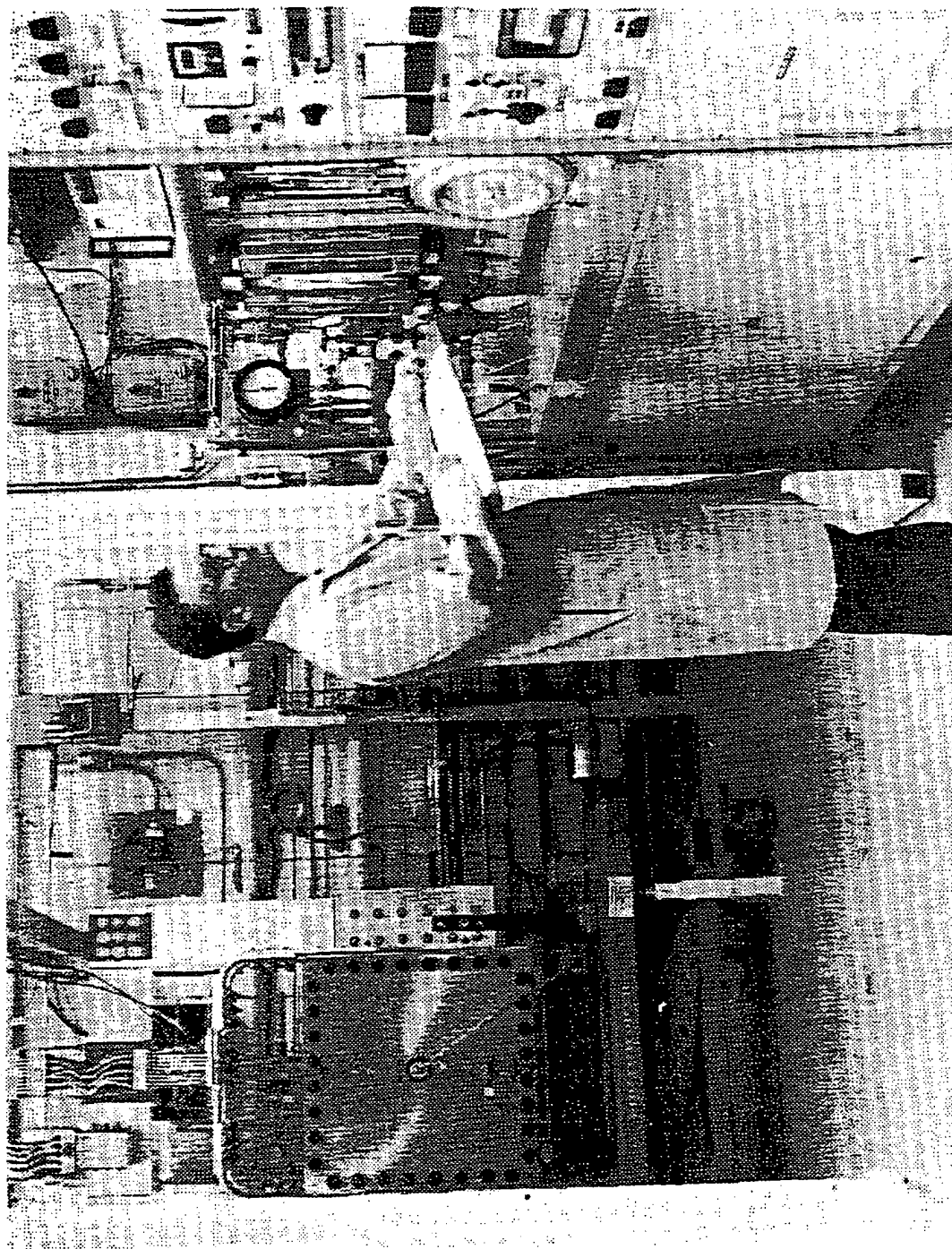
Figure 12. Single Module S/N DOE-5 Testing

22
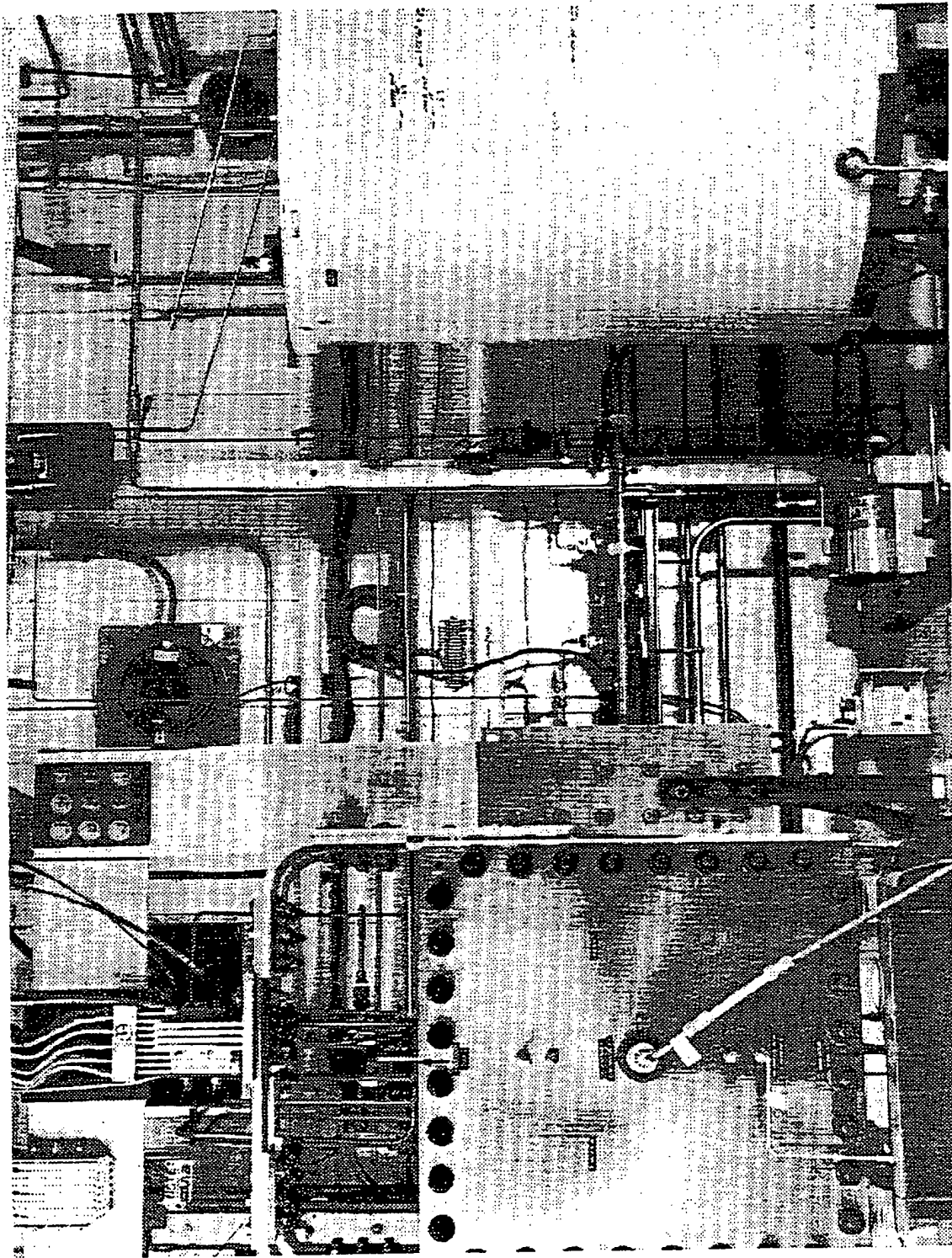
Figure 13. Single-Cell Module S/N DOE-5

DIRECT ENERGY CONVERSION PROGRAMS

Installation of a new electrical bus to allow hori-
zontal operation of stacks and the use of edge-wise
current introduction into the module bus plate.
(Horizontal operation is judged to have more mech-
anical reliability. Edge-wise current introduction
allows the use of a lower-cost bus plate.)

4.3   200 kW System Design

The basic system concept of the 200 kW Engineering Model
was an extention of the earlier 50 kW system. The packaging
concept, however, was considerably different. The 200 kW system
was packaged as a prototype for a "shippable" system; that is,
the system was modularized to allow for transport of individual
modules and to minimize on site installation activities.

4.3.1   200 kW System Definition

Heat and mass balance calculations were completed for
a 200 kW electrolyzer with off-design capability up to 300 kW.
Figure 14 shows the schematic for the system used for the heat
and mass balance calculations and Table 2 shows the computer
input/output for one set of operating conditions. The operating
conditions were varied over a temperature range of 180°F to
300°F and a pressure range of 100 psi to 300 psi.

To size the equipment, the maximum heat and mass loads
from all cases were chosen to ensure that each component would
be capable of full spectrum operation.

The removal of waste heat by an air coolant conditioner
was selected rather than water cooling, due to its more universal
acceptability.

Discussions were held with water treatment engineers to
finalize the water conditioning subsystem. The water conditioning
system was targeted towards treating Wilmington, Massachusetts
water, since it is both a convenient model and a diffucult water
to purify. This arises from its high organic and carbonate con-
tent.

A Rotojet pump instead of a piston pump was selected
for the feed pump because of anticipated fewer maintenance pro-
blems.

The heat and mass balance showed that, at 300°F,
some heat must be transferred from the cathode effluent water to
the anode loop; otherwise excessive stack cooling will take
place. A regenerative heat exchanger was included, therefore,
to allow steady state operation at 300°F.

24
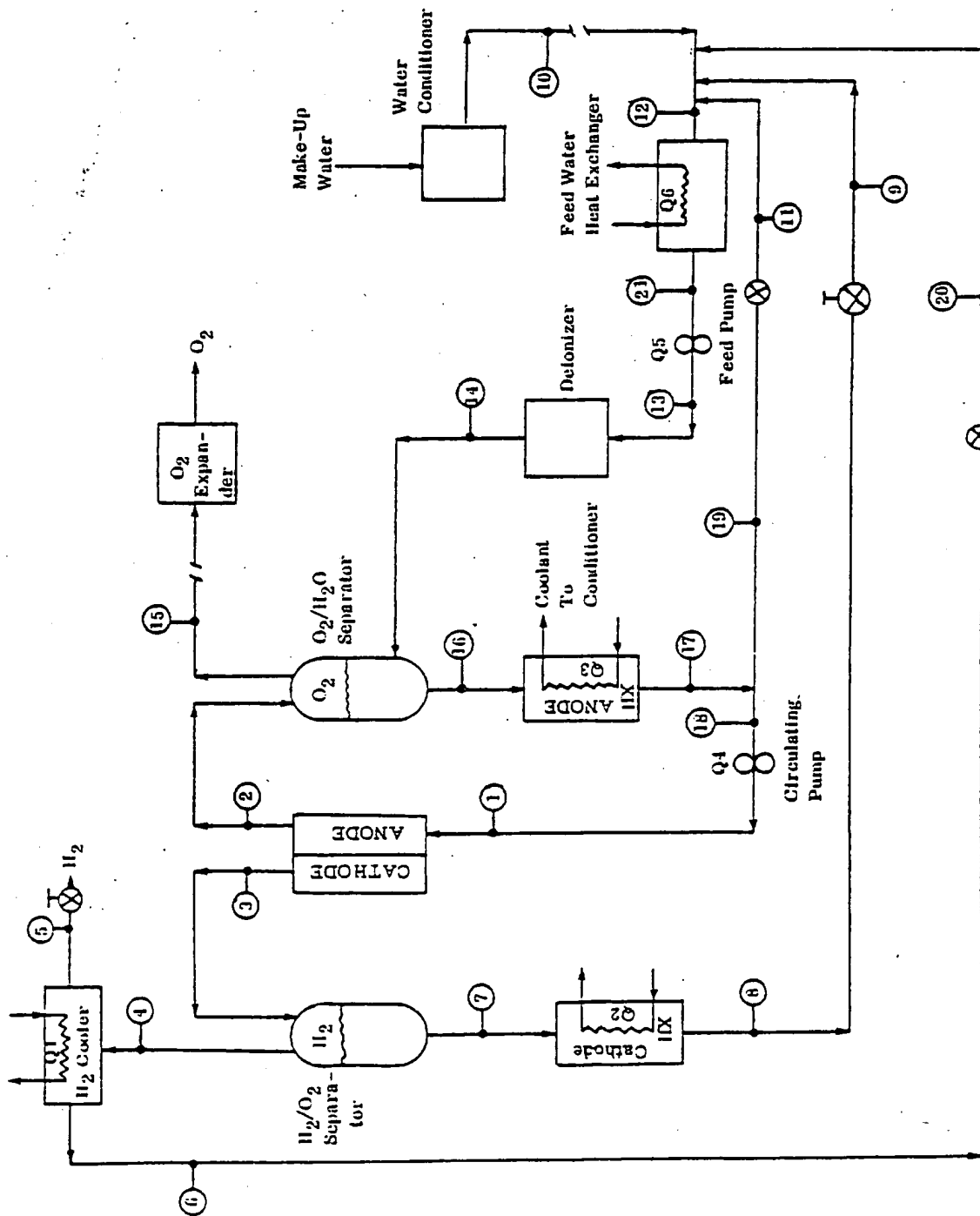
Figure 14. Water Electrolysis Heat and Mass Computer Model Schematic

TABLE 2

RUNH

27/06/78   11.274

```
ENTER HYDROGEN OUTPUT (SCFD)        ?83160
STREAM FACTOR (FRACTION)            ?1.0
CELL VOLTAGE (VOLTS)                ?1.780
TOTAL CURRENT DENSITY (ASF)         ?1500
DIFFUSION CURRENT DENSITY (ASF)     ?52.5
CELL OUTLET TEMPER (DEG F)          ?300
CELL ANODE OUTLET PRESS (PSIA)      ?290
CELL CATHODE OUTLET PRESS (PSIA)    ?340
MAKE UP WATER TEMPER (DEG F)        ?80
MAKE UP WATER PRESS (PSIA)          ?16
HYDROGEN OUTFUT TEMPER (DEG F)      ?100
CATHODE HX OUTLET TEMP (DEG F)      ?140
```

```
     83160   SCFD HYDROGEN SYSTEM STUDY


CELL TEMP(DEG F)=            300    STREAM FACTOR=      1
PRESSURE ANODE OUT=         290    CATHODE OUT=  340   PSIA
CURRENT DENSITY TOTAL=       1500    DIFFUSION= 52.5   ASF
CELL VOLTAGE= 1.78   VOLTS
CELL VOLT EFF(%)=      83.14607    CURR EFF(%)= 96.5
OVERALL CELL EFFICIENCY(%)=    80.23595
TOTAL ACTIVE AREA(SQ FT)=    148.9508
TOTAL NO OF 2.5 SQ FT CELL=   59.58032
NO OF MODULES FOR 1000 CELLS/MOD=    .0148951
HYDROGEN PRODUCTION RATE=    83160 SCFD OR   319097.3 WATTS
TOTAL POWER INPUT TO MODULES=    397698.6 WATTS
```

TABLE 2

SUMMARY OF MASS FLOWS IN THE SYSTEM BY STATION

STA NO	HYDROGEN LB/HR	VAPOR LB/HR	OXYGEN LB/HR	LIQUID LB/HR
1	.0000E 00	.0000E 00	.0000E 00	55.8647E 02
2	.0000E 00	23.9676E 00	14.1753E 01	40.8690E 02
3	17.8608E 00	39.1565E 00	.0000E 00	12.7684E 02
4	17.8608E 00	39.1565E 00	.0000E 00	.0000E 00
5	17.8608E 00	46.0937E-02	.0000E 00	.0000E 00
6	.0000E 00	.0000E 00	.0000E 00	38.6955E 00
7	.0000E 00	.0000E 00	.0000E 00	12.7684E 02
8	.0000E 00	.0000E 00	.0000E 00	12.7684E 02
9	.0000E 00	.0000E 00	.0000E 00	12.7684E 02
10	.0000E 00	.0000E 00	.0000E 00	18.4042E 01
11	.0000E 00	.0000E 00	.0000E 00	56.4290E 00
12	.0000E 00	.0000E 00	.0000E 00	15.5600E 02
13	.0000E 00	.0000E 00	.0000E 00	15.5600E 02
14	.0000E 00	.0000E 00	.0000E 00	15.5600E 02
15	.0000E 00	23.9676E 00	14.1753E 01	.0000E 00
16	.0000E 00	.0000E 00	.0000E 00	56.4290E 02
17	.0000E 00	.0000E 00	.0000E 00	56.4290E 02
18	.0000E 00	.0000E 00	.0000E 00	55.8647E 02
19	.0000E 00	.0000E 00	.0000E 00	56.4290E 00
20	.0000E 00	.0000E 00	.0000E 00	38.6955E 00
21	.0000E 00	.0000E 00	.0000E 00	15.5600E 02

STA NO	TEMPER DEG F	PRESSURE PSIA	ENTHALPY BTU/HR
1	260.0	310.0	12.7785E 05
2	300.0	290.0	11.3905E 05
3	300.0	340.0	40.7064E 04
4	300.0	340.0	62.6635E 03
5	100.0	330.0	46.5075E 02
6	100.0	330.0	26.3331E 02
7	300.0	340.0	34.4401E 04
8	140.0	330.0	13.7872E 04
9	140.0	16.0	13.7872E 04
10	80.0	16.0	88.4832E 02
11	260.0	16.0	12.9076E 03
12	136.3	16.0	16.2261E 04
13	120.0	300.0	13.6950E 04
14	120.0	290.0	13.6950E 04
15	300.0	290.0	36.6954E 03
16	251.0	290.0	12.3931E 05
17	260.0	280.0	12.9076E 05
18	260.0	280.0	12.7785E 05
19	260.0	280.0	12.9076E 03
20	100.0	16.0	26.3331E 02
21	120.0	6.0	13.6950E 04

ENTHALPY REFERENCE TEMPER IS 32 DEG F

HYDROGEN COOLER HEAT LOAD (BTU/HR)=   55379.42
CATHODE HEAT EXCHANGER LOAD (BTU/HR)=   206528.5
ANODE HEAT EXCHANGER LOAD (BTU/HR)=   -51452.08
FEED WATER HEAT EXCH LOAD (BTU/HR)=   25311.23
CIRCULATING PUMP HYDRAULIC POWER (WATTS)=   155.3374
FEED PUMP HYDRAULIC POWER (WATTS)=   390.1894

Figure 15 shows a simplified schematic of the 200 kW system and Figure 16 shows the finalized system flow diagram. The system operates as follows:

Process water for electrolysis is provided by passing city water through the Deionization-Reverse Osmosis equipment (DIRO system) and is stored in the anode reservoir tank.

The clean water is then fed into the system by the constant speed feedwater pump from the anode reservoir tank through the main deionizers. Water then passes through the filters, control valve, regenerative heat exchanger into the anode circulating water loop.

Feed rate is controlled by means of a modulating control valve which throttles flow as a function of O_2 separator level. Control valve modulation is accomplished by means of a capacitive level probe located in the O_2 separator and an electronic proportional controller.

Process water is circulated to the anodes by the water circulating pump. The two-phase effluent (H_2O, O_2) from the anodes passes to the O_2 separator, where gaseous O_2 is separated from liquid water. The O_2 is then vented via the O_2 off-gas line and the water passes through the anode heat exchanger where heat is rejected.

In the case of system operation under conditions of low pressure and high temperature, an anode regenerative heat exchanger is needed to add heat to the system. This heat exchanger, located in the feedwater line, transfers heat from the cathode return water to the feedwater supply, thereby preheating the feedwater prior to delivery to the circulating water loop. Heat rejection from, or heat addition to, the circulating water loop is accomplished by means of an electronic temperature controller which sequences heating and cooling water via appropriate control valves.

Two-phase effluent (H_2/H_2O) from the cathodes flows to the H_2 separator where gaseous H_2 is separated from liquid water. The H_2 passes to the user via the H_2 delivery piping. The water is drained under pressure from the H_2 separator by means of a modulating control valve. This valve is controlled by a capacitive level probe, located in the H_2 separator, and an electronic proportional controller. The drained water is then proportioned as a function of operating temperature to flow through or bypass the regenerative heat exchanger via the temperature controlled diverting valve. This water then passes through the cathode heat exchanger, where heat is rejected, and is returned to the cathode reservoir tank. The cathode reservoir is isolated from, but connected to the anode reservoir so that the cathode return water can be reused as feedwater, thereby conserving clean makeup water.

28
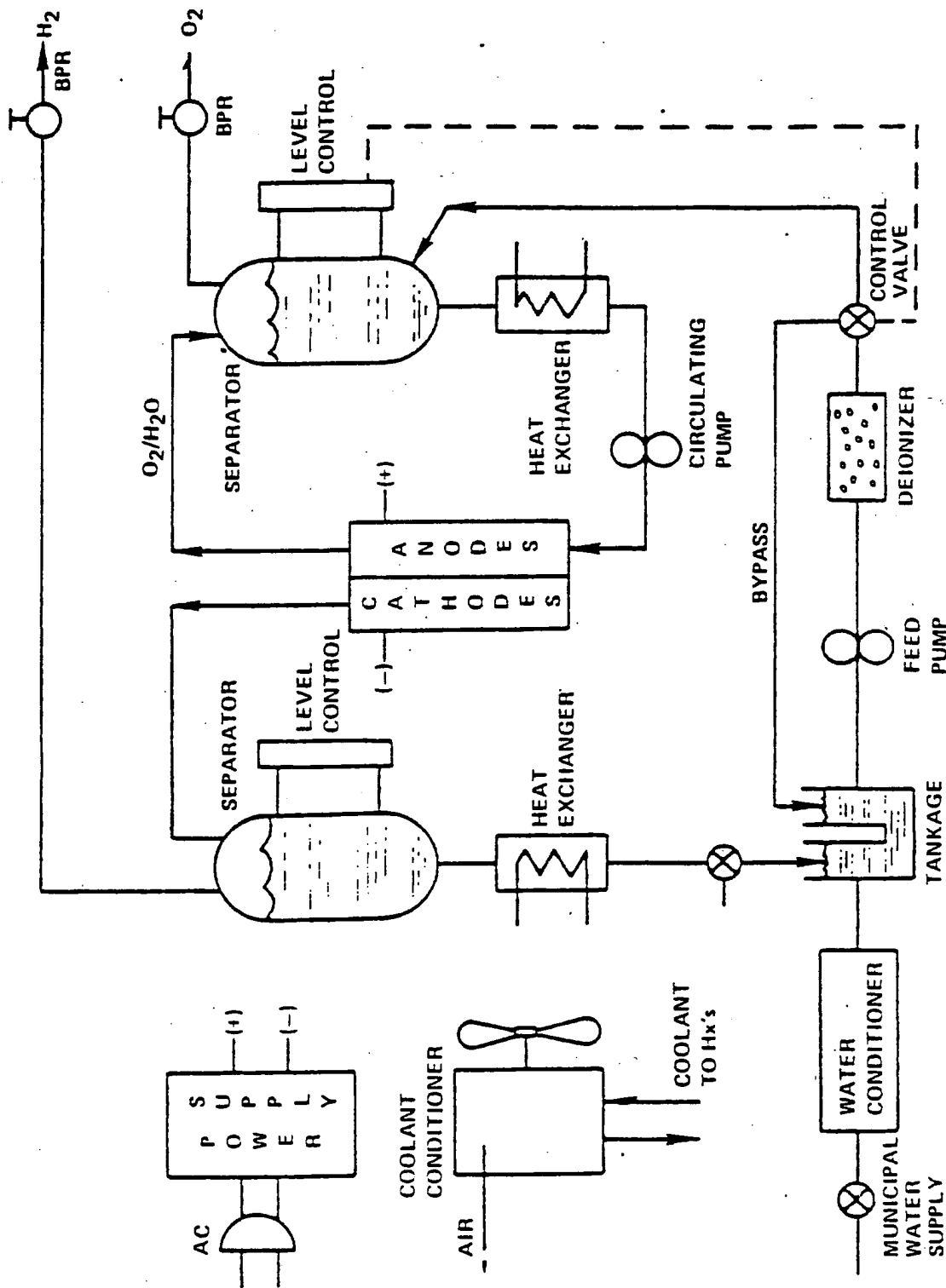
Figure 15. 200 kW System Schematic

Figure 16. System Flow Diagram
Bulk Hydrogen Generation
Sketch No. 78D491-642

DIRECT ENERGY CONVERSION PROGRAMS
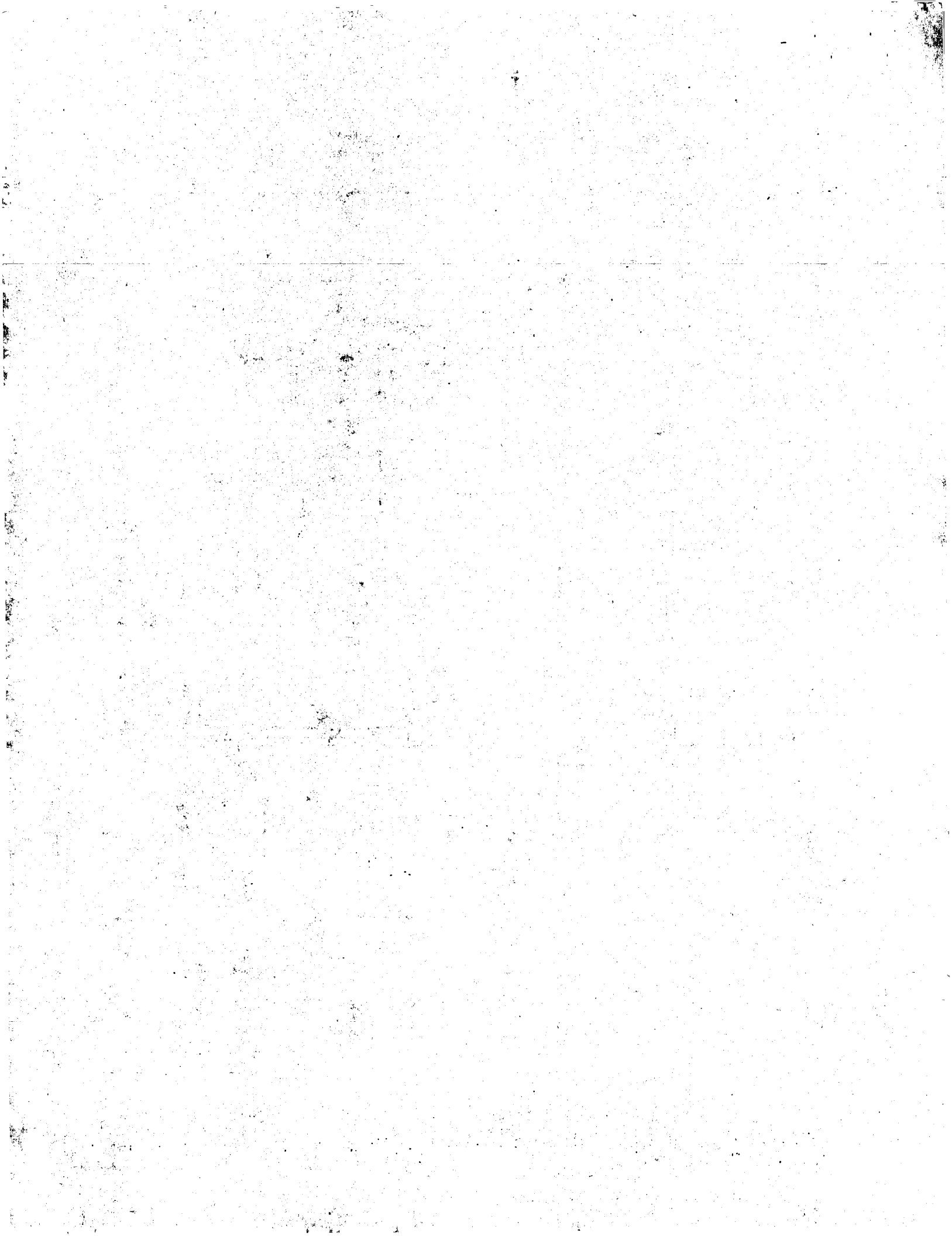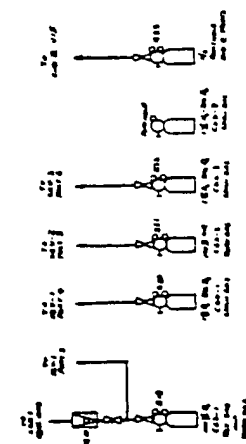
30
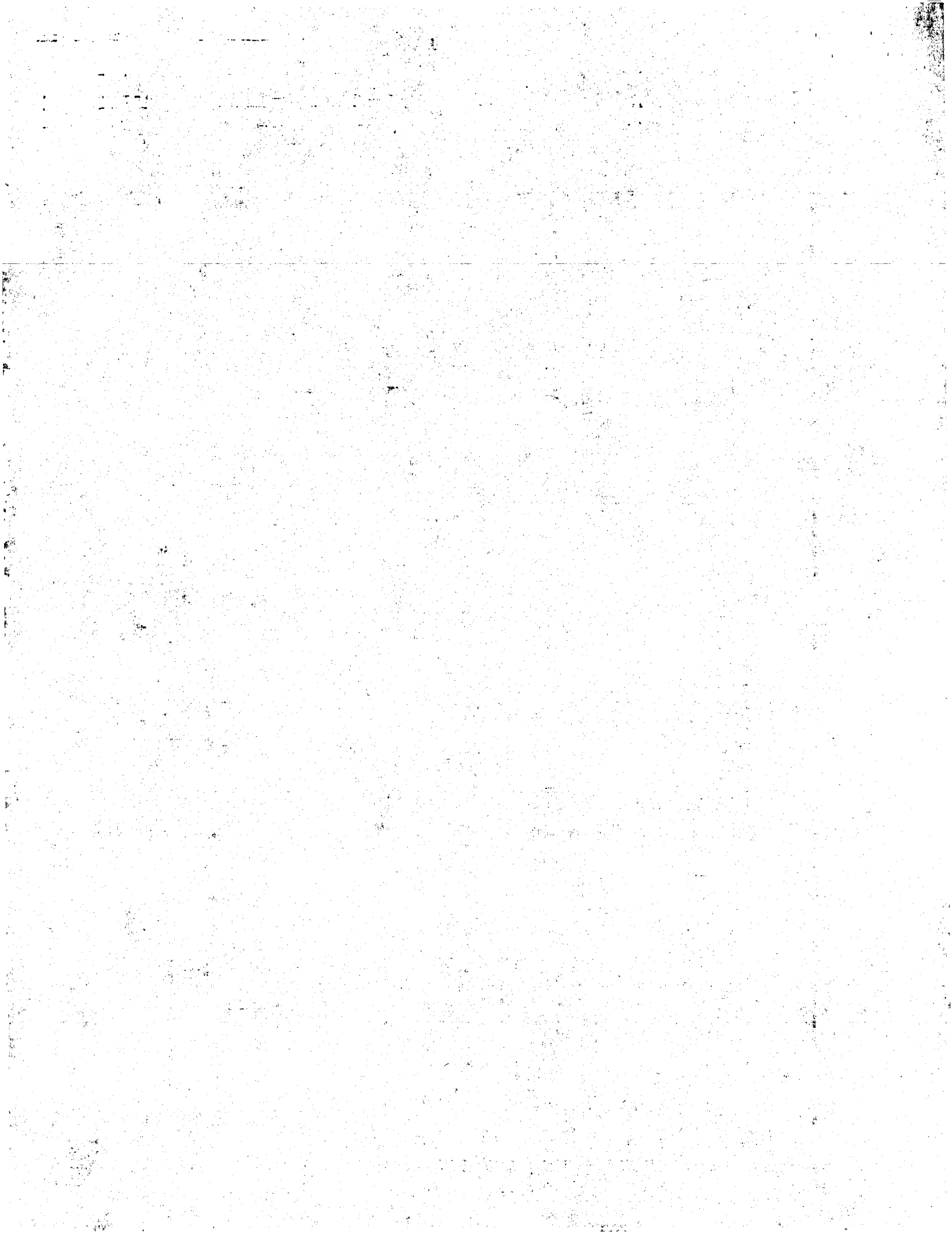
The cathode heat exchanger is used to reject heat from the cathode return water so that the reservoir tank water temperature does not exceed allowable limit acceptable for proper deionizer operation, 140°F.

Hydrogen is delivered to the user on demand by means of automatic controls.

Delivery pressure is adjustable by remote control using a dome-loaded back pressure regulator. Hydrogen production is automatically sequenced to an idle condition (100 ASF) when user consumption drops below the idle setting. This is accomplished using a system idle discharge line along with appropriate controls.

A system isolation valve is provided with a separate vent line and appropriate controls so that automatic purging of the electrolysis system can be accomplished without contamination of the customer's process.

A sampling line for automatic and continuous monitoring of H_2 purity is provided.

Electrolysis system pressure control is accomplished using:

a) H_2 back pressure regulator

b) O_2 back pressure regulator

c) Stack endplate pressure regulator

d) System pressure control regulator

e) Pressurized N_2 supply

f) Automatic purge pressure selector valve and regulator

The H_2, O_2 and stack endplate regulators are remotely controlled by means of dome loading pressure provided by the system pressure control regulator.

4.3.2   200 kW System Layout and Packaging

The 200 kW system was designed to be modular. That is, composed of connectable building blocks each of which is truck transportable. Figure 17 shows the arrangement of these subsystems in the GE/DECP test area. The subsystems are:
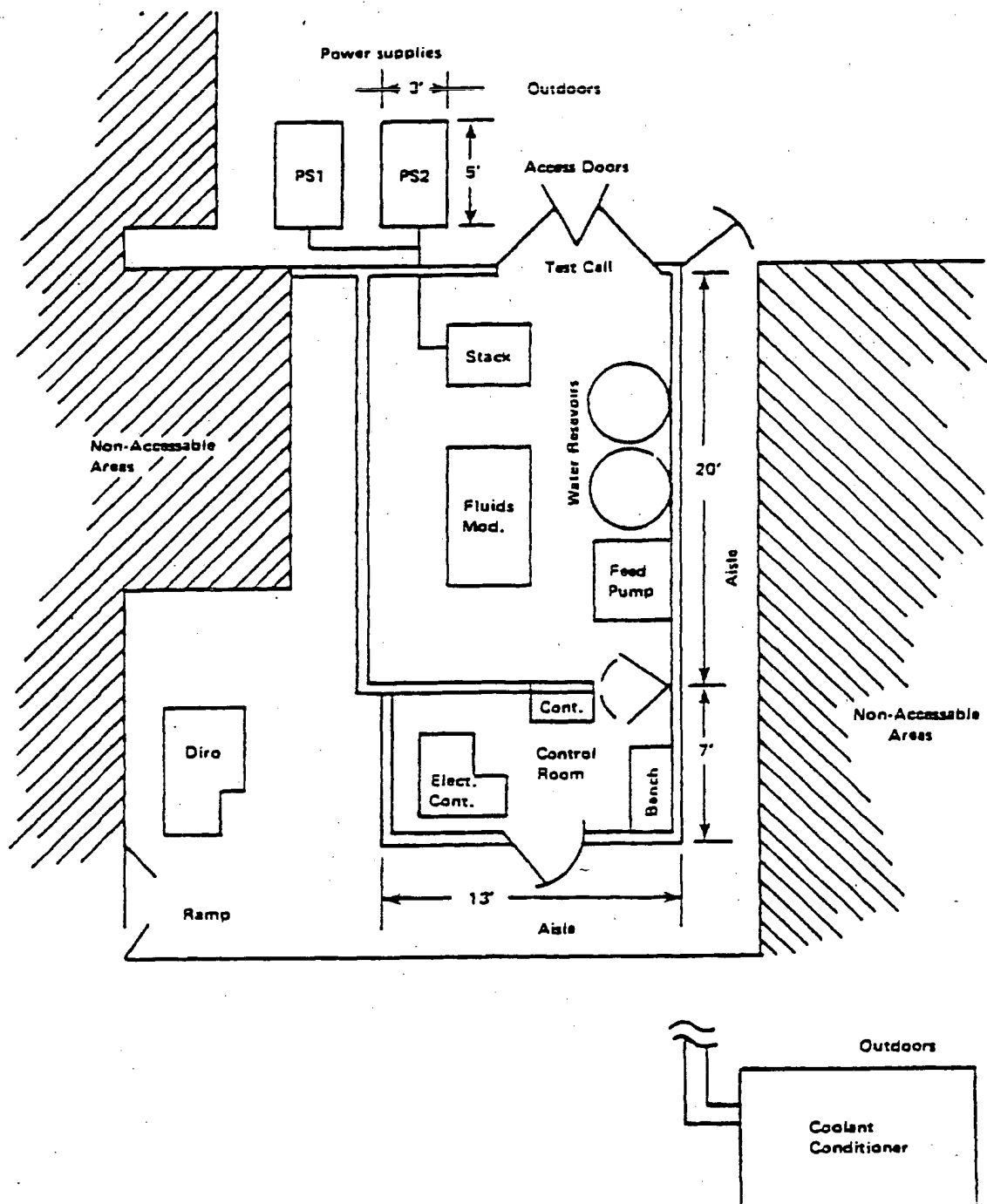
Figure 17. 200 kW System Layout Scale Drawing

1) Electrolyzer Module. This is a transportable electrolyzer on a test bed.

2) Fluids Components Subsystem. This consists of:

   a) H_2 and O_2 separators

   b) Pneumatic control and manual valves

   c) Transducers and instrumentation

   d) Deionizers and filters

   e) Regulators, flowrators, indicators

   f) Circulating pump

3) Feed Pump Subsystem. This consists of the feed pump and controls.

4) Reservoir Subsystem. This consists of anode and cathode water reservoir tanks with ultra violet light to kill bacteria and air filter.

5) Instrumentation and Control Subsystem. This contains all controls and instrumentation. It is located outside the test cell in an adjacent control room.

6) Coolant Conditioning Subsystem. This is located remotely from the test area for convenience in this installation only. The coolant conditioner supplies air-cooled glycol to the fluids module for heat rejection.

7) Power Supply Subsystem. Two DC power supplies are located just outside the test cell. Bus bars are run through the test cell walls to connect with the stack.

8) Water Conditioner (DIRO). Feed water is supplied from city water and processes through the deionizer - reverse osmosis (DIRO) unit. It is connected to the reservoir module and feed pump module.

The layout of the system was established with accessibility and maintainability being prime design considerations. Packaging density has been increased to the maximum feasible for a prototype system.

4.4   200 kW System Assembly

Assembly of the 200 kW system, started in January 1979 when many of the procured components had been received, was completed in May 1979. No major problems were encountered.

Figures 18 through 22 are photographs of the fluid control subsystem, the control panel, the gas monitoring panel, the water purifier, and the coolant conditioner, respectively. Figure 23 shows the 60-cell 200 kW module assembly.

After completion of assembly, and prior to operation, the interior of the piping and all components within the anode and cathode loops were flushed with a cleaning solution and then distilled water. The circulating pump was used to circulate the solutions during cleaning. The flow was bypassed around the module through a filter in order to remove all free particles.

The coolant loop was filled with ethylene glycol solution and then operated for several days. System wiring was completed and tested. Minor problems in the logic circuits were corrected.

The power supplies were tested in the current-controlled mode by placing a shorting strap across the output of each supply. Operation was satisfactory at the tested current of 2500 amps.

Operational testing commenced shortly after system assembly.

4.5   200 kW System Operation

Operational testing of the 200 kW system was initiated on May 25, 1979 using 6-cell module DOE 17 as a slave. Initial system operation, at nominal pressures and temperatures, presented no major anomalies although several minor problems were identified and corrected.

Since initial operation of Module DOE 17 in May 1979, a total of 8 more modules were operated in the 200 kW system for a total of over 3,100 hours. These were:

Unit	No. Cells	Hours of Operation in 200 kW System
DOE 17	6	4
DOE 21	12	163
DOE 25	6	1312
DOE 29	12	151
DOE 31	12	213
DOE 32	30	31
DOE 33	60	707
DOE 43	12	164
DOE 45	12	431

34
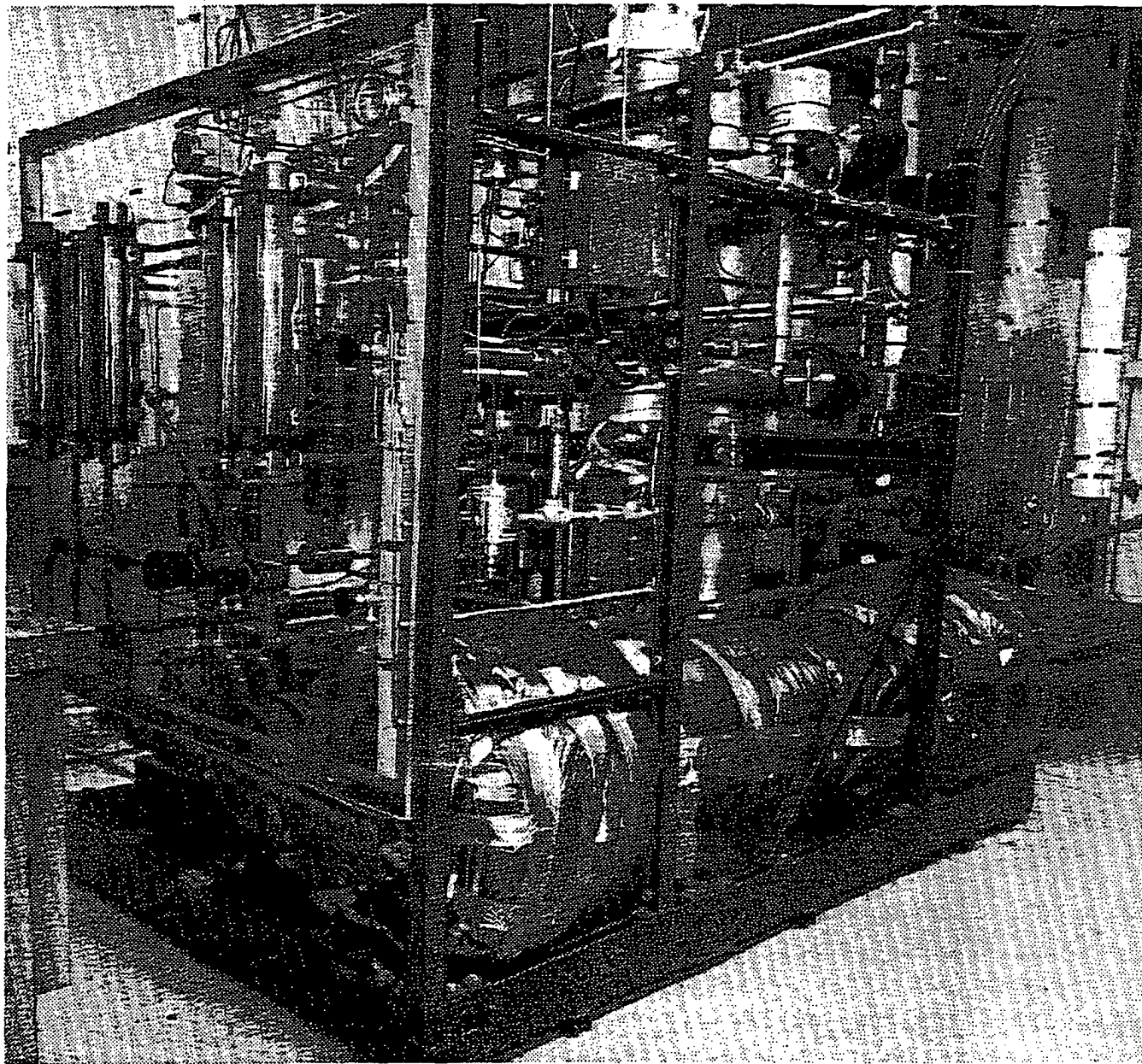
Figure 18.   200 kW Electrolysis System

35
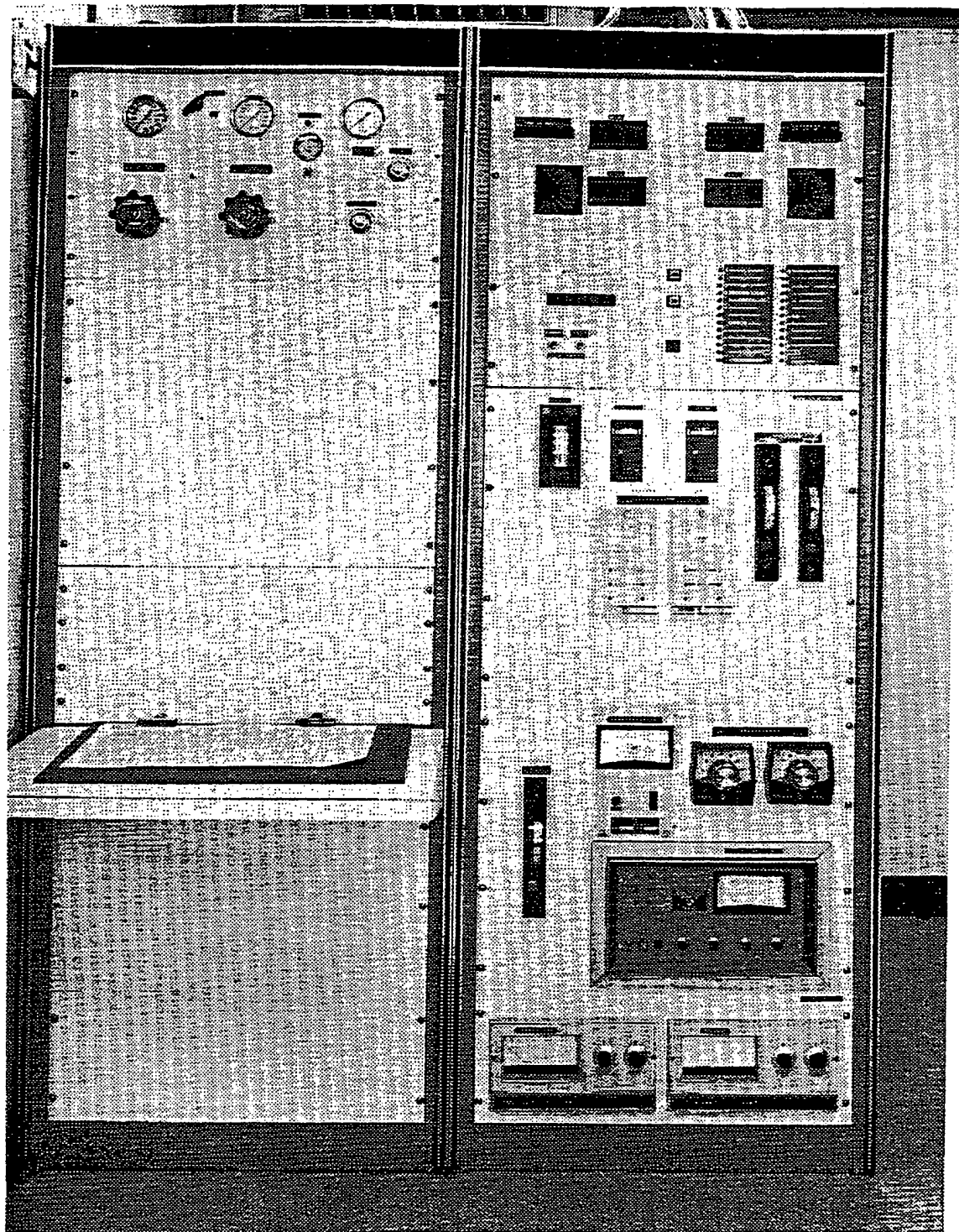
Figure 19.   200 kW System Control Console
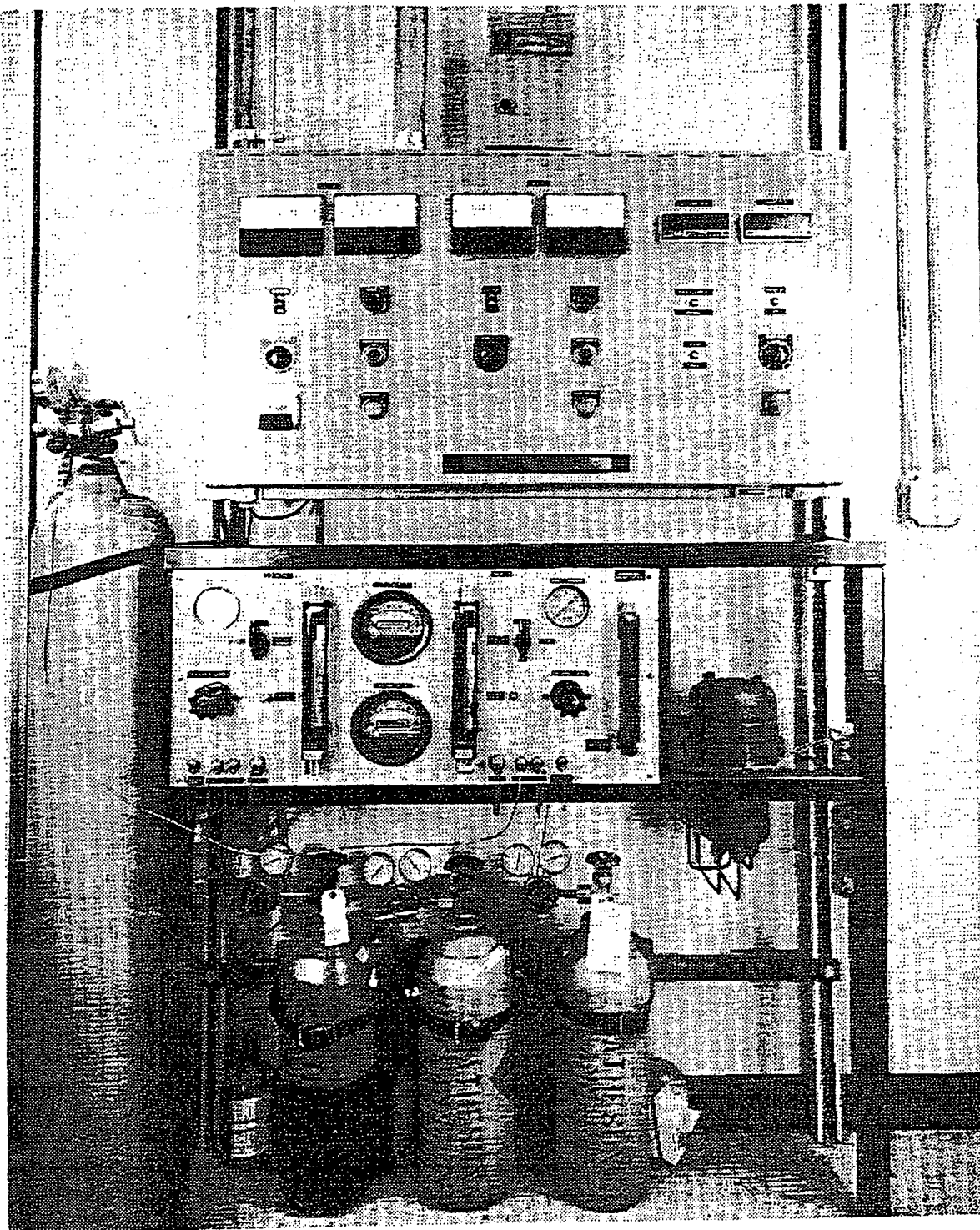
Figure 20. Gas Monitoring Panel
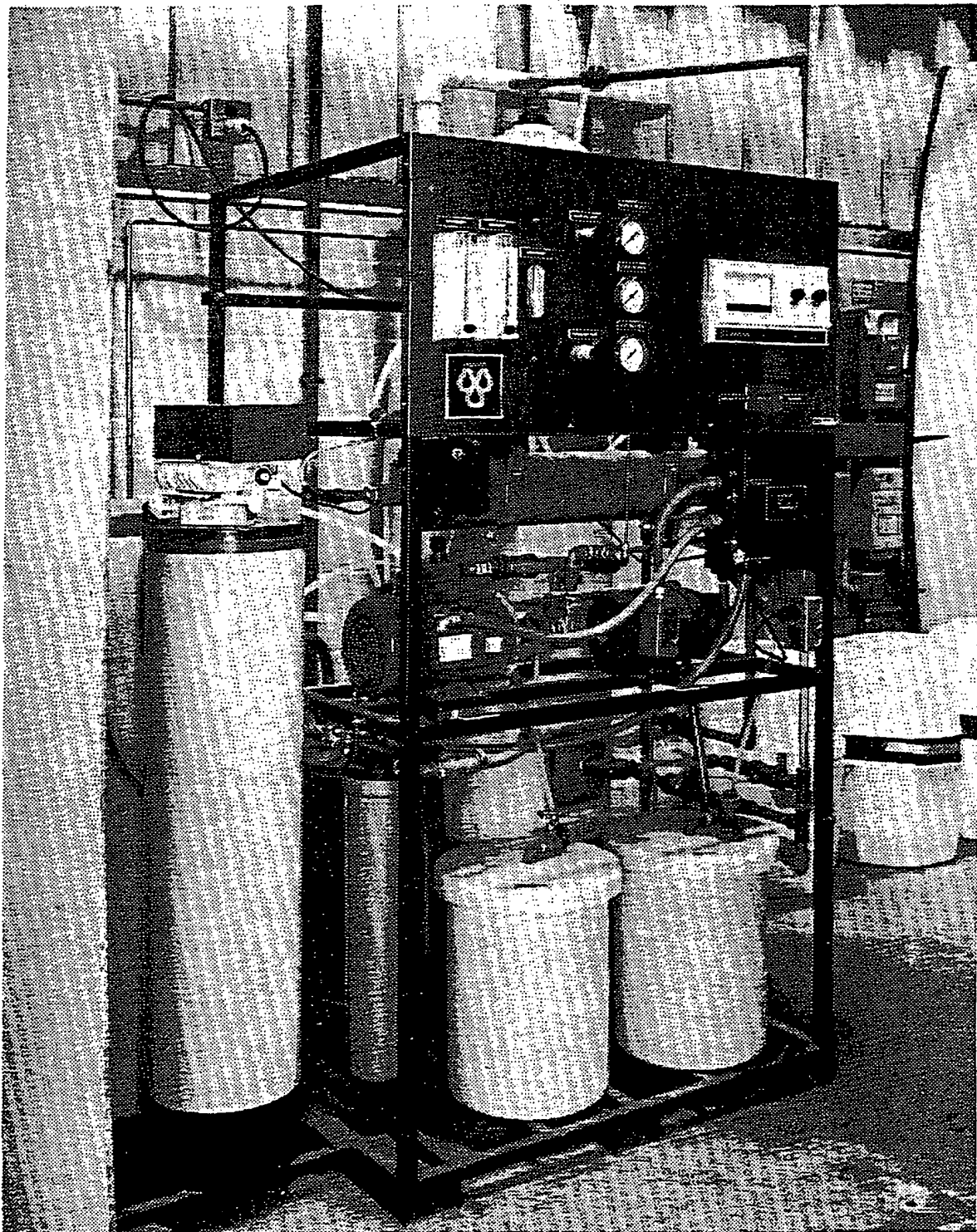
Figure 21.   Water Purifier
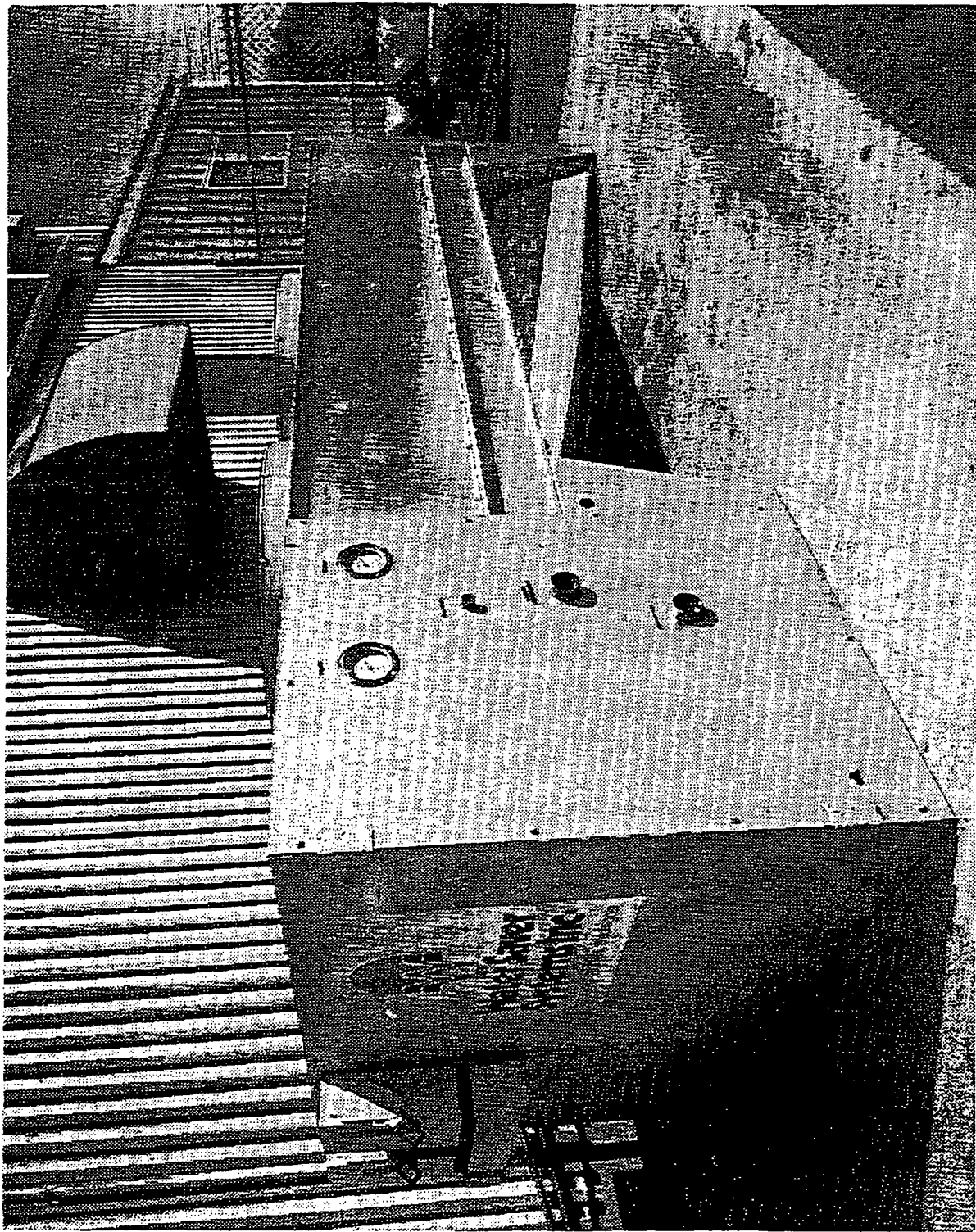
Figure 22. Coolant Conditioner
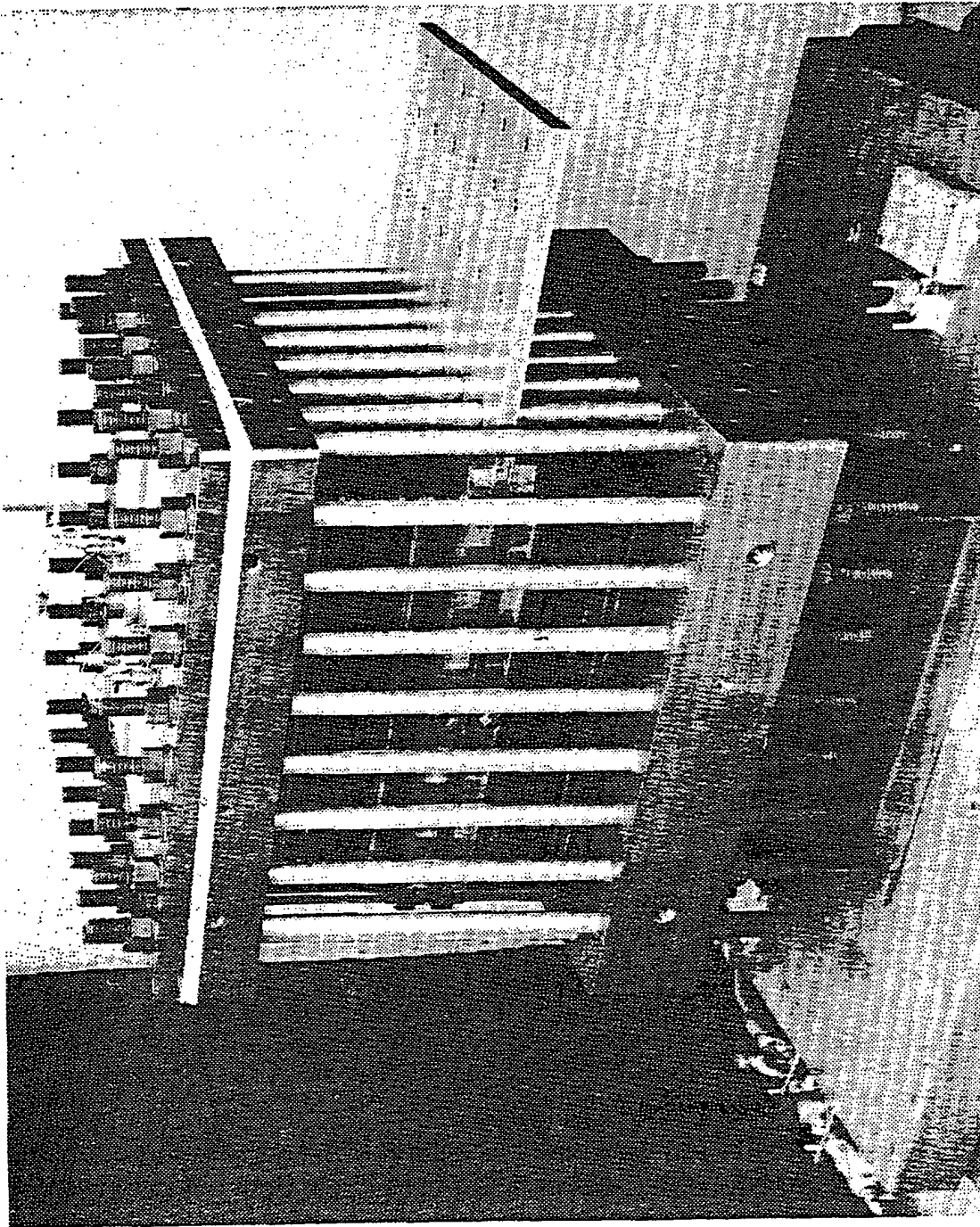
Figure 23.   200 kW (60-Cell) 2.5 Ft^2 Module

DIRECT ENERGY CONVERSION PROGRAMS

Each of these modules are discussed in detail in section 4.6. During the 3,100+ hours of operation, the basic system operated quite well, with only three areas requiring modification.

Deionizers

The initial deionizer configuration had parallel de-ionizers, each containing a mixed bed (both strong anion and cation resins) with a small amount of cation beads only at the outlet. It was found on the 60-cell module (DOE 33) that this configuration led to contamination of the module by amines which elute from the mixed bed as a result of gradual degradation of the anion beads. To drop these amines dependably, the two deionizers were arranged in series with the upstream deionizer containing a mixed bed and the downstream deionizer filled completely with cation resin only. The cation beads effectively drop the amines and prevent them from entering the anode loop.

DIRO Subsystem

The DIRO (deionizer-reverse-osmosis) subsystem is a vendor-supplied component which passes potable water through a reverse-osmosis module at 200 psi, reportedly removing 90% of the total dissolved solids (TDS). The purified water then passes through a strong anion/strong cation mixed-bed deionizer, bringing the water to 18 mΩ-cm, or ultra-pure levels. As incorporated into the GE system, this water is then fed to the electrolyzer to support the electrolysis process.

The unit was tested by regenerating the deionizer and running the subsystem to a cut-off point of 1 mΩ-cm, product water. The highest purity water obtained during the test was 8 mΩ-cm, indicating that the resin bed was imperfect or the regeneration was not complete. Also, from the water resistivity at the RO inlet (4000 ohm) to RO outlet (16,000 ohm), the rejection was calculated to be 69%, rather than 90%. This indicates a raw-water leakage problem in the RO module. Figure 24 shows that if the RO rejection were 90% using Wilmington, MA water, the subsystem would produce 23,000 gallons of water, enough to run the 200 kW unit for 1200 hours. At a rejection of 69%, the unit would produce 8400 gallons of water, sufficient for 440 hours of operation. In the test, the subsystem produced 3000 gallons (157 hr).

It was determined that the DIRO (Deionization/Reverse Osmosis) system for makeup water purification does not perform well for extensive periods of time using Wilmington, MA water. The high colloidal silica content of the water in this area coats the reverse osmosis fibers and reduces the salt rejection, in this case from 90% to 69%.

OPERATION ON WILMINGTON, MA WATER
p = 4,000 to 5,000 OHM-CM
R = REVERSE OSMOSIS REJECTION
ADVERTIZED R = 90%
ADVERTIZED DEIONIZER CAPACITY =
15.6 Kgr AS $CaCO_3$
ELECTROLYZER USAGE RATE = 96 $\frac{gal}{(hr)(mw)}$

R=90%

R=69%

MEASURED

THEORETICAL

☐ MEASUREMENT 13-16 JUNE '80
AFTER "IMPROVED" REGENERATION
OF D/I. p = 8 TO 1 Meg

WATER RESISTIVITY AT DEIONIZER INLET, OHM-CM

1,000

10,000

100,000

1,000,000

DEIONIZER CAPACITY, GALLONS

1,000

10,000

100,000

Figure 24. Facility No. 5 DIRO Characteristics

42

The type of water purification equipment for an application is very site-specific: That is, the equipment must be tailored to the water impurities present in the actual water supply. Thus the system which would be appropriate for in-house testing at GE/DECP might not be the type of equipment required for demonstration systems at other locations.

Module ASD Purge System

The initial system approach to removing hydrogen from the hydrogen side of the module in the event of an ASD (automatic shutdown) was to purge the hydrogen side with nitrogen. It was found, however, on DOE 33 that the flow of dry nitrogen over the cells at elevated temperatures led to drying of the cell with subsequent mechanical stresses and possible cell damage. To correct this situation, a cathode water purge was incorporated to prevent cell dehydration during the nitrogen purge which follows a high-temperature ASD. This modification is shown in Figure 25. During a shutdown under the new system, an air-driven water pump feeds deionized water through the cathode chambers and back to the reservoir tank. An electric timer limits the duration of the purge, after which the system becomes dormant.

General System

All other aspects of system operation were satisfactory. The "Udylite" power supplies performed well as did the coolant conditioner, the pitot tube feed pump, and the bulk of the fluid control components. The control system, once debugged, was reliable although somewhat sensitive to electrical glitches.

4.6   Operational Evaluation of 2.5 Ft^2 Modules

This section contains a discussion of each of the 2.5 ft^2 module operational evaluations which took place during this program. The modules were numbered sequentially, as assembled, starting with DOE-1. Not all modules assembled were operationally evaluated. The first module to be operationally evaluated was DOE-5.

4.6.1   DOE-5

A single cell was assembled and designated DOE-5. It was leak-checked at room temperature before and after heating the stack to 180°F by hot water flow to the anode compartment. Leak tests were run using nitrogen gas to pressurize the anode, and subsequently measuring the gas rate at the cathode. Figure 26 shows that, initially, the cell was leak-tight to 50 psig (300 psig endplate pressure), but that it did leak above 50 psig. After heating the stack to 180°F for about four hours and then cooling it to ambient temperature, the stack showed only normal gas permeability up to 150 psig. Between 150 and 200 psig, the cell began to leak in excess of the normal membrane diffusion rate.

43
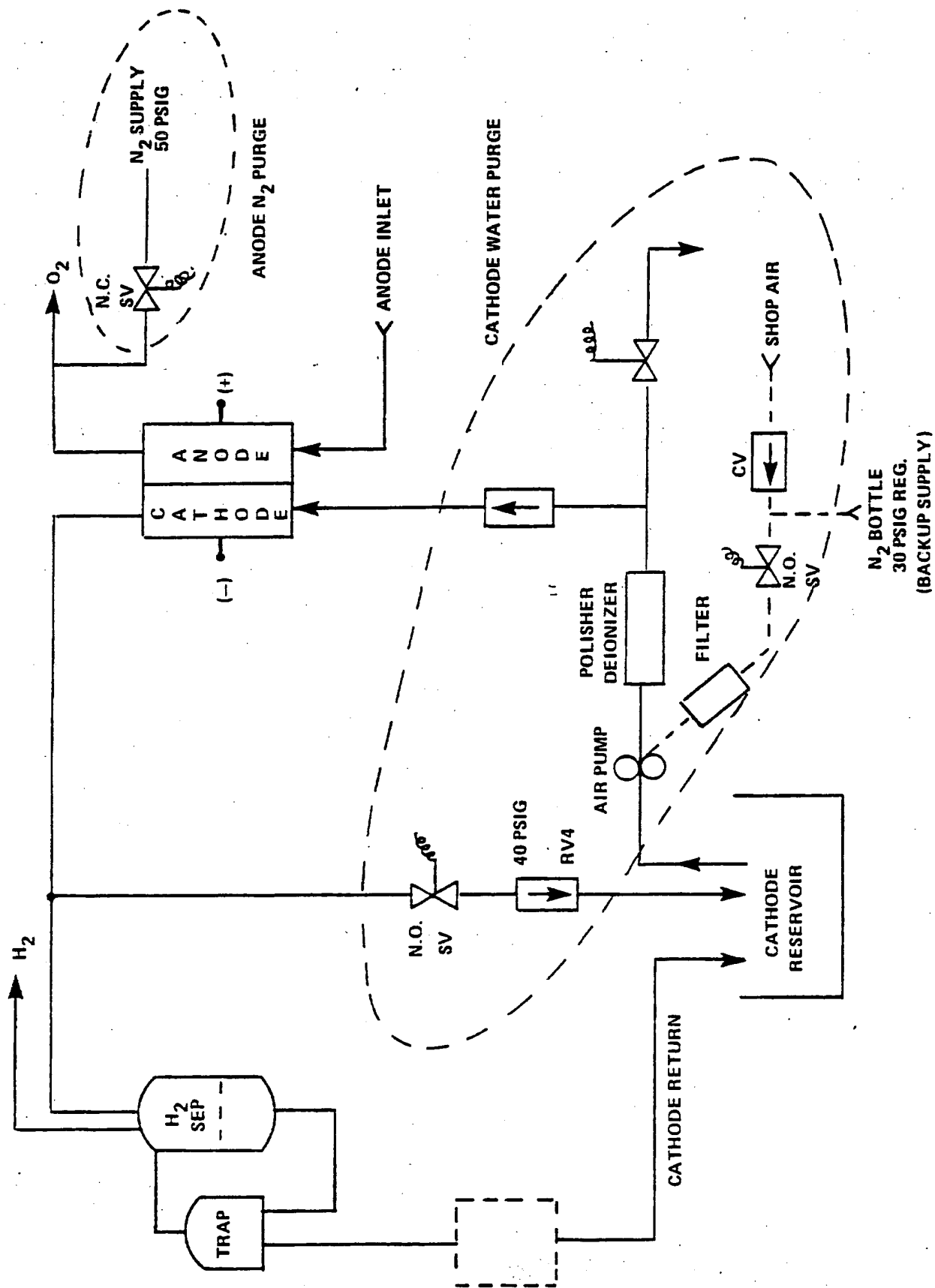
Figure 25. ASD Cathode Purge Subsystem

44
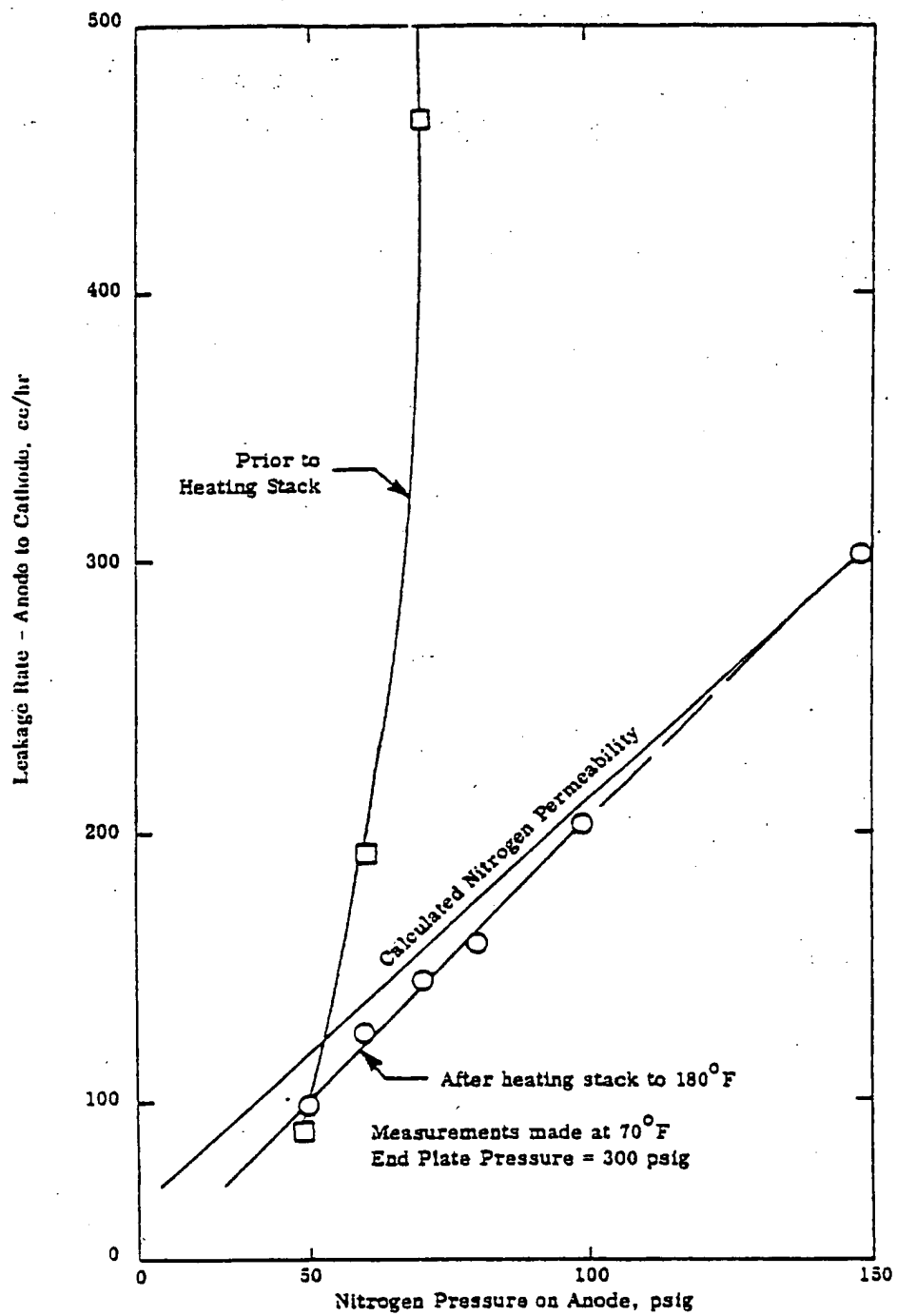
Figure 26.   Results of Leak Test DOE-5

The cell was also checked for overboard leakage by connecting the anode to the cathode and then pressurizing the system with nitrogen at room temperature. The leakage was calculated from measurements of pressure decay, using the perfect gas law and the known system volume.

Figure 27 shows the leakage rate using nitrogen as the pressurizing fluid. The leakage at 100 psia was about 400 cc/hr, considered minimal when contrasted to the hydrogen production rate at 1000 ASF, which is about 1,040,000 cc/hr. The leakage, therefore, amounts to about 0.04% of production rate.

Satisfied that leakage rates were small, the cell was energized at 180°F for gas production runs. Figure 28 shows the operating characteristics. It can be seen that the operating voltage was higher than anticipated. The performance was insensitive to endplate loading in the region of 200 to 400 psig. (A total of 20 hours operation up to 1000 ASF, was accumulated on the single cell stack.)

The cell was disassembled. Sections of the M&E were cut out and run in lab hardware (1/20 Ft^2). It was found that the M&E performance was normal with only about 20 mv loss attributable to contamination. Component tests indicated that the performance loss was most probably due to high contact resistances associated with the collector foil.

DOE-6

To evaluate the location of the contact resistance loss, a 6-cell stack (DOE-6) was assembled with cell No. 1 instrumented with voltage tabs on each cell component.

During the assembly, misalignment between M&E's and the current collectors occurred which resulted in one cell (#3) being shorted. After replacement of the misaligned M&E's, the 6-cell stack was installed in the test facility and heat-soaked at 180°F (by passing hot water through the stack) for >72 hours.

Even with this testing, external and internal leakage was still excessive. The stack was removed from the test facility, disassembled and analyzed. This analysis indicated that force amplifiers would be helpful in achieving reliable seals.

4.6.2   DOE 9, 10 and 11

Three single cell modules were used to determine the effect of adding force amplification to the cell seals.

DIRECT ENERGY CONVERSION PROGRAMS
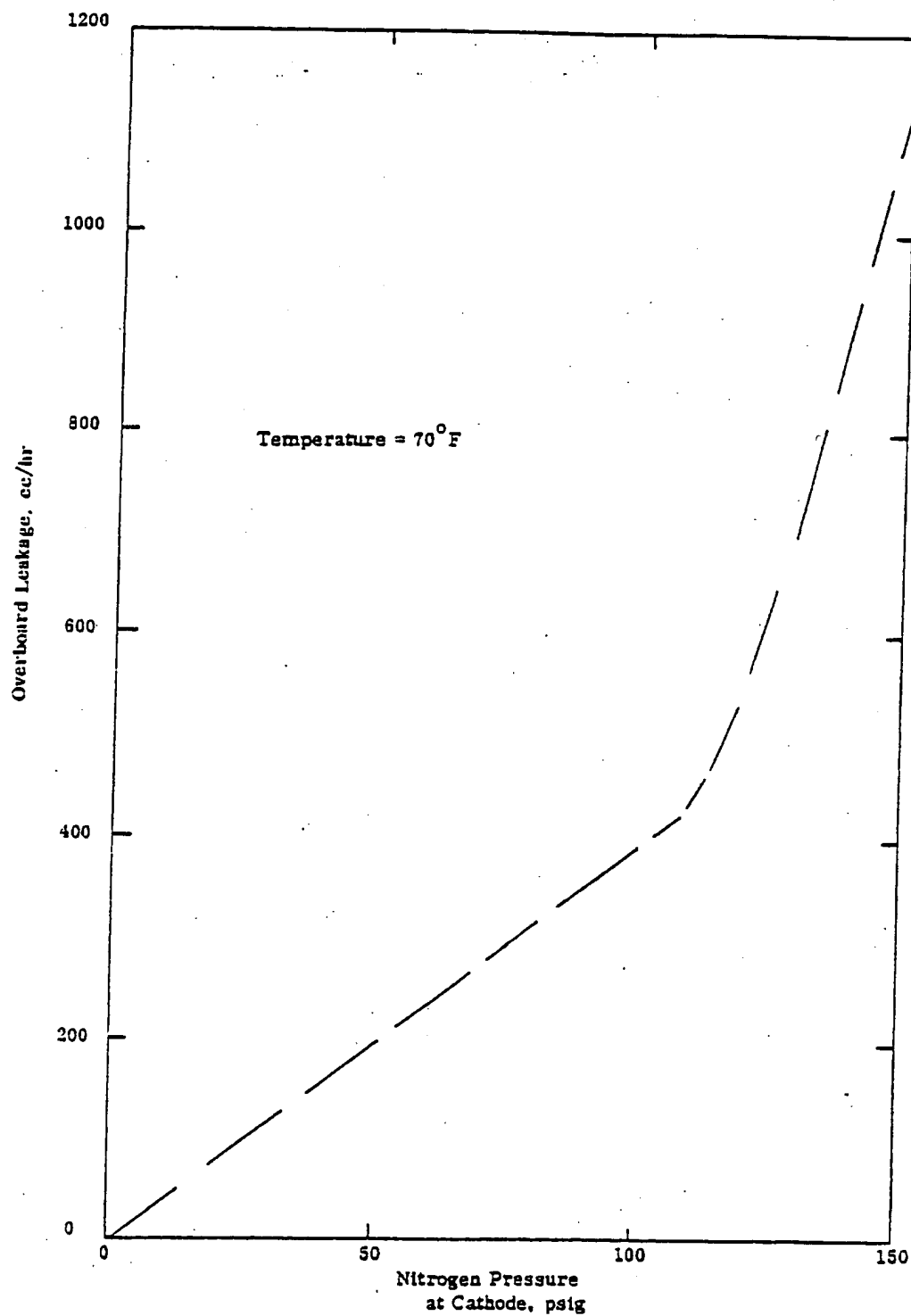
Figure 27.   Results of Overboard Leakage Test

DIRECT ENERGY CONVERSION PROGRAMS
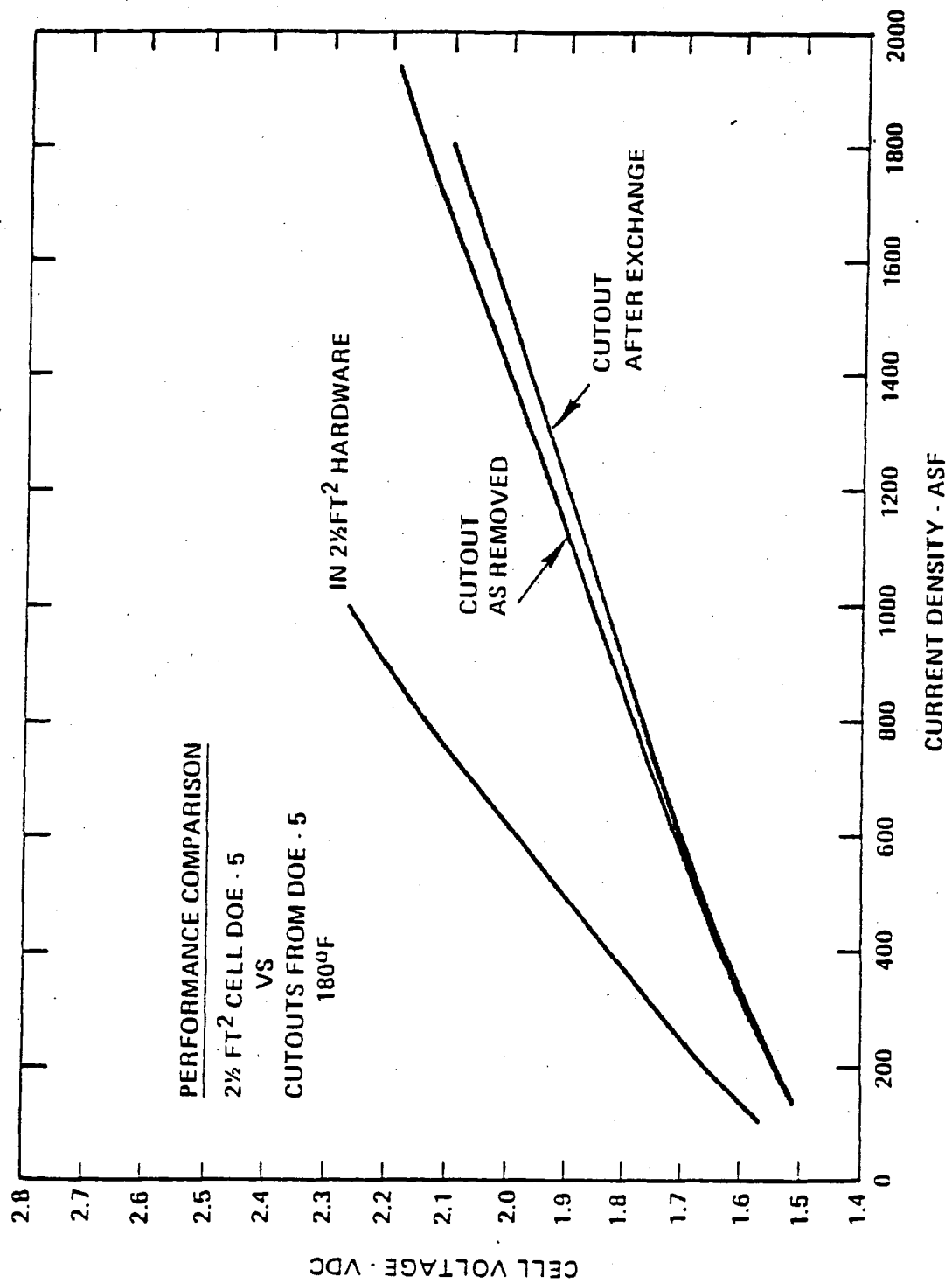
Figure 28. Performance Comparison

48

DOE-9: This buildup contained two new collectors. A standard center collector was used as an oxygen end collector with two sheets of carbon paper used on the non-active hydrogen compartment to provide a flat surface. The hydrogen end collector contained two sheets of carbon paper on the active hydrogen side, the other side being the standard flat O_2 end surface. At room temperature and 300 psi on the pneumatic endplates, the cell was leak tight only to 10 psi of nitrogen pressure applied to the anode chamber. Above this point, cell leaked slightly from anode to cathode (see Figure 29).

DOE-10: This buildup used the same components as DOE-9, with the addition of 2-mil thick titanium rings in the internal port regions, and a 2-mil KEL-F strip around the periphery of the active hydrogen compartment outboard of the manifolds. These components were added to increase the compression force in the manifolds and around the collector for better sealing. This cell maintained a seal up to 50 psi, a definite improvement over the sealing of DOE-9.

DOE-11: The same basic configuration used for DOE-10 was employed for the DOE-11 buildup, but with a new membrane and electrode assembly and the thickness of the Ti-rings and the KEL-F strip increased to 3 mils and 4 mils, respectively. DOE-11 exhibited the same leakage characteristics as DOE-10, indicating that no substantial benefit was gained from thicker force amplifiers. DOE-11 was installed in the test facility and heated by circulating hot water up to 250-275°F to allow membrane creep for sealing. Subsequent leak checks showed no abnormal internal or external leakage at 50 psi. Operational evaluation of DOE-11 commenced on December 2, 1978, with initial operation showing performance considerably better than that exhibited by previous 2 1/2 Ft^2 cells, being 1.97 volts at 1000 ASF and 165°F.

These tests showed the desirability of reducing the contact area in seal regions to amplify the contact pressure, thus improving the seal. It was planned to incorporate molded-in pressure amplifying port rings and edge rings into the collector mold when sufficient collectors were on hand to allow rework of the mold.

4.6.3   Performance Improvement with Cell Development

The chronological development of the last three operating 2.5 Ft^2 stacks is worthy of mention. Figure 30 shows the performance at 180°F for stacks DOE-8, DOE-11, and DOE-12.

Two cells from DOE-8 exhibited high voltage entirely attributable to high cell resistance. Three possible origins of this high resistance were postulated:

49
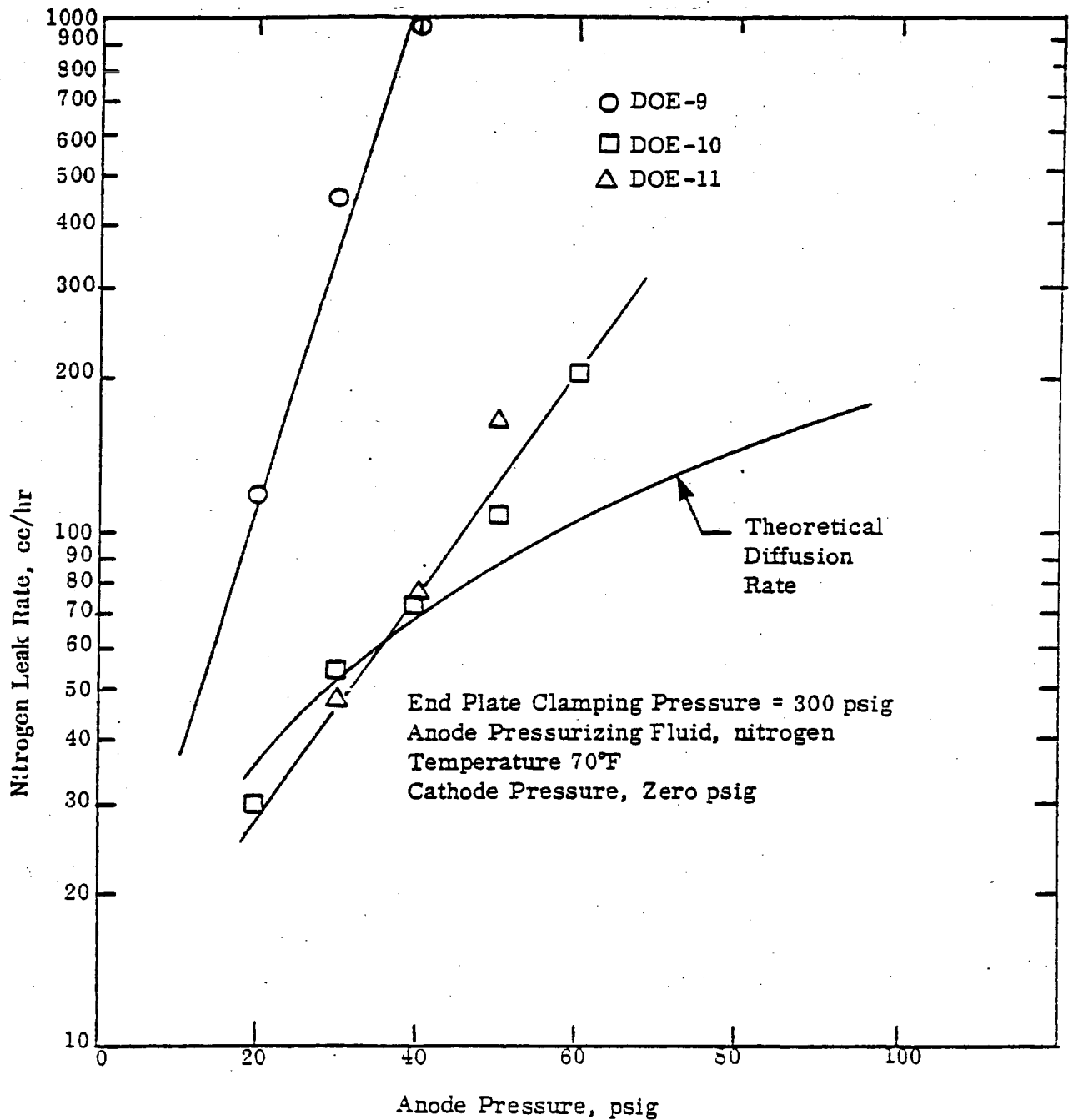
Figure 29.   Leakage from Anode to Cathode Chambers
for Various 2.5 Ft^2 Single Cells

		m	p
		$\underline{\text{ohm Ft}^2}$	$\underline{\text{ohm Ft}^2}$
○	DOE-8 Cell 1	7.2 E-4	8.5 E-4
☐	DOE-8 Cell 2	6.8 E-4	8.3 E-4
△	DOE-11	4.7 E-4	4.1 E-4
⬡	DOE-12	4.0 E-4	3.3 E-4
⬢	DOE-12 After High J Operation	-	-

m is the slope of the linear portion of polarization curve

p is measured cell resistance, 1000 Hz bridge
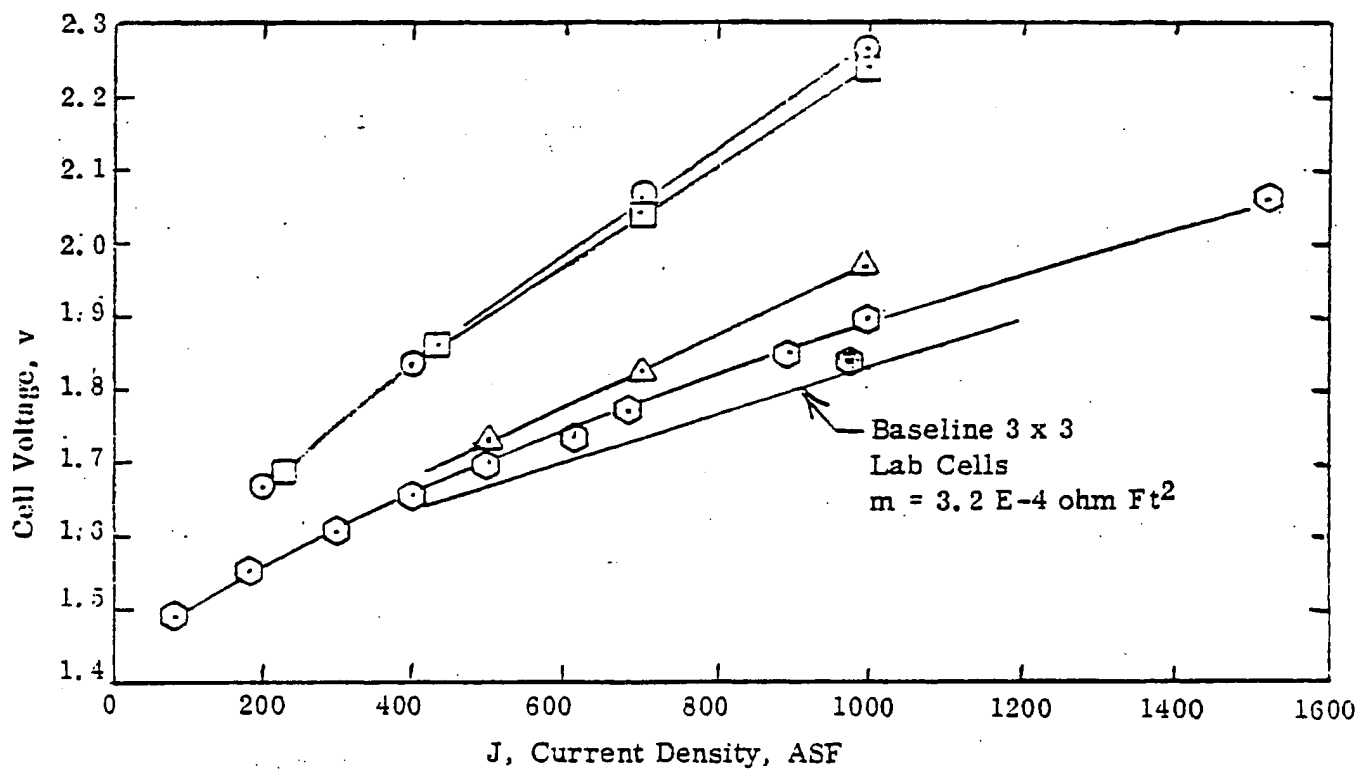
Figure 30. History of Performance Improvements for 2.5 Ft^2 Water Electrolyzers Operating at 170 to 180°F

a)   Inadequate thickness of the cathode support.   The
cathode support is afforded by porous carbon sheet.   In DOE-8,
only one sheet of carbon paper 12 mils thick was used in a cath-
ode chamber 17 mils deep.   This could have resulted in part of
the M and E being inadequately supported, and thus in only a por-
tion of the cell carrying current.

Referring to Figure 31, a too thin carbon support is
shown diagrammatically.   The anode end collector tends to deflect
under the influence of pneumatic endplate pressure to clamp the
M and E.   However, if the collector is not entirely compliant,
a region of M and E near the outer periphery of the cathode
chamber will not be supported.   It is therefore better to "over-
fill" the cathode chamber with cathode support and allow the sup-
port material to compress into the cathode chamber and support
the M and E over its entire area.   Of course, too thick a layer
will prevent the collector edges from sealing and care must be
exercised to optimize the support thickness.

End Plate Pressure

Anode End Collector
Contact

M and E

Carbon Support   Unsupport

Cathode End Collector

Cathode Chamber depth = 17 mil
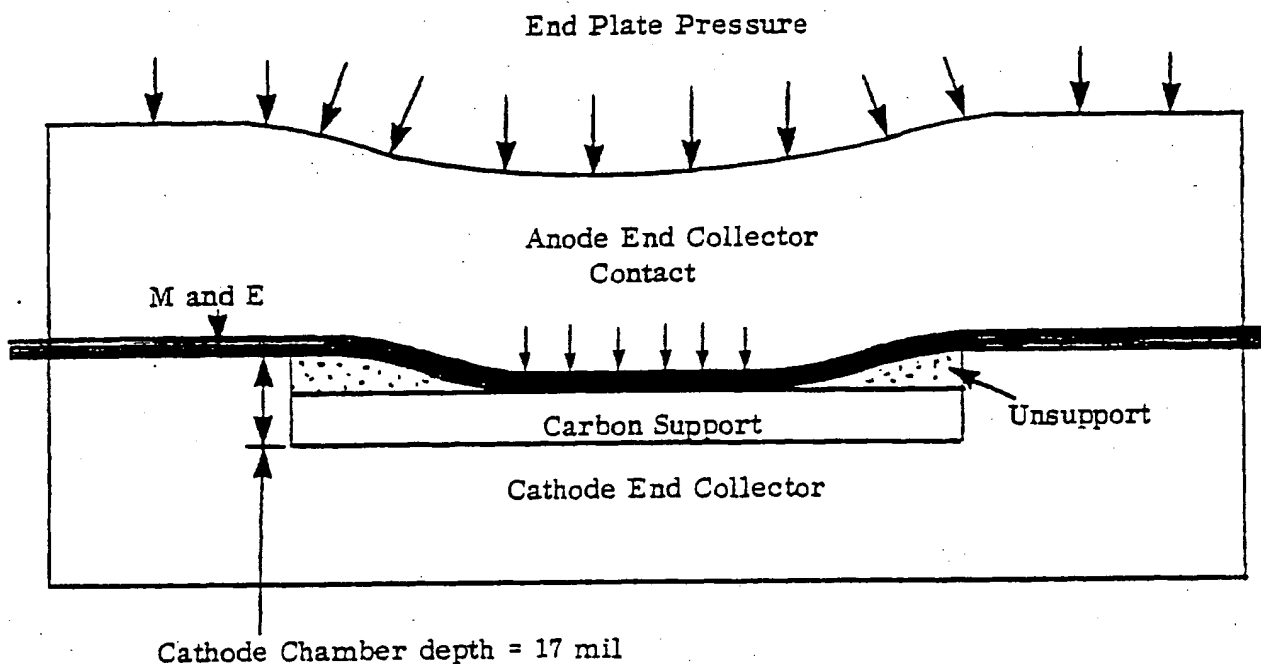
Figure 31.   Possible Unsupported Regions in a Cell Deficient
in Carbon Support

b) <u>Membrane Contamination</u>. If the water in the anode recirculating loop is impure, the membrane will lose conductivity. Separate tests on small laboratory cells using water from the DOE-8 recirculating loop showed performance impairment which was subsequently alleviated by using pure feed water. The water in DOE-8, then, was indeed impure enough to cause performance problems. Some contamination could have come from a water filter downstream of the main deionizer. Chemical analysis showed that the filter material was replaced with one having much lower cation content.

c) <u>Electrical Contact Resistance</u>. Some molded collectors have exhibited a high electrical contact resistance between the carbon/phenolic and the titanium foil molded to it.

After disassembly of DOE-8, each collector was installed into the 1000 Hz 2.5 Ft^2 resistance fixture described elsewhere. By applying voltage tabs on each component, the contact resistivity was measured and found to be high:

DOE-8 Cell 1 (Collector No. 105) p = 3E-4 ohm Ft^2
DOE-8 Cell 2 (Collector No. 111) p = 5E-4 ohm Ft^2

These measurements were made at room temperature with a 300 psi mechanical load.

These measurements led to the decision to mold some collector plates using pre-platinized Ti foil.

When DOE-8 was disassembled, it was found that wherever unprotected carbon contacted bare solid polymer electrolyte on the anode side, the carbon structure was severely corroded due to the high anodic potentials in the presence of oxygen and water. In running small lab cells allowing bare carbon to contact the membrane has been successful as long as water and oxygen are totally excluded from the seal area. In the case of the larger cells, the sealing was not yet perfected and, in unsealed areas, water and oxygen combine with anodic potential to cause corrosion. An interim solution was to protect the anode side seals with Teflon to eliminate membrane contact with the carbon.

In cell DOE-11, the following corrective actions were taken:

1) Two layers of carbon paper, a total of .024 inch thick were used as support in the .017 inch deep cathode chamber. This was done to provide better contact between the M and E and collectors, and to decrease bending of the collectors resulting in better seal contact.

2) The anode collector was chosen with a pre-platin-
   ized foil to eliminate contact resistance.

3) The bleed water rate from the anode loop was in-
   creased so that the loop would run cleaner. It
   was also necessary to relocate the bleed to a
   point downstream of the circulating pump for
   cleaner operation.

The bare carbon collector was not protected from the
solid polymer electrolyte. It was thought that better sealing
would result from action No. 1 above, thus preventing corrosion.

As seen in Figure 30, the performance of DOE-11 was
far superior to that of DOE-8. The voltage increase above base-
line was due to increased resistance. Here again, however,
severe corrosion occurred on the anode side of the carbon collec-
tor in the sealing area.

4.6.4   DOE-12

In DOE-12, all previous corrective actions were used.
In addition, the exposed carbon seal faces on the anodic side of
the solid polymer electrolyte were protected with 3-mil Teflon
tape having a silicone pressure sensitive adhesive. Seal pres-
sure amplifiers were not used. Instead, some reliance was put
on the gasketing qualities of the Teflon tape to effect a good
seal.

As seen in Figure 30, DOE-12 shows the best perfor-
mance, almost to baseline. Indeed, after operating briefly at
1500 ASF and returning to 1000 ASF, baseline performance was
achieved.

Subsequent to operation, leak checks showed leakage
occurring at 60 psi, which could not be reduced by clamping the
endplates as high as 500 psi. The cell was disassembled and
the M and E bubble checked at 4 psi.

It was determined that the M and E had a cross-mem-
brane leak in the active area. Microscopic examination revealed
a small glassy particle imbedded in the membrane, probably in-
cluded in the catalyst when it was applied to the membrane.
Also, the collectors were cracked in the region where excessively
thick voltage probes were inserted between the collector and
endplate and the collector and fluid plate.

The following corrective action was taken based on the
experience of DOE-12.

54

Stress-concentrating components such as the excessively thick voltage probes between the collector and rigid stack hardware will be avoided, since they can crack the collector.

● Teflon tape was applied to the bare carbon surfaces having anodic potential to prevent corrosion. This practice will be continued until an electrically non-conductive film can be applied directly in the molding process.

● M and E inspection was improved to discover and remove foreign objects before assembly into stacks. This is being done by detailed microscopic examination before assembly followed by removal of any particles found and and separate leak-checks of M and E's.

● M and E manufacture was improved to eliminate foreign objects in the catalyst. This has been accomplished by a change in catalyst preparation which eliminates the present step currently suspected of causing the problem.

4.6.5   DOE-13

Another single cell, DOE-13, was then assembled. The purpose of this buildup was to demonstrate high-pressure sealing. To achieve this, the following configurations and techniques were used:

● Anodic areas were protected by Teflon tape as in DOE-12, which has demonstrated zero corrosion.

● Three-mil thick force amplifiers were installed in all manifold port areas.

● The M and E was thoroughly inspected for foreign matter inclusion.

● The M and E was separately leak-checked with 4 psig nitrogen on one side and water at atmospheric pressure on the opposite side, to detect bubbles.

● The cell assembly was cold-pressure-checked to 40 psig to verify initial assembly integrity. The assembly was then heated to 250°F at the endplate pressure of 500 psi over a weekend. This was done to allow the membrane to creep and seal.

55

The oxygen side collector foil was not platinized
before molding the collector. The collector was
resistance-checked and found to be satisfactory.

After assembly and heat treating, DOE-13 was pressure-
checked up to a chosen limit of 150 psig: no leakage was demon-
strated.

The cell was then operated with the following results:

- Cell voltage was 2V at 1000 ASF, 180°F. This is
  about .15 volts higher than baseline.

- Water flow into the anode was found to be restricted
  to 0.02 gpm versus a desired rate of 0.12 gpm, limit-
  ing operation to current densities below 1350 ASF.
  The restriction was later found to be caused by mem-
  brane creep into the anode internal manifold slots.
  Corrective action to avoid this condition in subse-
  quent cells was taken.

- Excellent sealing characteristics. With the endplate
  clamped at 400 psig, 370 psig of N_2 gas at the anode
  was sealed for 10 minutes against an ambient pressure
  cathode. Breakthrough leakage was experienced at
  395 psig, only 5 psi below endplate pressure.

- Zero overboard leakage was demonstrated at 300 psi.
  Testing above 300 psi was not done.

- After breakthrough leakage at 395 psig, the unit was
  resealed at 200 psi and kept the seal until 395 psi
  was again imposed.

Cell DOE-13, therefore, showed that excellent sealing
can be achieved with high temperature (250°F), high endplate
clamping (500 psi) over an extended period of time (60 hours).
However, sealing under these conditions produces the undesirable
effect of flow restriction due to membrane creep into manifold
slots. By reinforcing the span over the slots, the creep could
possibly be avoided.

4.6.6   Cell DOE-14

Cell DOE-14 was constructed with an anode support in
the manifold slot area which was reinforced with perforated foil.
The cell was heat-soaked at 220°F, with endplates clamped to 300
psi for 60 hours (weekend). Water flow was unrestricted, indi-
cating the effectiveness of the added support. The cell was
then operated and exhibited very poor performance, indicating
that the cell had been fabricated with anode and cathode catalyst
reversed. This was later verified at disassembly. Leakage test-

56

ing demonstrated a good seal up to 280 psig, with endplates at 300 psig, verifying that a good seal can be achieved at moderate clamping pressures.

4.6.7 Cell DOE-15

Cell DOE-15 was constructed similarly to DOE-14, and with proper M and E installation. After only 16 hours of soaking at 220°F, with 300 psi pressure on the endplates, the cell was leak-tight up to 150 psi, at which point, leak-checking was terminated and testing begun.

At 1000 ASF and 189°F, the voltage was 2.08V. After running at 2000 ASF and returning to 1000 ASF, the voltage improved to 1.89V. The cell was shut down for facility work, and during leak checks prior to restart, a large cross-cell leak was noticed. After disassembly, a slit was found in the membrane near the seal area. This also corresponded to a region where a mechanical interference was caused between the carbon paper support and the edge of the oxygen manifold cover. Action was taken to:

- Cut back the carbon paper to avoid the mechanical interference.

- Discontinue use of the RTV assembly aide, using water and surface tension forces to hold the carbon in place.

4.6.8 DOE-16

DOE-16 was a single cell using all the corrective actions previously devised. It showed good sealing to 100 psi with 300 psi endplates immediately after assembly.

The above test showed that the scale-up development and corrective actions have led to the achievement of good cell sealing on single-cell buildups. The next step was to demonstrate sealing in multi-cell stacks.

4.6.9 DOE-17

Cells in this 6-cell stack contained previously developed components and configurations to insure integrity and sealing, namely:

- Teflon-taped anode side collectors - for corrosion resistance.

- Force amplifying rings at internal ports - for sealing.

57

- Titanium foil supports at internal manifold slots (anode side) - to prevent SPE creep.

An overnight heat soak at 250°F with endplates at 400 psi, was sufficient to achieve an internal and external seal.

The seals were checked to 100 psi, which was sufficient for initial stack operation.

Figure 32 shows the performance of each cell in the stack. It was apparent that there was a spread in voltage of about 100 millivolts at practical current densities. Cell numbers 4 and 5 showed the best performance. These cells contained collectors with pre-platinized titanium foils on the anode side of the collectors. The conclusion, based on this test, was that the effort to manufacture this type of collector should be continued and compared to non-platinized types on a statistical basis.

At 800 ASF, all cell voltages rose out of proportion in comparison to laboratory cells. It was determined that phenolic collectors in contact with the hydrogen side of the solid polymer electrolyte cause voltage to increase in this current density region. This is caused by the adsorption of oxygenated carbon compounds on the catalyst, masking the electrochemical reaction. It was also well documented that the chemical species can be desorbed by running the cell to about 2000 ASF, thereby polarizing the hydrogen electrode to lower voltages.

Operation at higher current density was precluded due to the following factors:

- High cathode piping pressure drop, causing the back pressure to increase above desired limits, and

- Anode flow restriction caused by the 250°F/400 psi heat soak to seal the stack.

The cathode back pressure problem was alleviated by substituting 1/2 inch diameter tubing in place of 1/4 inch. However, operation was limited to 1000 ASF by the flow restriction which decreased the anode water flow from a desired 1.0 gpm to 0.4 gpm (at 30 psi pumphead), a level which is not sufficient to cool the stack properly at elevated current density.

DOE 17 was shut down and installed into the new 200 kW test facility for use as a checkout vehicle for that new facility.

Due to leakage in the pneumatic end domes, the unit had no clamping pressure other than the physical weight of the endplate during the month-long period of assembly into the 200 kW facility, and completion of the system assembly.

58

Pressure Conditions

End Plate:	406 psig
Anode Out:	127–135 psig
Anode ΔP:	31–34.3 psig
Anode In:	158–169.3 psig
Cathode Out:	13.0–99.6 psig
Cathode ΔP	0.2–10.0 psig
Cathode In:	13.2–109.6 psig

Cell Voltage, v

Current Density, ASF

O	Cell 1
□	Cell 2
△	Cell 3
▲	Cell 4
◇	Cell 5
×	Cell 6
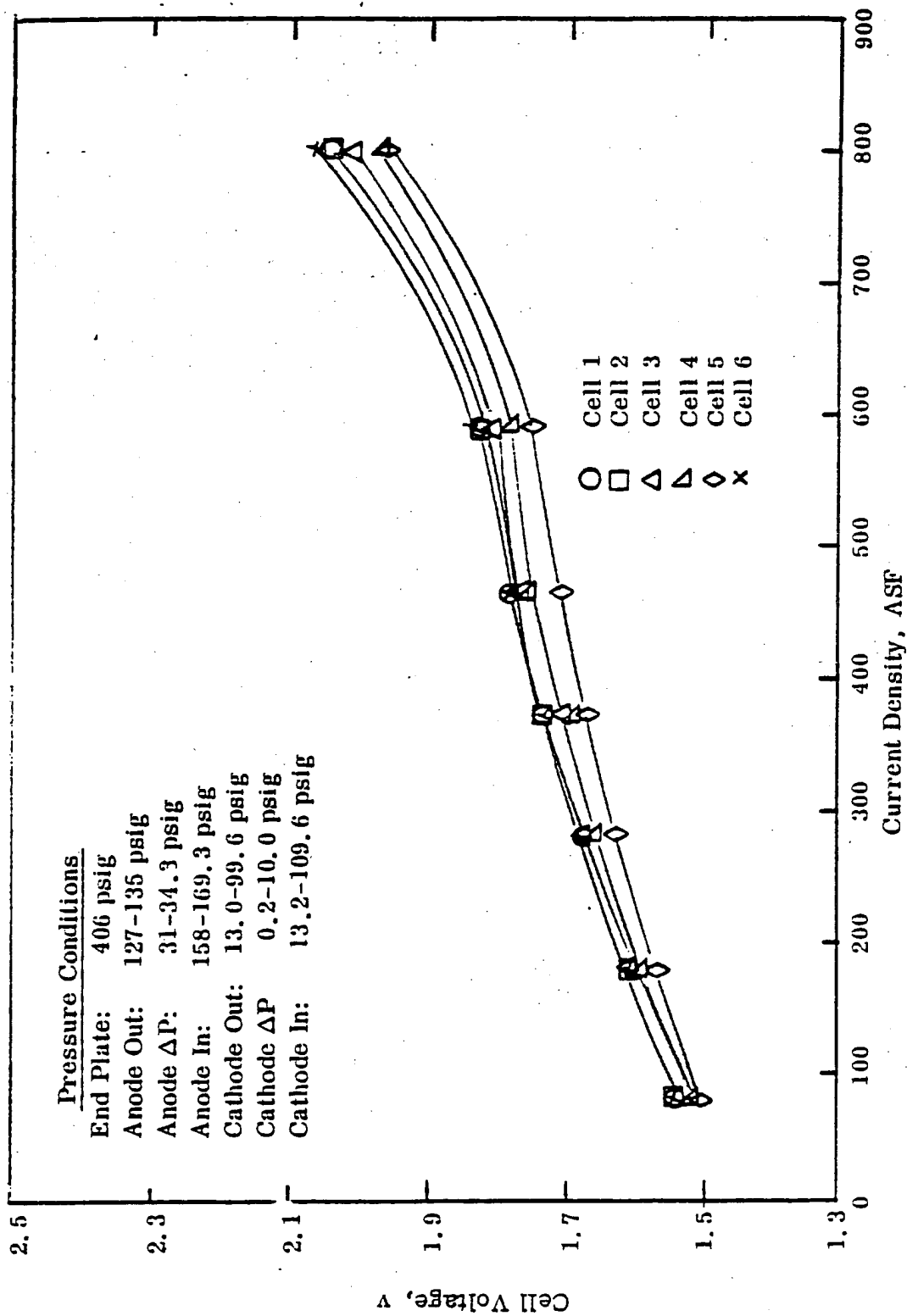
Figure 32. Performance of (6) Cell Stack (DOE–17) at 187°F

59

During the subsequent initial operation of the 200 kW system, the module voltage was considerably higher than previously experienced in the 50 kW facility and was characterized by anode exhaust temperatures much higher than normal for the water flow rate provided. Leak-checks indicated excessive H_2-to-O_2 side leakage, but normal O_2-to-H_2 side leakage, a condition which indicates a seal leakage as distinguished from a through-membrane leak. Operation in the 200 kW system was with a hydrogen overpressure (the direction of the seal leakage) whereas previous operation in the 50 kW facility was with an oxygen overpressure, at which condition no seal leakage was apparent.

Disassembly of the module showed:

- Many signs of high heat as a result of hydrogen-to-oxygen side leakage, including severe oxidation of the collectors in the oxygen outlet manifold area, surface cracks in the collector border area near the oxygen outlet manifold, and discoloration on the oxygen outlet cover plates.

- There was no evidence of through-membrane leakage, substantiated by leak-check of the individual cells. This confirmed leakage was seal-related.

- Misalignment of the perforated foil anode support in cell No. 6, and a number of high heat spots on the same anode support, particularly at the welded seams. This indicated poor uniformity of contact, possibly aggrevated by the misalignment.

- Operation of a 3" x 3" cutout of cell No. 1 from DOE-17 showed performance behavior typical of phenolic contamination.

The DOE-17 test experience:

- Emphasized the need for improved internal sealing. Mold modifications to incorporate force amplifiers to improve both internal and external sealing characteristics.

- Emphasized the need to avoid phenolic contamination by utilizing a non-contaminating binder for the carbon in the molded collectors. No further phenolic collectors were molded and all future full-size cell testing utilized the fluoropolymer/carbon collectors developed under the parallel technology development program.

60

- Emphasized the need to improve the pneumatic endplate sealing. Improved sealing though softer, more compliant rubber seals and a compatible lubricant was subsequently achieved.

- Emphasized the need for reduced anode side pressure drop to allow more water flow. Introduction of the stiffer porous plate anode support, was made to mitigate this problem.

4.6.10   DOE-18

Twelve-cell module DOE-18 was comprised of two 6-cell stacks in parallel. Each cell had preplatinized foils on the phenolic collectors. After a number of heat-soak attempts, half-stack "A" exhibited unacceptable internal leakage. Half-stack "A" was isolated from the fluid system and electrical bus. Half-stack "B" passed all pre-operational checks, and was subsequently operated. These six cells were operated for 113 hours at 1000 ASF and 165°F with an average voltage level of 2.1 VDC.

This stack demonstrated improved water flow characteristics over previous stacks, due to lower pressure heat-soaks for sealing. It was therefore possible to operate at 2000 ASF to investigate the existence of phenolic contaminants. The stack was operated with excursions to 2000 ASF, during which time cell B-1 was monitored on an x-y plotter, depicting current density and voltage. As the cell ran at 2000 ASF, the voltage dropped from 2.6 volt to 2.2 volt in one minute. A subsequent setting of 1000 ASF resulted in the cell operating at 1.85 V, equal to a "baseline" cell. Voltage slowly climbed while at 1000 ASF. This behavior is characteristic of phenolic-contaminated cells. The testing did show that, with pre-platinized protector foils, the goal performance could be reached. It reinforced the need to develop the fluoropolymer-bonded collectors, which do not contaminate the catalyst.

During the operational period, several automatic shutdowns occurred which were caused by control "glitches". Subsequent to one such automatic shutdown, excessive external leakage in half-stack "B" was indicated. The module was removed from the test system and disassembled.

Disassembly showed that internal leakage in half-stack "A" had been caused by an imbedded crystalline particle which had punctured the membrane. External leakage in half-stack "B" resulted from three cracked graphite collectors. A 1/2" circular membrane punch-out from a manifold hole was found in the vicinity of the collector cracks. A die with positive membrane punch-out removal was designed and procured to eliminate this problem.

61

4.6.11   DOE-19

Module DOE-19 was a single-cell module using carbon/ fluoropolymer current collectors. The purpose of the test was to demonstrate improved performance with non-contaminating collectors. The anode support was the standard perforated titanium foil, and all other cell components were standard.

The performance shown in Figure 33 was 150 to 200 mV better than steady state performance demonstrated on previous cells (with phenolic collectors) and very stable throughout the 137-hour test. There was no evidence of electrode contamination.

Although improved due to elimination of the phenolic contamination, the 130 mV above baseline performance of DOE-19 was attributed to a cell resistance approximately 60 micro-ohms above normal.

The oxygen side flow drop characteristics of DOE-19 were consistent with previous cells utilizing perforated foil anode support, i.e., marginally adequate water flow for operation at 1000 ASF but insufficient flow for extended operation at 1500-2000 ASF without very high outlet temperatures and potential membrane drying.

After 137 hours, DOE-19 was removed from test to incorporate a porous titanium plate anode support for enhanced water flow.

4.6.12   DOE-20

This was a single-cell module utilizing the fluoropolymer collectors from DOE-19, but incorporating a porous titanium plate for anode support. This cell showed excellent anode flow properties; the plate spanned the flowfield gaps without deforming into them, thus leaving the field unobstructed.

This cell had performance identical to DOE-19, indicating that low water flow was probably not the cause for the higher-than-normal resistance of DOE-19. However, performance (Figure 34) was nearly linear up to 2000 ASF. The unit was operated for 462 hours.

4.6.13   DOE-21 through 24

Subsequent to DOE-20, four separate modules employing cells of 2.5 ft^2 active area were operationally evaluated in order to define the cause of high cell resistance. Details of these modules are shown in Table 3. The salient results of these evaluations are summarized below.

62

Single Cell Module S/N DOE-19   (Fluoropolymer Collectors)
2.5 Ft^2 Active Area – Anode Feed
Chamber #4

○— 31.5 Hrs; Testing: 5/31/79; 183.8°F Ave.Anode Temp.

□— 113.5 Hrs; Testing: 6/4/79; 184.6°F Ave.Anode Temp.

Note: Decreasing Cur Dens

PRESSURE RANGE

End Plate   : 300 PSIG
Anode-Out   : 94.5-108.2 PSIG
Anode-△P   : 29.7-30.9 PSI
Anode-In   : 124.2-139.1 PSIG
Cathode-Out : 55.3- 72.0 PSIG
Cathode-△P   :   3.0- 10.0 PSI
Cathode-In   : 58.3- 82.0 PSIG

CELL VOLTAGE VDC

Current Density (ASF)
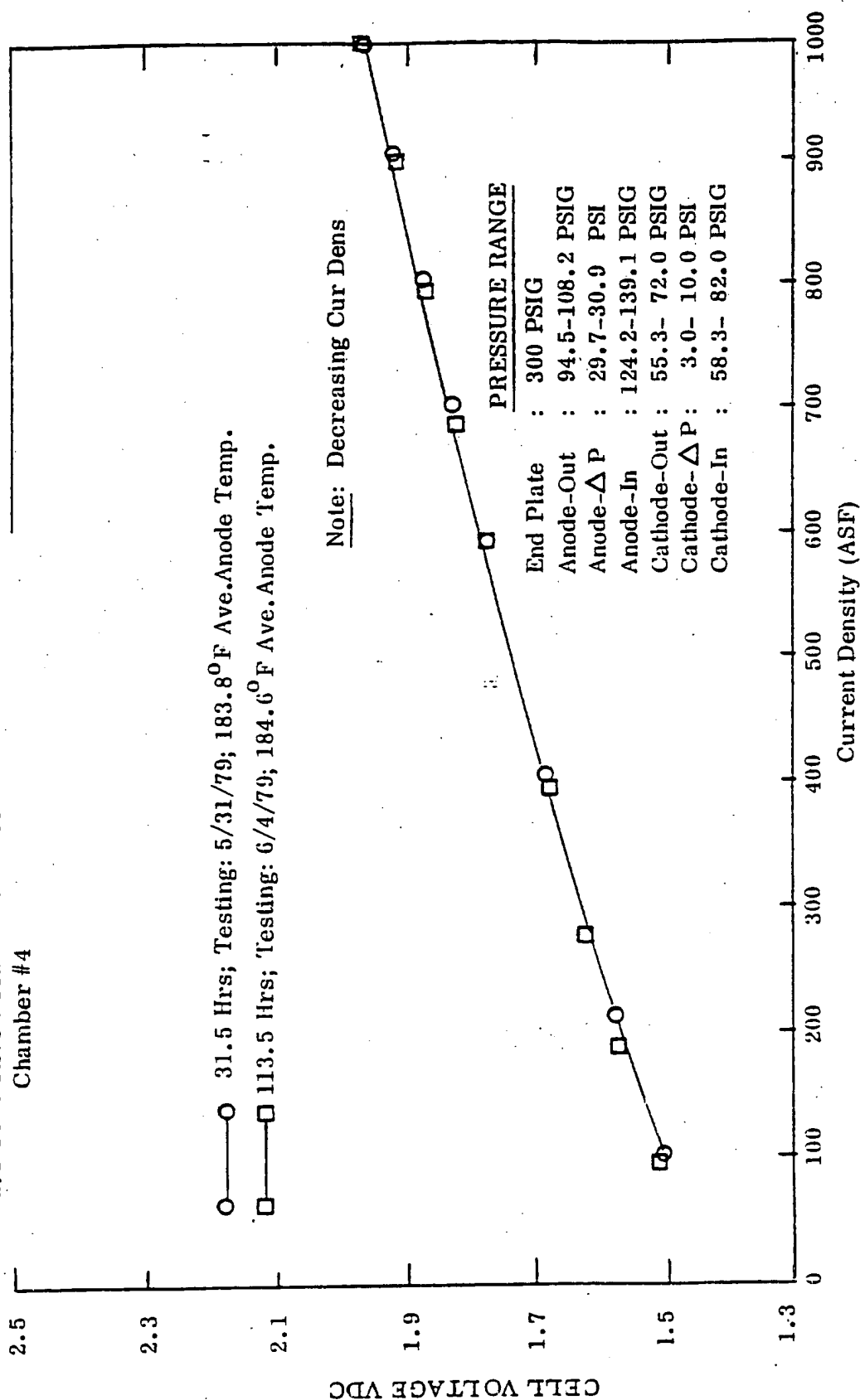
Figure 33. Polarization Characteristics

63

DIRECT ENERGY CONVERSION PROGRAMS

PERFORMANCE CURVE

Module DOE - 20
Single 2.5 Ft^2 Cell
Fluoropolymer/Carbon Collectors
Porous Ti Plate Anode Support

180°F, 100 PSIG
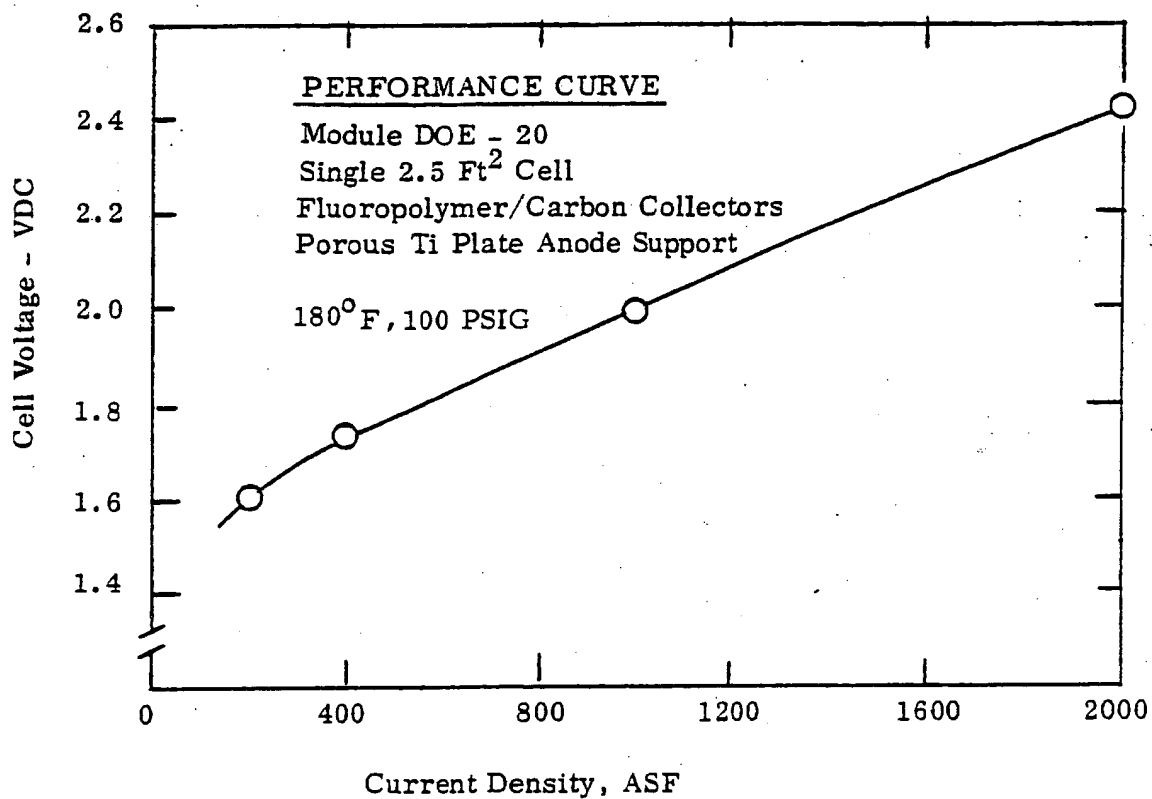
Figure 34.   DOE-20 - Performance

64

TABLE 3. Summary of 2.5 ft² Modules with Kynar/Graphite Current Collectors

General: Anode Support: Porous Titanium Plate.
Cathode Support: (2) Layers Carbon Paper.
DOE-20 - DOE-27 had no Ti Foil on Collector.
Modules with Serial Numbers Higher than DOE-22 had M&E's treated with HNO_3.

Module No.	No. of Cells	Anode Catalyst	Total Operating Time Hrs.	Cathode Overboard Seal Augmentation	Anode Water Flow (70 to 105°F) Nonoperating gpm/Cell	Pressure Drop PSI	Heat Soak to Achieve Seal °F Days	Cell Voltage at ( )ASF and 180°F V	Anode Cathode Teflon Tape
DOE-20	1	E-50	462	None	0.2	25	243 F for 2.5 days	1.99 V (1000 ASF)	
DOE-21	12 (6 per stack)	E-50	163	None	.0088(A) .057(B)	57 57	220°F for 20 days A-Stack Note 1	2.0 V (600 ASF)	
DOE-22	1	E-50	80	None	0.2	25	229°F for 3/4 day	1.97 V (1000 ASF)	
DOE-23	1	E-50	19	None	0.18 (48X) Note 2	24	197°F for 3/4 day	1.96 V (1000 ASF) 155°F	
DOE-24	1	E-50	607	4-mil wire Si glued in place	0.20 (54X) Note 2	20	None for cross-cell or overboard	2.03V (1000 ASF)	(1) layer 10-mil TFE None
DOE-25	6	E-50	1,312	4-mil wire Si glued in place	.417 (112X) Note 2	57	200°F, 3 days cross-cell none for overboard	1.93 to 1.98 (1000 ASF)	(1) layer 10-mil TFE None
DOE-26	1	WE-3	51	4-mil wire Si glued in place	.16 (43X) Note 2	20	None	1.94 (1000 ASF)	(3) layers 3-mil Kynar (2) layer 3-mil Kynar
DOE-27	1	WE-3	297	4-mil wire Si glued in place	.14 (38X) Note 2	20	None	1.89 (1000 ASF)	(1) layer 10-mil TFE (1) layer 3-mil Kynar
DOE-28	1	WE-3	70	Molded-in ridges	.21 (56X) Note 2	20	None	1.84 (1000 ASF)	(1) 3-mil Kynar (1) 3-mil Kynar
DOE-29	12	WE-3	151	Molded-in ridges	.42 (113X) Note 2	30	237 F 16 hr. (None for cross-cell)	1.87 to 1.93 (1000 ASF)	(1) 3-mil Kynar (1) 3-mil Kynar
DOE-30	12	WE-3	30	Molded-in ridges 4 mil	.34 (61X) during operation	25	237F 16 hr Some leak persisted	1.90 V (av), 1.82 V to 1.99 V 1000 ASF	(1) 3-mil FEP none on cathode
DOE-31	12	WE-3	950	Molded-in ridges 4-mil plus bead of Si glue			238F 16 hr	1.85 V (av), 200F 1.77 V to 1.94 V 1000 ASF	(1) 3-mil FEP none on cathode
DOE-32	30 Including 11 cells from DOE-31	WE-3	734	Molded in 4-mil ridge plus bead of Si glue	4.6 (41) during operation	48	238F 16 hr	1.85 V (av) 196 F 1.79 V to 2.06 V 1000 ASF	(1) 3-mil FEP none on cathode
DOE-33	60 (30 cells in addition to DOE-32	WE-3	705	Molded-in 4-mil ridges plus bead of Si glue	9.2 (41) during operation	42.6	238F 16 hr.	1.30 V (av) 205F low ASF 700 hours	(1) 3-mil FEP none on cathode
DOE-34 (Single edge bus)	12	WE-3	.1014	Molded-in 4-mil ridges plus bead of Si glue	3.3 (74)	57	190F 16 hr.	1.93 V (av) 1000 ASF 150 hr.	(1) 3-mil FEP none on cathode

Note 1 Both stacks A and B sealed cross-cell
Only stack A sealed overboard

Note 2 At 2500 amp (1000 ASF) water electrolyzed
is .00272 gpm
Cell Stoich.

65

Sealing

Modules-with cells containing force amplifiers in the manifold ports, but none in the overboard seal areas-readily achieved internal (H_2-to-O_2) sealing. Heat-soaking for prolonged periods up to 250°F was required to achieve external seals.

Overboard seal force amplifiers were simulated in modules DOE-24 and DOE-25 through application of a thin bead of silicone glue along the hydrogen seal area of the collector, about 0.25 inch in from the edge. After the solvent evaporated, a 4-mil wire was laid up on the glue. With this arrangement, single-cell DOE-24 sealed internally and externally up to 100 psi without a heat-soak using an endplate clamping pressure of 300 psi.

Multi-cell stack DOE-25 sealed overboard prior to a heat-soak, but leaked internally. This was probably due to the larger total overboard seal stack-up (six, 4-mil-thick seals at the overboard region vs. six, 2-mil-thick seals at the manifold ports). However, the stack sealed after a weekend at 200°F. These tests illustrated that the force amplifying ridges are effective, and that when the heights of the porthole ridges and overboard ridges are equal, minimal heat-soaking will be required for sealing both internally and externally.

Anode Water Flow

Cells using the 1-mil perforated titanium foil as anode support achieved only about 2 to 15 times theoretical electrolyzed water for 1000 ASF operation, compared to the level of 30 to 70 times necessary to modulate temperature at that current density. For this reason, the cells in DOE-21 could only achieve 600 ASF operation. Cells using porous titanium plates provided water flow rates up to 112 times theoretical water and could achieve current densities in excess of 1000 ASF. Porous titanium supports did not deflect into the grooved anode side of the collector and was more effective in attaining high anode water flow compared to perforated foil.

Performance

As the development of modules DOE-20 through DOE-22 progressed, diagnostic tests of the M&E from DOE-19 indicated that performance loss was attributable to catalyst contamination. Cell performance could be brought back to baseline only by treating the M&E with dilute nitric acid. Therefore, modules from DOE-23 and onward contained M&E's treated with nitric acid. Although some performance improvement was made with nitric acid treatment, some deviation from baseline still exists. This deviation was attributed to contact resistance. In the case of

DOE-24, a voltage probe was installed on the porous titanium plate. As shown in Figure 35, the voltage from collector to collector was 2.02 volts (at 1000 ASF). The voltage drop from oxygen collector to the porous plate accounted for 150 mV, bringing the net cell voltage almost to baseline.

Plotting cell resistance for five cells against temperature (Figure 36) revealed that the difference between the ideal (expected) resistance and the actual resistance was fairly constant with temperature. The only types of resistance which would be constant over this temperature range are metallic resistance or contact resistance, as distinguished from ionic (membrane) resistance. Since the metal components were thin, they had small resistance and thus the major effect was most probably contact resistance.

Various resistances measured in the full-size 2.5 ft^2 fixture are listed in Table 4.

TABLE 4

COMPONENT RESISTANCES MEASURED IN 2.5 FT^2 RESISTANCE
FIXTURE WITH 50 AMP 1000 Hz BRIDGE

	R ohm-Ft^2 x 10^4	Voltage Drop at 1000 ASF, mV
Contact Between Carbon Paper and Collector	.55	55
Contact Between 2 Carbon Papers	.30	30
Resistance of Porous Ti Support	.05	5
Contact Between Porous Ti and Collector	.35	35
		125

There was considerable contact resistance between supports and collectors which was not present in smaller laboratory cells.
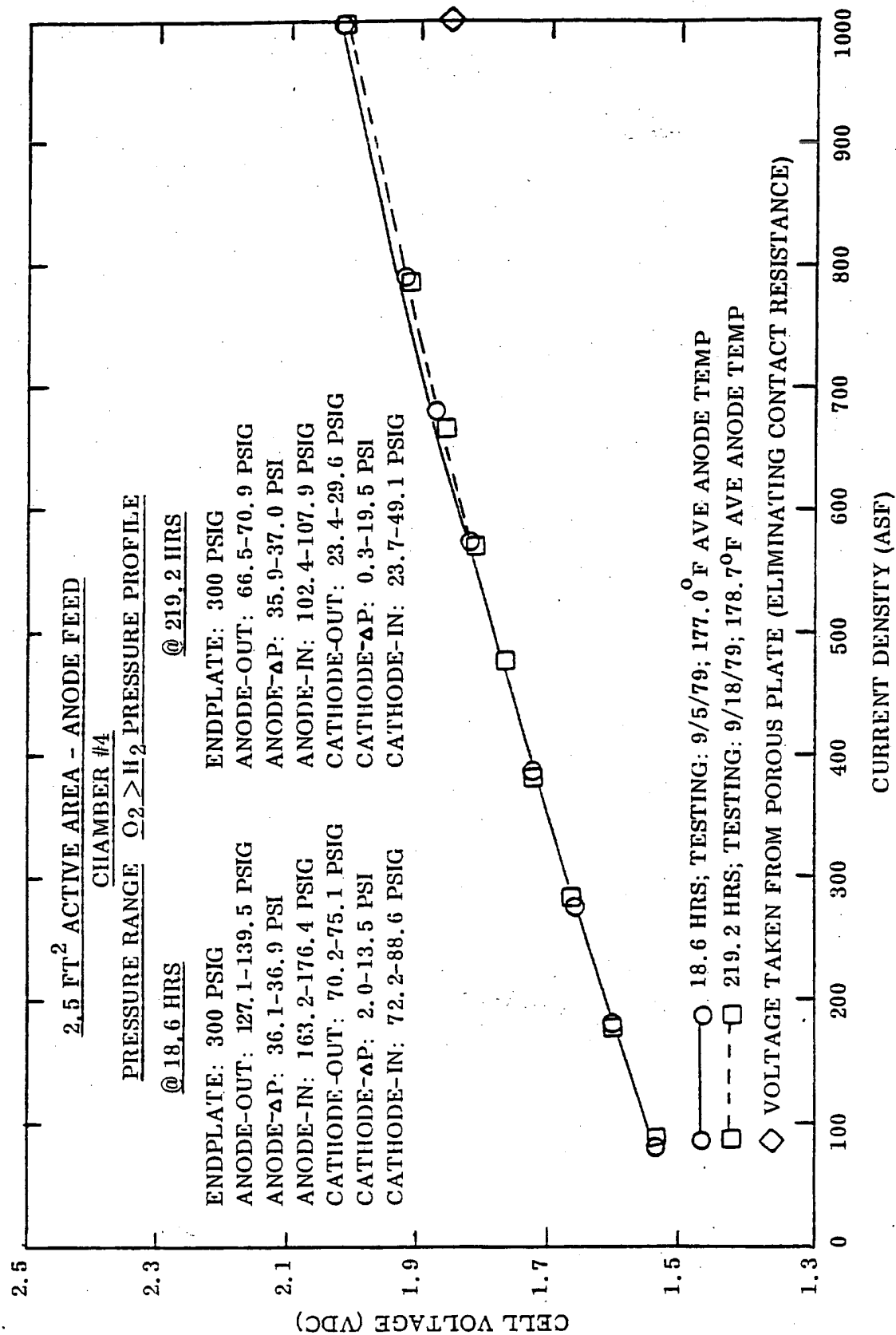
Figure 35. Performance of DOE-24

2.5 FT^2 ACTIVE AREA - ANODE FEED
CHAMBER #4

PRESSURE RANGE O$_2$ > H$_2$ PRESSURE PROFILE

@18.6 HRS

ENDPLATE: 300 PSIG
ANODE-OUT: 127.1-139.5 PSIG
ANODE-ΔP: 36.1-36.9 PSI
ANODE-IN: 163.2-176.4 PSIG
CATHODE-OUT: 70.2-75.1 PSIG
CATHODE-ΔP: 2.0-13.5 PSI
CATHODE-IN: 72.2-88.6 PSIG

@219.2 HRS

ENDPLATE: 300 PSIG
ANODE-OUT: 66.5-70.9 PSIG
ANODE-ΔP: 35.9-37.0 PSI
ANODE-IN: 102.4-107.9 PSIG
CATHODE-OUT: 23.4-29.6 PSIG
CATHODE-ΔP: 0.3-19.5 PSI
CATHODE-IN: 23.7-49.1 PSIG

○—— 18.6 HRS; TESTING: 9/5/79; 177.0°F AVE ANODE TEMP
□--- 219.2 HRS; TESTING: 9/18/79; 178.7°F AVE ANODE TEMP
◇ VOLTAGE TAKEN FROM POROUS PLATE (ELIMINATING CONTACT RESISTANCE)

CELL VOLTAGE (VDC)

CURRENT DENSITY (ASF)

Figure 36. Resistance of Cells with Fluoropolymer/Graphite Collectors

DIRECT ENERGY CONVERSION PROGRAMS

4.6.14   DOE-25

Six-cell stack DOE-25 was constructed using the same features employed in DOE-24 (see Table 3). After initial pressurization of the endplates to 300 psi and a leakage test at 70°F, the overboard seal was found to be excellent, but the internal leakage was 70 times theoretical at 50 psi. This illustrated that the cumulative stackup of 4-mil sealing wires in the overboard seal regions, compared to the 2-mil porthole rings, had been sufficient to hold one or more internal seals off their seats. An overnight, 180°F heat-soak brought the cross-cell leakage to 3 times theoretical. A heat-soak at 220°F sealed the leaks.

Performance of the stack in the 200 kW system is shown in Figure 37. Individual cells performed from 60 to 150 millivolts above baseline, a level attributed to the same contact resistances observed in DOE-24.

The stack ran in the 200 kW system for 1312 hours at which time the electrical conductivity of the anode exhaust water increased abruptly and the system automatically shut down. Subsequent tests showed cross-cell leakage, and the unit was disassembled.

It was found that some physical damage to the cell had occurred. The damage was confined to cell No. 1 (located next to the pneumatic diaphragm) which has sustained a hole through the M&E in the region of the oxygen exhaust. The hole was a slot about an inch long and about .04 inch wide.

The cause of the M&E failure was determined to be the arrangement of a titanium protector foil spanning the gap between the porous Ti support and the oxygen manifold cover. The protector foil had covered about a quarter inch of active catalyst on the membrane. If catalyst is shielded from contact with water, the mambrane will dry out and degrade. The use of the protector foil had been an interim expedient to give support to the membrane in the manifold region. In future units, the porous plate was extended into the manifold area to give a smooth continuous support.

4.6.15   DOE-26

The geometry of unit cell was:

• Anode Catalyst: WE-3.

• Current Collectors: Kynar/Graphite with simulated force amplifiers and Ti protector foil removed.
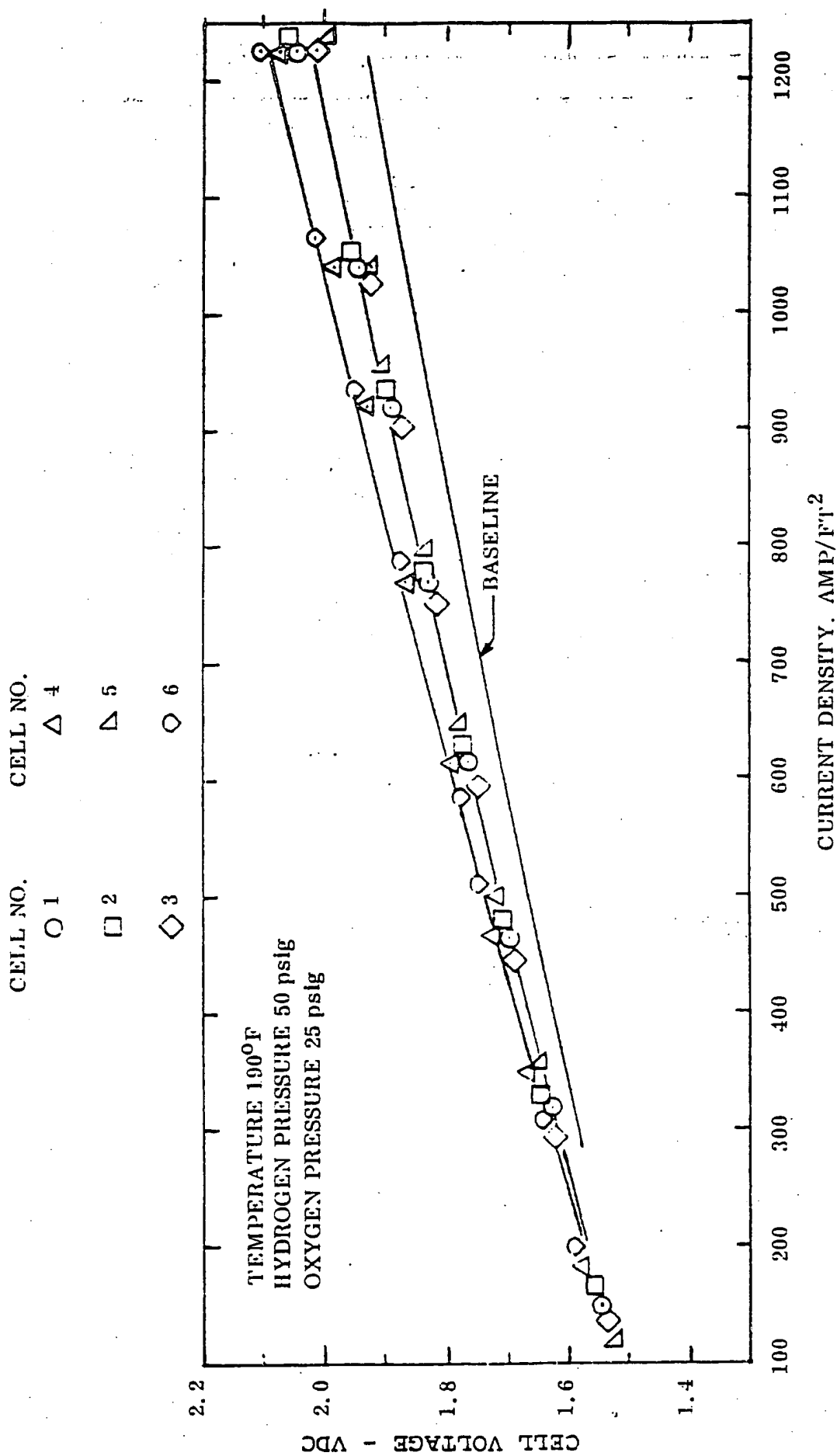
• Cathode Support: Carbon fiber paper (2 layers).

Figure 37. Performance of Cells in 6-Cell Stack DOE-25, E-50 Anode Catalyst

71

- Anode Support: Porous Titanium.
- (3) layers of 3-mil Kynar tape on anode edges.
- (1) layer 3-mil Kynar tape on cathode edges.

The purpose of the test was to verify performance of the new WE-3 catalyst in scaled-up (2.5 ft^2) cells. To improve sealing, an uninterrupted Kynar tape frame was utilized, cut from a roll wide enough to span the width of the collector. In order to build up the 9-10 mil cavity necessary to hold the porous Ti plate, three layers of the available 3-mil thick Kynar were required. The leakage rate was improved but, after 50 hours of operation, the layers of tape extruded out of the stack due to the multiplicity of slip planes in the tape fabrication.

Figure 38 shows the performance of this buildup as compared to a similar unit (DOE-24) employing E-50 catalyst. Performance of WE-3 was about 90 mV better than that of E-50 and remained stable for the 50-hour test period.

4.6.16   DOE-27

The configuration of this unit consisted of the following:

- Anode Catalyst: WE-3.
- Current Collectors: Simulated sealing & ridges (Same as DOE-26).
- Cathode Support: Carbon fiber paper (2 layers).
- Anode Support: Porous Ti (Same as DOE-26).
- (1) layer 10-mil TFE tape on anode edges.
- (1) layer 3-mil Kynar tape on cathode edges.
- Improved fluid plate O-rings.
- Polished current contacts.

The collectors employed in DOE-26 were used in DOE-27. The standard segmented 10-mil TFE tape was installed on the anode edges. To improve sealing of the fluid plate ports, the O-rings were changed to a larger size, allowing the O-ring to touch the outer diameter of the face seal grooves. This provided a more positive seal against internal pressure. In addition, the contact surfaces of the fluid plate and electrical bus plates in this buildup were polished with conducting silver grease to increase conductivity and eliminate current density skewing in the stack. Examination of the data from DOE-27, displayed in Figure 38, shows that performance was about 50 mV better than that of the previous cell. The cell was run for 300 hours at 180°F, generating hydrogen at 30 psig. Voltage was essentially invariant over that time period. Higher pressure operation was not attempted because of the onset of leakage in the circulating pump.

72
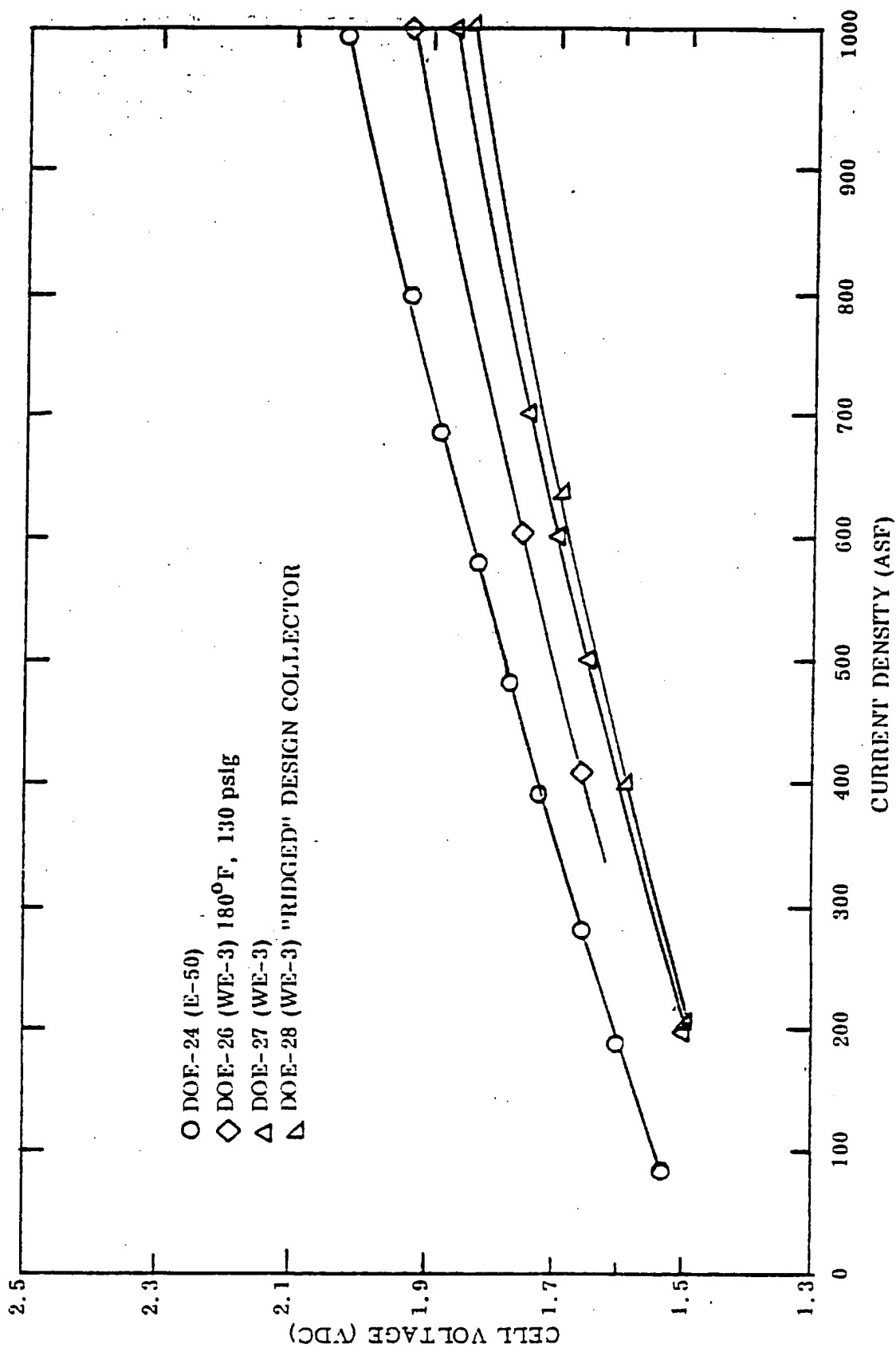
Figure 38. Comparison of WE-3 and E-50 Catalysts in 2 1/2 Ft^2 Cells at 180°F

CURRENT DENSITY (ASF)

CELL VOLTAGE (VDC)

O DOE-24 (E-50)
◇ DOE-26 (WE-3) 180°F, 130 pslg
△ DOE-27 (WE-3)
△ DOE-28 (WE-3) "RIDGED" DESIGN COLLECTOR

DIRECT ENERGY CONVERSION PROGRAMS

At the halfway point in the test (150 hours), the unit was torn down to remove the fluid plate. At that point, the surfaces between fluid plate and the hydrogen collector which were not previously polished, were silver-polished. The voltage was found to improve slightly (20 mV). This indicates that care must be taken to eliminate contact resistance on each buildup.

The unit was voluntarily shut down to trouble-shoot the circulating pump, refurbish the endplates with Rulon-F* and install a cell with the modified collectors incorporating sealing ridges.

4.6.17   DOE-28

The configuration of this unit was as follows:

● Anode Catalyst: WE-3.

● Current Collectors: Modified-design, Kynar/carbon with molded-in seal ridges and molded-on titanium protector foil.

● (1) layer 3-mil Kynar tape on anode and cathode edges.

● Improved fluid plate O-rings.

The purpose of this cell was to investigate performance and sealing of the modified-design, Kynar/carbon collectors with the molded-in sealing ridges.

The modified design collector also uses an extension of the porous Ti plate itself as a manifold cover plate. This simplified assembly, reduced cost and provided uniform stresses on the membrane by virtue of the unbroken surface between active area and internal manifolds.

As seen in Table 3 and Figure 38, this cell had the best performance to date. However, resistance losses were still present and caused the voltage to be about 90 mV higher than WE-3 anodes in smaller laboratory-size cells.

4.6.18   DOE-29

A descriptive summary of this stack is as follows:

● Twelve-cell (50 kW).

● Anode catalyst: WE-3 - Catalyst area scraped back to 18.75 inch square.

● Current collectors: Modified design with molded-in force amplifiers (4-mil) plus (10-mil recess to hold the porous Ti plate.

* ® Registered trademark, Penn Dixon Co., Westboro, Mass.

74

Cathode support: 2 layers carbon fiber paper.

Anode support: Porous Ti plate.

(1) layer 3-mil Kynar tape on anode and cathode edge
for corrosion protection.

It had been previously learned that masking the active
anode catalyst would lead to membrane degradation.   Therefore,
since all the M&E's were already manufactured, the anodes were
scraped back from 19 inches square to 18.75 to avoid masking due
to misalignment of collectors.

The other important feature of this stack was the use
of modified current collectors with molded-on Ti foils and sealing
ridges.

The stack was originally installed in the 50 kW facil-
ity, where cross-cell sealing was adequate to 200 psi, but over-
board sealing was poor.   The stack was heat-soaked by having
heated water pumped through the anodes while applying controlled
electric heat to the endplates.   The heat-soak lasted 16 hours,
during which time the stack reached 237°F.

Some extrusion of the membrane and collector border
tape occurred during the heat-soak.   However, subsequent leak
tests showed internal sealing to 300 psi and hydrogen-side exter-
nal sealing to 200 psi, so operation of the module was initiated.

Unit operation revealed water flow limitations due to
ingestion of gas in the oxygen side water separator at the high
flow rates associated with twelve-cell operation.   This limited
the water flow rate so that the temperature rise across the stack
reached 150°F (240°F anode outlet temperature) at 1000 ASF.   The
stack was operated briefly at reduced currents, and then moved
to the 200 kW facility to take advantage of the larger separator
installed in that facility.

The module was leak-checked at 100 psi and put into
operation.   Water flow was 70 times stoichiometric, producing a
stack temperature rise of 30°F at 1000 ASF.   The unit was run
at 186°F (average stack temperature) with hydrogen and oxygen
delivered at 80 and 25 psig, respectively.   Cell voltage ranged
from 1.87 to 1.93 volts per cell.   During the course of opera-
tion, system pressure was raised to 150 psi, H_2, and 100 psi, O_2.

During a weekend on unattended operation, the unit shut
down at about 150 hours due to low endplate pressure.   A nitro-
gen pressure bottle valve had mistakenly been left closed.   On
the following Monday, the endplate pressure was zero.   After purg-
ing anodes and cathodes with nitrogen, leak-checks were done at
75 psig.   The unit was restarted with back pressure regulators

75

still at their previous settings (150/100 psi). Two minutes into the restart, with the unit at 500 amps (200 ASF), hydrogen pressure was 168 psig and oxygen was 116 psig. Module temperature was 90°F. At this point, the operator made a downward adjustment on the back pressure regulators, with no immediate response. Two loud bangs in quick succession were heard from the test cell. The unit automatically shut down.

Failure Analysis: After securing the test cell, the system was inspected. Two pieces of the center carbon collector had been blown out of the stack and had been caught by the surrounding blanket of fiberglas insulation. The cathode cover plate from the damaged collector had split at the center porthole and was protruding from the stack. The collectors between the pneumatic diaphragm and the damaged collector had been pushed down to fill the void left by the missing pieces of the center collector. The rubber seal behind the pneumatic diaphragm had blown out in the region where the diaphragm and collectors had deflected.

The stack was disassembled and examined. Most of the hydrogen ports in all the membranes were elongated, while the oxygen ports were not. In many cases, the holes had become elongated well beyond the two porthole sealing ridges which surround the portholes. The Kynar tapes at the hydrogen ports followed the membrane beyond the sealing ridges, leaving the adhesive behind. This condition most probably led to cross-cell leakage and collector overheating.

Since this type of extensive membrane and tape movement was unusual, the tape and adhesive became suspect. It was found that the adhesive on the tape was not silicone-based, as had been intended, but rather acrylic-based. Acrylic tape is not functional above 140°F, and should not be used in wet, high-pressure, oxygen environments.

The demonstrated fluidity of the acrylic adhesive led to a re-evaluation of taping both sides of the current collector. Figure 39 (a) shows the arrangement of tape, adhesive, collector, and membrane, as installed. Because of the slip planes provided by the adhesive, the membrane will move under lateral forces. Figure 39 (b) shows how the membrane and tape generally looked after module disassembly. The tape and membrane had moved together past the porthole sealing ridges. At that point, the hydrogen and oxygen were sealed from each other only by the adhesive left behind and the sealing pressure of the flat (non-ridged) portion of the collector. A hydrogen leak at that region would tend to leak into the oxygen side, since the overboard sealing ridges were all engaged.

Figure 39 (c) shows that the removal of one slip plane (the tape on the hydrogen side) would allow the membrane to contact the rigid collector and cover plate directly. Since the

76

PORT HOLE SEALS

HYDROGEN PORT HOLE

ANODE SIDE OF COLLECTOR

ADHESIVE

KYNAR

M & E

KYNAR

ADHESIVE

CARBON

PAPER

H₂ MANIFOLD

COVER PLATE

(a) AS ASSEMBLED TAPE ON BOTH SIDES

CATHODE SIDE OF COLLECTOR

OVERBOARD SEAL

KYNAR

CARBON

KYNAR

PAPER

H₂ MANIFOLD

ANODE SIDE OF COLLECTOR

SLIP PLANE

ADHESIVE

KYNAR

CREEP

M & E

KYNAR

COVER PLATE

SLIP PLANE

CATHODE SIDE OF COLLECTOR

(b) MOTION OF M&E AND TAPE

H₂ MANIFOLD

ADHESIVE

FEP

M & E

COVER PLATE

SLIP PLANE REMOVED

CATHODE SIDE OF COLLECTOR

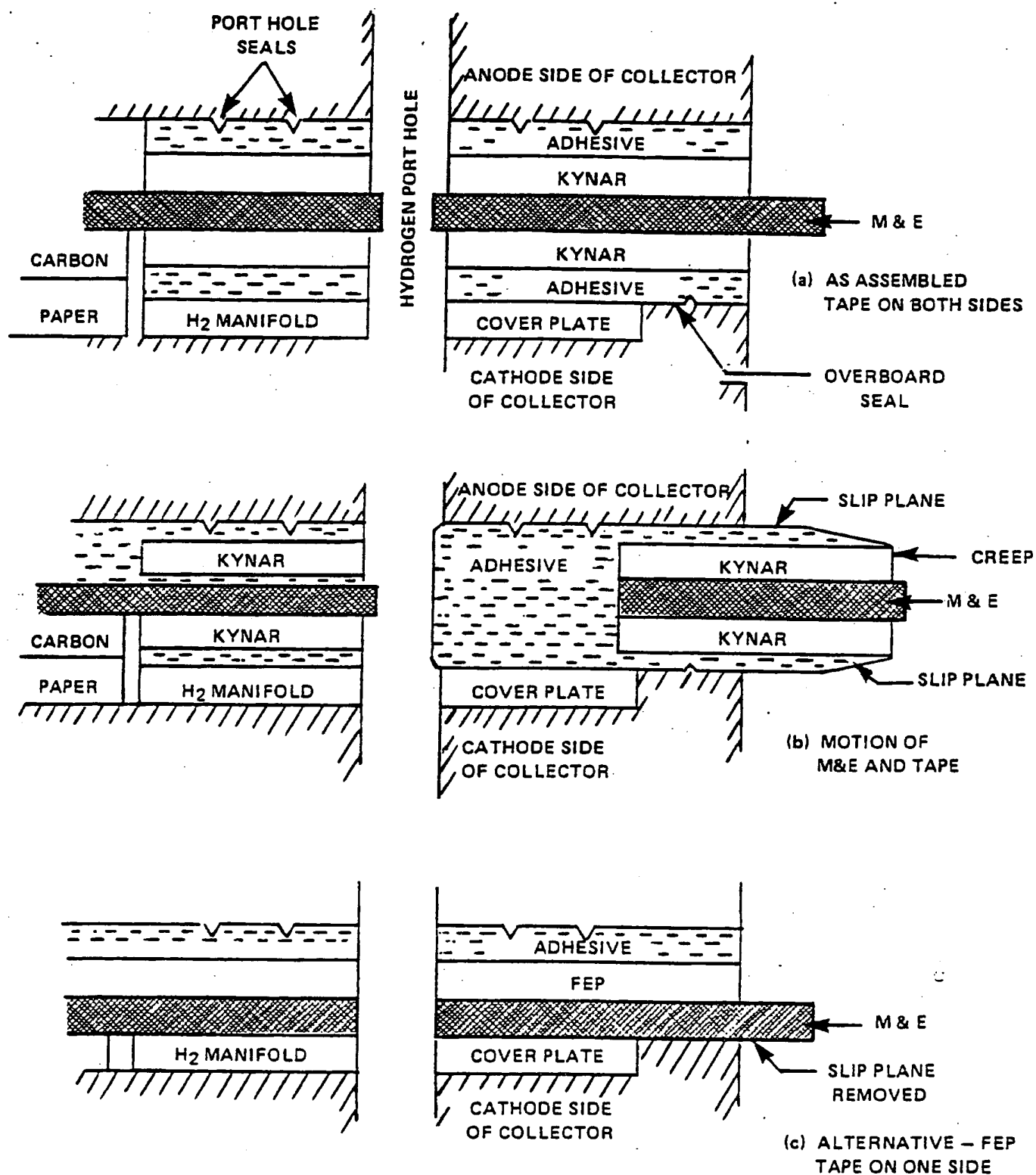(c) ALTERNATIVE – FEP TAPE ON ONE SIDE

Figure 39. Effect of Collector Tapes on Membrane Creep

77

membrane resists shear flow, it would remain in place even though the other side contacts tape. The corrective action taken, therefore, was to remove the tape from the cathode side completely and to change the tape on the anode side of the collector from Kynar-acrylic to Teflon*-silicone. Teflon-silicone tape was available in full-size sheets to make an uninterrupted tape frame.

It was interesting to note that the oxygen portholes in the membrane did not elongate. The reason for this is that the tape on the anode side of the collector contacts the extension of the porous titanium anode support. The adhesive intrudes into the pores of the titanium, allowing the tape backing to contact the surface of the rigid anode support.

Other observations during disassembly were:

1) A hole was found in M&E number 7 next to the failed collector. This portion of M&E was stripped in aqua regia; there was no evidence of chemical degradation. This indicated that the hole was the result of the failure (most probably from intense heat) rather than a cause of the failure.

2) Cell number 4 showed indications of having been exposed to high temperature on the titanium foil and porous plate. Two cracks were also found in the M&E at the edge of the catalyst at the oxygen end. Again, the cracks were not the result of membrane degradation, having been most probably caused by high heat resulting from seal failure.

3) Several collectors had deposits of adhesive in the hydrogen exhaust ports between the ribs supporting the hydrogen manifold cover plates. If these grooves are blocked, the pressure inside the cathode cavity will increase, tending to increase the pressure differential between cathode and anode. Elimination of the acrylic-based tape should prevent this in the future.

4) There were cracks on the hydrogen side of the collectors which had bent to fill the space left by the ejected pieces of the failed collector. However, these cracks did not penetrate through to the anode side. This attests to the inherent ductility of the collector.

5) A niobium hydrogen manifold cover plate was ejected from collector 7, touching both the collector (about 12 volts) and the grounded piping. A fused portion on the cover plate matched some slag on the piping. The contact probably produced a spark which ignited the hydrogen and oxygen emitting from the open stack; the probable origin of the second report heard during the incident.

* Registered trademark, E.I. duPont de Nemours & Co.

78

In summary: The cause of the failure was the movement of membrane, as a result of the fluidity of two tape covers, past the sealing ridges in the hydrogen porthole regions. The result was gas mixing and excessive heat, causing the collector to soften and blow out. Gas was emitted into the space between the stack and insulation. A niobium cover plate ejected from the stack touched the grounded piping, causing a spark and the second report.

4.6.19   DOE-30

DOE-30 was a 12-cell stack having the following construction:

- Kynar/graphite molded collectors with molded-in sealing ridges (4 mils high) and titanium foil.

- FEP tape (2-mil film with 1 mil of silicone adhesive) on the anode side of the collector frames for corrosion protection.

- No tape on the cathode side of the collector frames, in order to prevent the tape slippage problem of the previous DOE-29.

- Porous titanium anode supports, which also formed anode manifold cover plates.

- Two layers of carbon paper as cathode supports.

- Anode catalyst trimmed to avoid local water starvation.

A series of heat-soaks was performed to determine the effect of temperature. After a weekend heat-soak at 180°F, cross-cell leakage tests showed that a good seal was achieved up to the chosen point of 200 psi (see Figure 40). Some overboard leakage did occur at a low level of nitrogen pressure on the cathodes, however. Heat-soaks were continued. Final sealing was achieved at 75 psig after soaking at 236°F.

Performance of DOE-30 is shown in Figure 41. Average cell voltage at 1000 ASF was 1.9 V.

The marginal sealing and performance of this module led to efforts to improve the overboard seal and the quality of the M&E's in future buildups.

4.6.20   DOE-31

Twelve-cell stack (DOE-31) was constructed and tested in the 200 kW facility. The cells in this stack featured:

- Kynar/graphite molded collectors with molded-in sealing ridges (4-mil high) and titanium foil.

79

ANODE>CATHODE N$_2$ CROSS-LEAKAGE
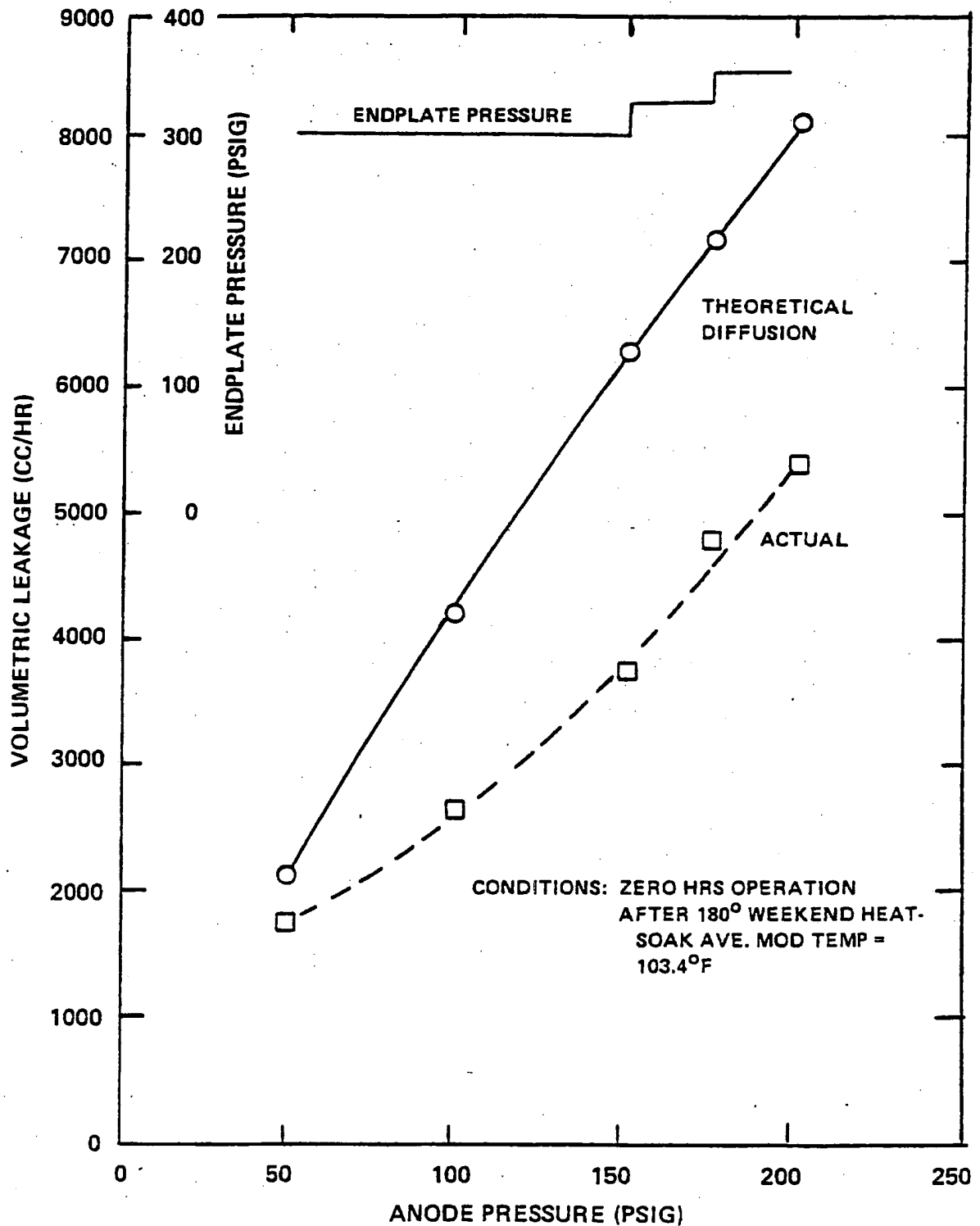12-CELL SERIES MODULE S/N DOE-30

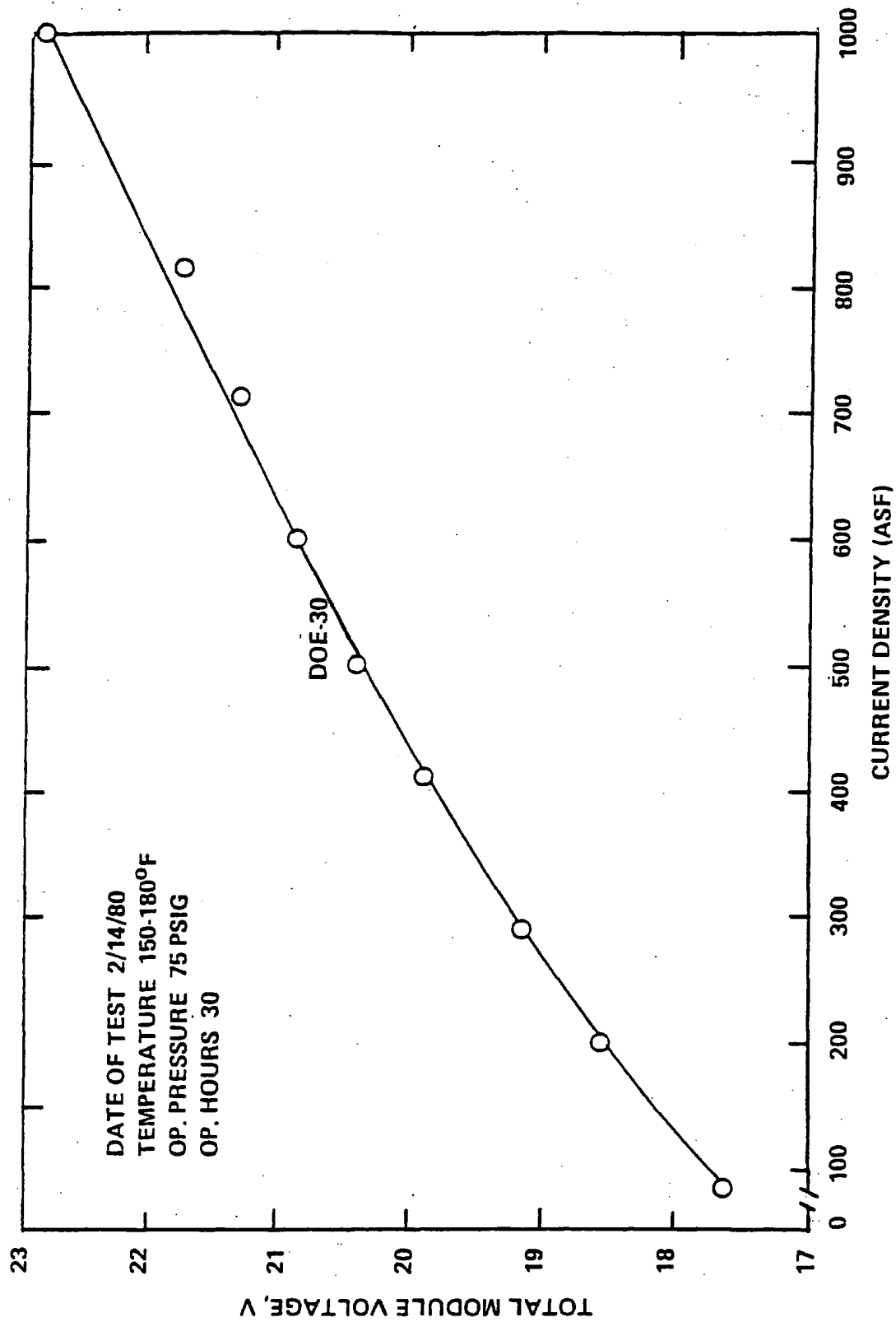Figure 40. Cross-Cell Sealing of DOE-30

Figure 41. Performance of 12-Cell Stack DOE-30

DATE OF TEST 2/14/80
TEMPERATURE 150-180°F
OP. PRESSURE 75 PSIG
OP. HOURS 30

DOE-30

CURRENT DENSITY (ASF)

TOTAL MODULE VOLTAGE, V

- M&E's reboiled and repressed to provide minimum resistance.

- Porous titanium anode supports which also formed anode manifold cover plates.

- Two layers of carbon paper as cathode supports.

- Anode catalyst trimmed to eliminate local water starvation.

The stack was first heat-soaked to 238°F with water flowing over the anodes and cathodes. Results of subsequent leak-checks using nitrogen gas on the cathode side are presented in Figure 42. The cross-cell seal was good to 100 psi.

The overboard leakage behavior of DOE-31 is shown in Figure 43. Initially the leakage rate was 2000 cc/hr. at 50 psi and 4500 cc/hr. at 100 psi. The unit was leak-checked after extensive nitrogen purging. The sequence of testing is listed in the legend of Figure 43.

Curve No. 1 in Figure 43 shows that after the module had been purged and stored under dry nitrogen, the leakage rate seemed high (10 to 20 l/hr.). After a short-term rewetting of the anodes to 90°F, the leakage did not decrease significantly.

After overnight rewetting of anodes and cathodes under pressure, dry nitrogen was applied to the cathodes; the resulting leakage behavior is depicted in curve No. 2. Note that the leakage rate was initially very small, but increased over time. The unit was allowed to sit with dry nitrogen at 70 psi (1300 cc/hr) for a period of one hour. The leakage increased to 50 l/hr, which indicated that the water in the seal regions was being removed, allowing gas leakage. Curve No. 3 shows the results of a test after rewetting the module again. Leakage initially decreased, probably due to the transient dissolution of the measuring gas into the cells. (Leakage is measured by trapping a volume of gas in the unit and then observing the pressure decay. A higher-than-normal pressure decay indicated that gas is dissolving into the membranes.) Once again, if dry gas was kept on the unit for a long time, the leakage increased. It was proven several times that the "wet seal" could be consistently regained by rewetting, giving confidence that overboard sealing had been achieved.

It should be remembered that in the normal operating mode, the hydrogen compartments (cathodes) contain both hydrogen gas and liquid water which has been protonically pumped across the membrane. Therefore, water exists at all times during operation and will continually provide an adequate overboard seal.
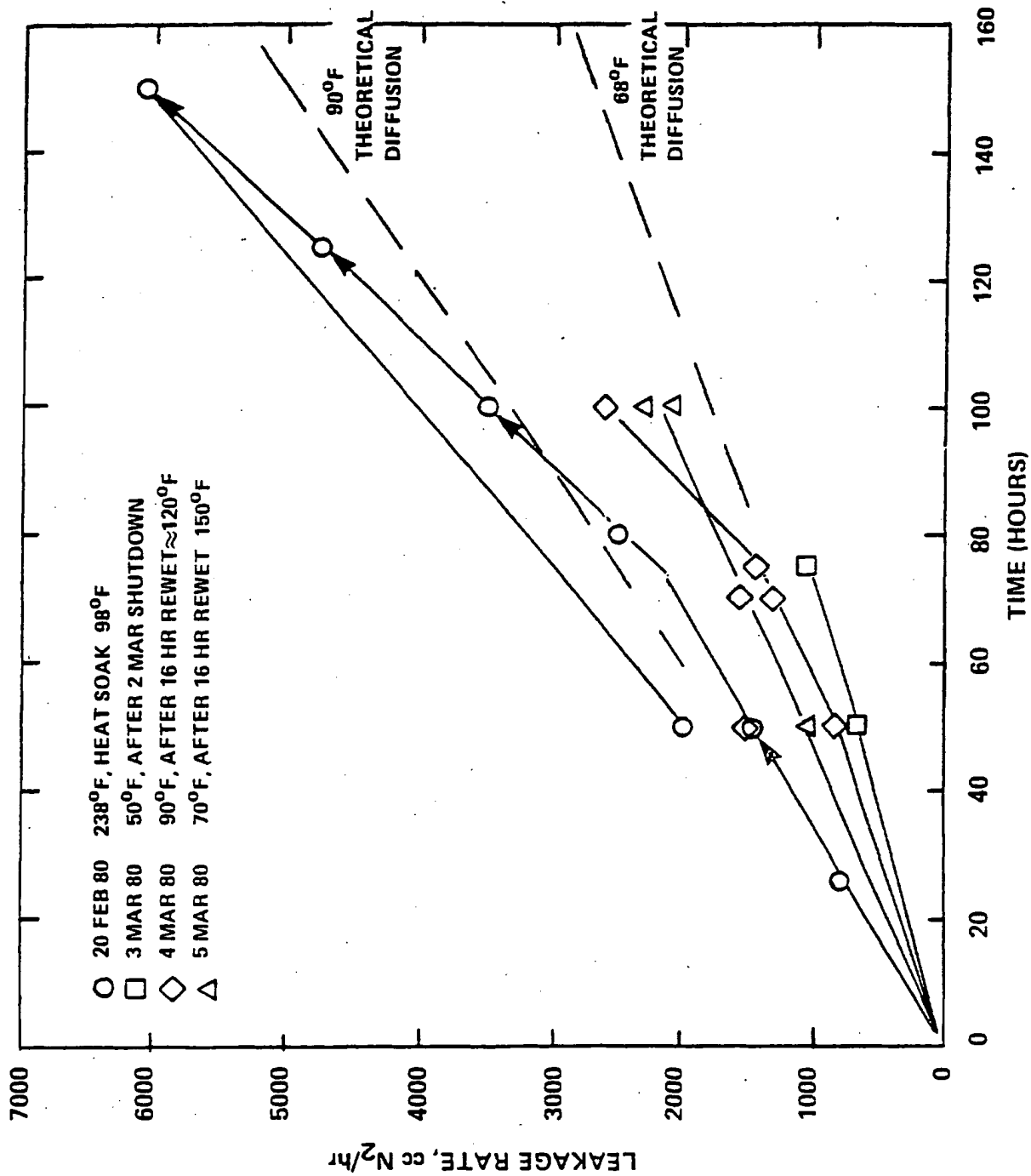
82

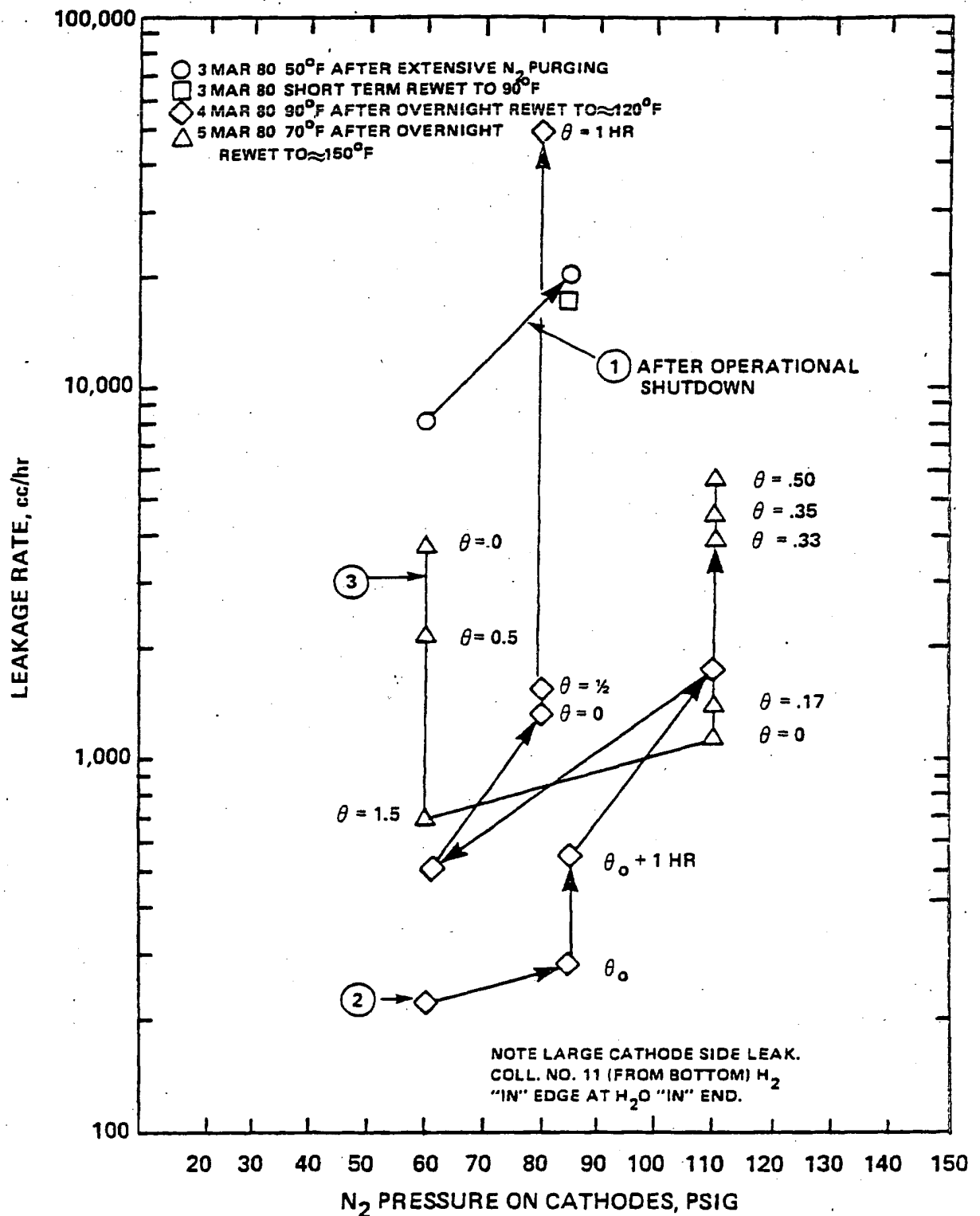Figure 42. Cross-Cell Leak Test DOE-31 (12 Cells)

83

Figure 43. Cathode Overboard Leakage History DOE-31 12 Cells (238°F Heat Soak)

DIRECT ENERGY CONVERSION PROGRAMS

The stack was operated at 180°F and 100 psi hydrogen pressure. The stack's performance is shown in Figure 44. The average cell voltage is 1.82 volts at 1000 ASF. The cell voltage correlates with the resistance of the cells as installed, the higher voltages corresponding to higher resistances. The resistance of each cell was calculated from polarization data at operating temperature. Cell number 6 demonstrated essentially the ideal resistance of laboratory cells. When the data was normalized by subtracting the voltage attributable to excess resistance, the results were quite similar to performance of laboratory cells. It may be concluded that:

● The performance discrepancy is resistive, and therefore the catalysts are good and the fluid flow is adequate.

● Several cells had good resistance, particularly Cell 6, which had ideal resistance.

Figure 45 shows the operating history of DOE-31. The average voltage was kept below 1.85 V/cell during 216 hours of operation by slight increases in temperature from 190° to 196°F. A goal of 1.85 V/cell at 1000 ASF, 100 psi has been set for operation of the 60-cell, 200 kW stack which is scheduled for a 400-hour life test, and therefore the testing of DOE-31 was tailored after that model.

4.6.21   DOE-32

DOE-31 was then removed from the test facility and built up to 30 cells by removing the oxygen end collector and M&E No. 1. The second collector was cleaned of the silicone glue and a fresh bead of glue applied. Subsequently, 19 cells were added to the stack and the resulting module was re-numbered DOE-32.

DOE-32 was heat-soaked to 230°F and leak-checked to 100 psi. The stack was operated at 75 psi hydrogen pressure for 20 hours to compare it to DOE-31. Performance was essentially the same, 1.85 V/cell at 1000 ASF and 196°F. The unit was then successfully leak-checked at 125 psi in preparation for 100-psi operation.

4.6.22   DOE-33

Another 30-cell stack was added to DOE-32 to complete the assembly of a full 60-cell, 200 kW module designated DOE-33.

Figure 46 shows the average cell voltage over the life of the test by module, including data points broken out for the 12-cell group common to all three modules. An inspection of the average cell voltage of the original 11-cell group shows that a 30 mV rise in voltage occurred each time a new module was built

DIRECT ENERGY CONVERSION PROGRAMS
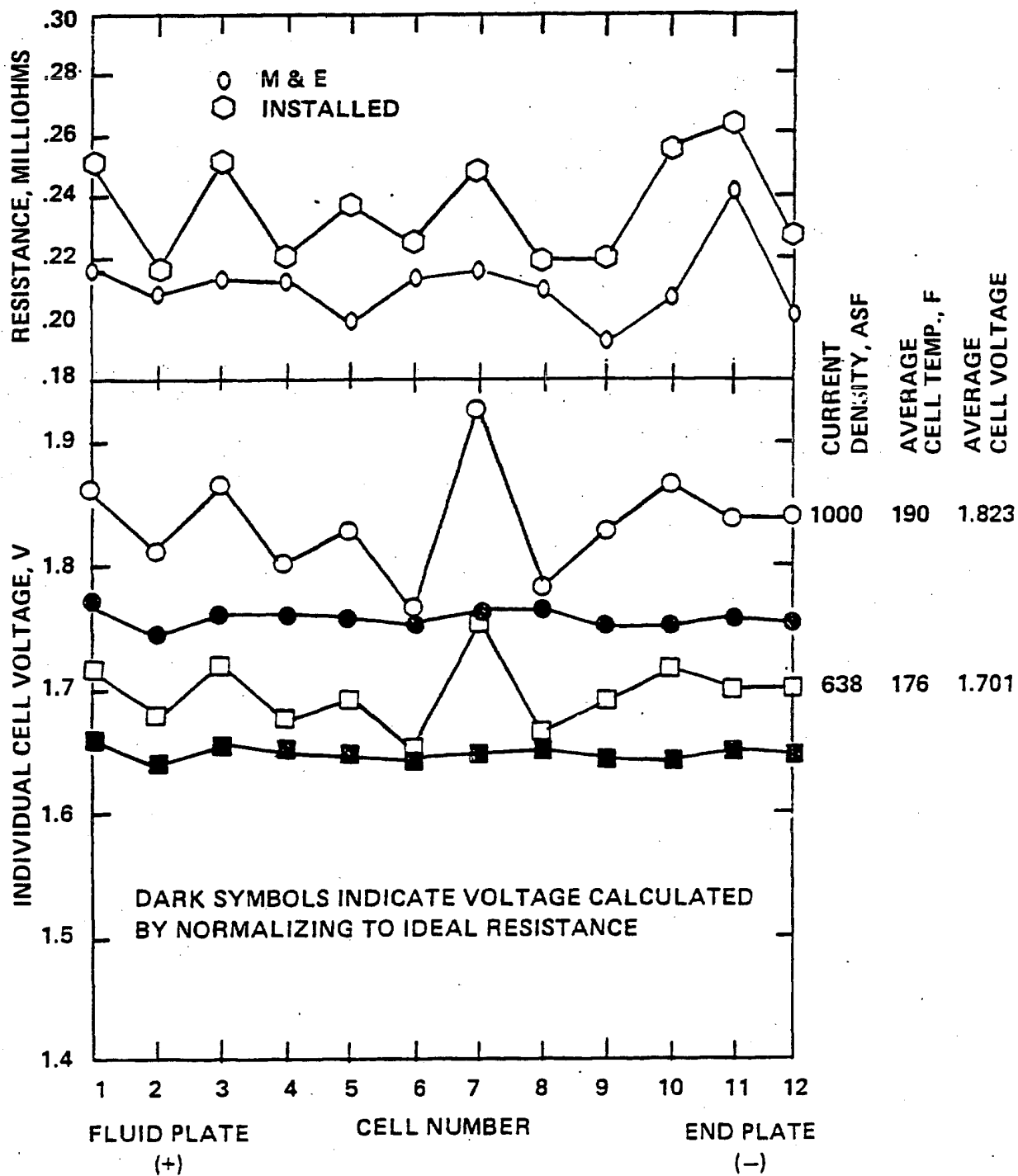
Figure 44. Performance of 12-Cell Stack DOE-31
100 PSI Hydrogen Pressure

DIRECT ENERGY CONVERSION PROGRAMS
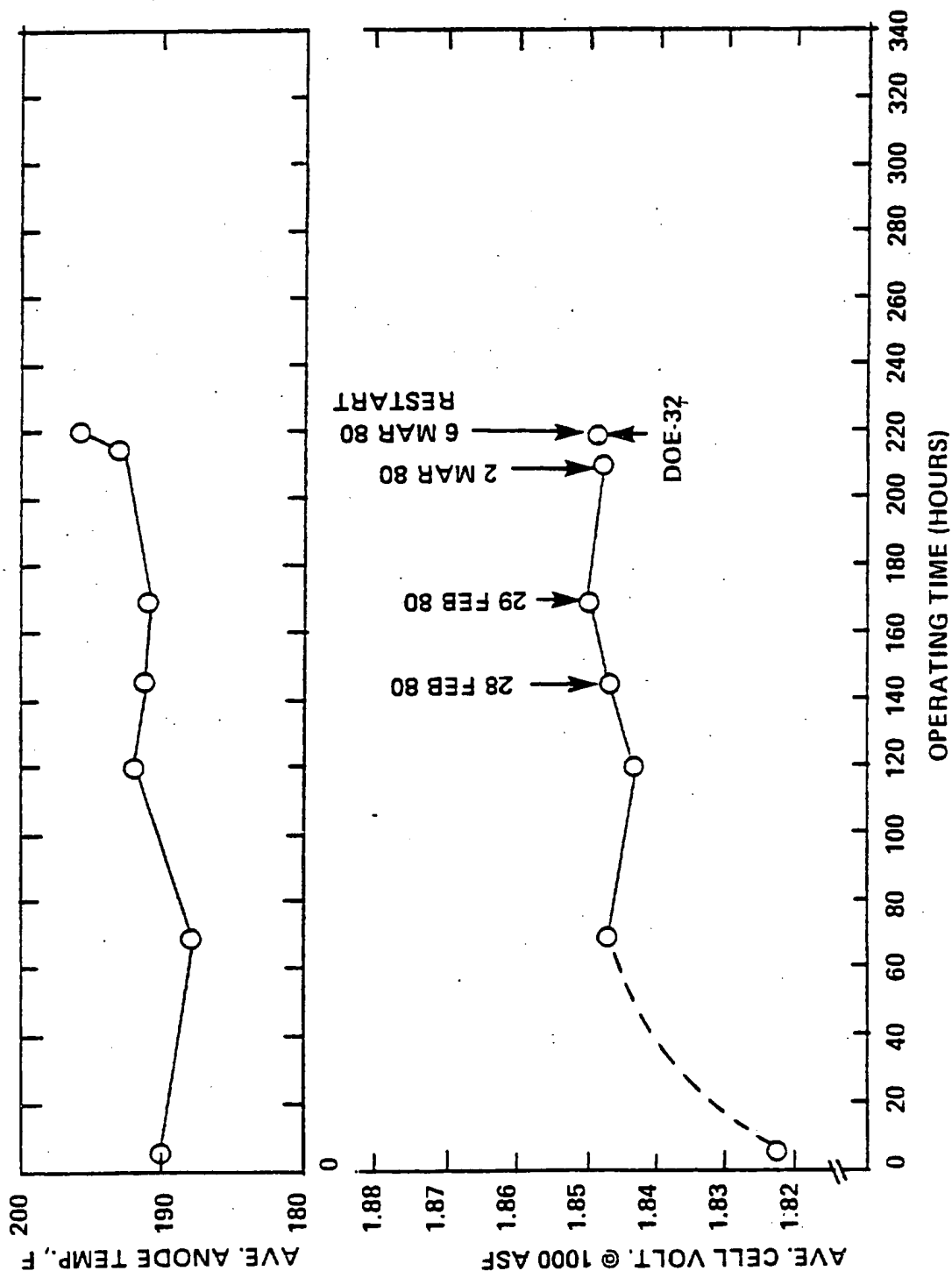
Figure 45. Performance History of DOE-31

DIRECT ENERGY CONVERSION PROGRAMS

Figure 46. Performance History DOE-31, 32, 33   180 to 208°F, 1000 ASF, 100 psi Hydrogen

□ ORIGINAL 12 CELLS (DOE-31) 11 CELLS REUSED IN DOE-32 AND DOE-33B
△ (19) CELLS ADDED TO (11) FROM DOE-31 TO MAKE DOE-32.   REUSED IN DOE-33B
○ (30) CELL STACK DOE-33A

88

up. This was caused by the depressurization of the endplate which was required each time additional cells were added. Indeed, the same effect was produced at a later time in 12-cell stack DOE-34 by depressurizing and repressurizing endplates without disassembling the module. The voltage rise was probably caused by partial detachment of the Ti foil molded to the collector, especially if water was present at the foil/collector interface due to some porosity in the molded carbon/Kynar.

From Figure 46, it is evident that DOE-31 exhibited a voltage better (lower) than the goal of 1.85 V/cell. The performance of similarly-configured DOE-32 can be seen in Figure 45 in the 220 to 250-ho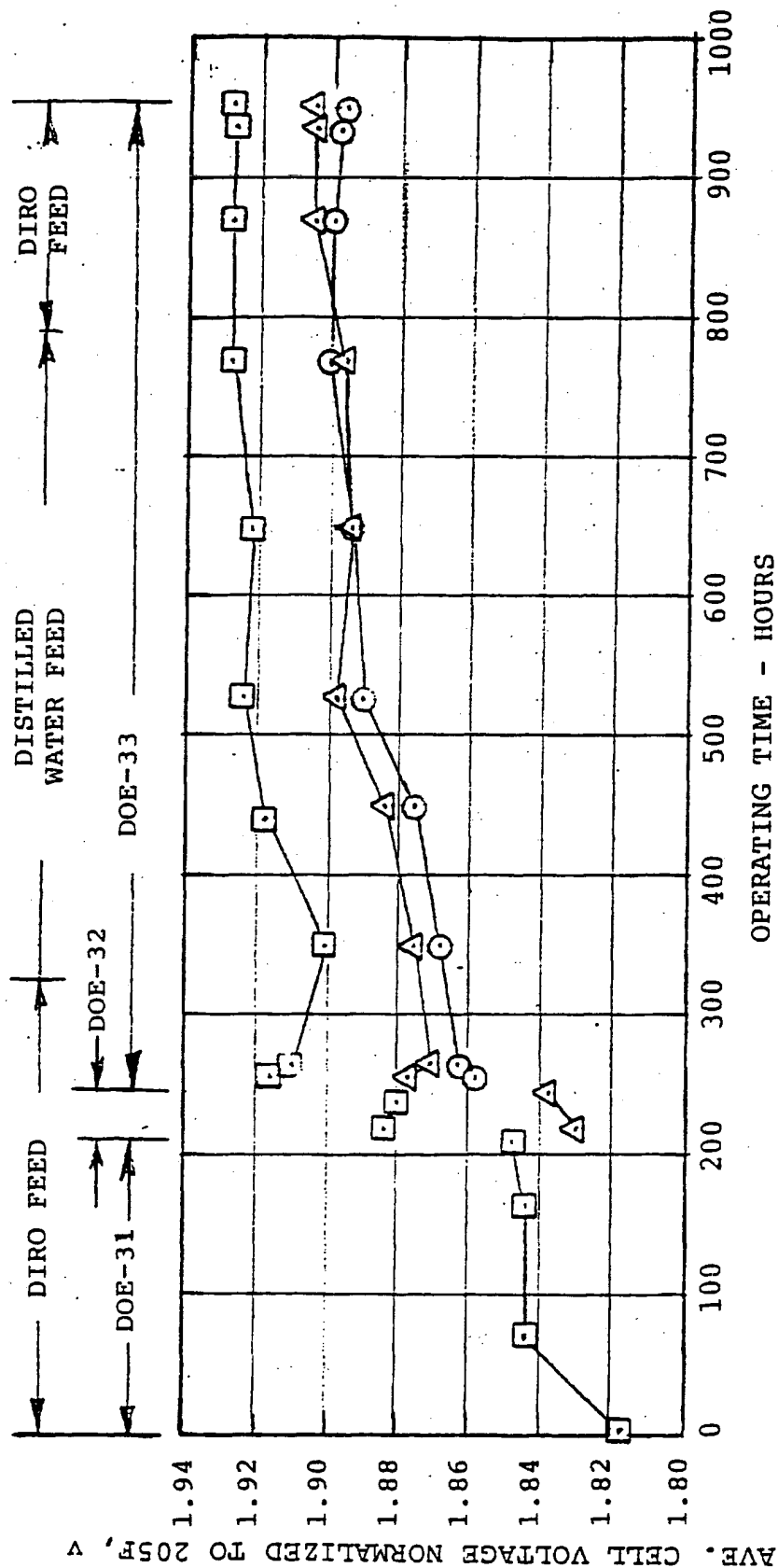ur region. The average performance of all of the cells during this period was 1.85V. Older cells were running at a higher voltage (as discussed above) while the newer cells showed about the same voltage as did the new cells at a similar point in the operation of DOE-31.

The new cells in Stack 33A started with an average voltage about 40 mV higher than that of the original 11 cells, probably because the best cells and parts had been used for earlier stacks.

After 950 hours of testing (i.e., 950 hours accumulated on the original 11 cells), the average cell voltage was 1.90V at 1000 ASF and 205°F. The module was operating in the automatic mode at this point, when an automatic shutdown occurred, the result of a spurious electrical signal. As designed, the nitrogen blanket to the module was immediately activated to maintain system pressure while the system was cooling. However, the cathode water return valve had not closed completely during the shutdown process, which allowed the cathode separator to empty. This loss of pressure on the system when the stack was still at 230°F caused the moisture in the cells to vaporize and be carried out with the nitrogen venting across the cathodes, thus dehydrating the cells. Subsequent leak-checks showed excessive overboard and cross-cell leakage in both stacks. Heat-soaking restored the overboard seal, but the cross-cell leakage, while reduced, was not eliminated.

In an attempt to locate the source of the internal leakage, an electrochemical test was conducted which consisted of introducing air to the anodes and 1% H_2-in-N_2 to the cathodes while maintaining a potential of 1 V/cell on the stack. It was theorized that a leak in any cell would be evidenced by a drop in voltage due to hydrogen leaking from the high-pressure cathode side to the anode side, depolarizing the cell. However, the results of using this procedure were inconclusive.

Finally a hydraulic method was used, whereby one reactant side was filled with water and subsequently pressurized with nitrogen. Depending on the attitude of the cells, the water level could be measured when it dropped to the location of the leak and caused gas to be expelled to the opposite reactant chamber. By orienting the stack on its X, Y, Z axes, the leak could then be triangulated to within about 1/2 inch of its location, that is, to within about 3 cells of the actual leak-point.

Teardown Analysis

The module was disassembled and cells removed from the areas indicated by the hydraulic tests. Leakage was found in one cell of each stack. In both cases, the leakage was due to membrane degradation at the edge of the active area near the corner of the hydrogen outlet and oxygen outlet manifolds.

In order for membrane degradation to occur, the membrane must become dehydrated in the presence of catalyst. The rate of attack is also temperature-sensitive. In this case, the damage was in an area where:

a) The anode catalyst had been deliberately removed (by scraping) prior to assembly to prevent any masking of anode catalyst by the collector sealing edge. It is very likely that though the membrane had been scraped, some catalyst particles remained embedded in it.

b) The porous plate anode support had been platinized. Although not as active as WE-3, platinum is also an anode catalyst and can affect the membrane under the right conditions.

c) The porous Ti plate was found to be hydrophobic in the area where it touched the scraped region of the membrane, most probably due to oxidation of the titanium. This could lead to local membrane dryness.

d) Cathode catalyst was present.

This area is shown schematically in Figure 47.

Two steps were taken to prevent a reoccurrance of a membrane attack of this nature:

● The electrode spreading molds were modified to ensure proper placement of catalyst, and

● The porous plate platinization masks were modified to ensure that platinization is restricted to the proper areas, i.e., areas in which anode catalyst is present.

90
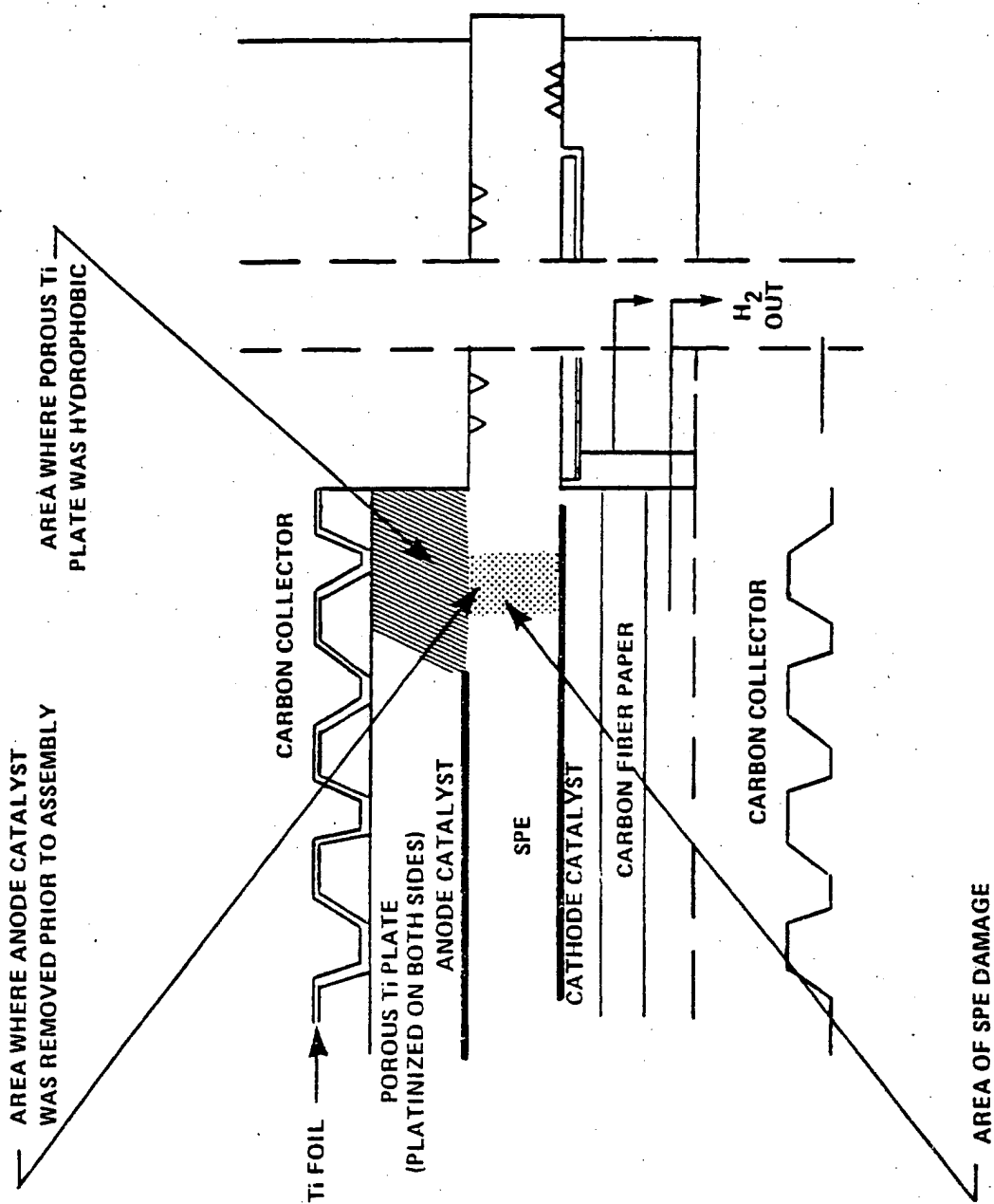
Figure 47. Location of SPE Leakage in 2 Cells of 60-Cell Module

AREA WHERE POROUS Ti PLATE WAS HYDROPHOBIC

AREA WHERE ANODE CATALYST WAS REMOVED PRIOR TO ASSEMBLY

CARBON COLLECTOR

Ti FOIL

POROUS Ti PLATE (PLATINIZED ON BOTH SIDES) ANODE CATALYST

SPE

CATHODE CATALYST

CARBON FIBER PAPER

CARBON COLLECTOR

H_2 OUT

AREA OF SPE DAMAGE

91

During the teardown analysis, it was found that the porous titanium plate contained regions which appeared to be denser and were less hydrophilic than the rest of the plate. This was qualitatively proven by applying a drop of water to the dense region and observing that the water would spread at a much slower rate than a drop applied to a normally porous region. The dense regions were areas where the vendor had found it necessary to patch voids in the plate which arose in manufacture. Membrane which had been in contact with the patched (non-porous) regions was found to be delaminated. Delamination is the result of operating the M&E without sufficient water. This condition demonstrated the need for better manufacturing control of the porous plates by the vendor, and the avoidance of the patching process.

It was also found that some of the anode flow field grooves were blocked with carbon/Kynar mold flash. This also produced membrane delamination. In the future, the field grooves were inspected and cleaned of flash prior to assembly of the component into a module.

It was also noticed that some of the anode flow field grooves were plugged with solid material, which was analyzed by SEM techniques and found to contain the elements present in the anode catalyst. A means of filtering out loose catalyst particles before they can be recycled back to the anode inlet was required.

Post-Operative Performance Analysis

In an experiment to analyze certain aspects of the performance of DOE-33, a section of an M&E was cut up and immersed in hydroxide solution. A smell typical of an amine species resulted.

The anion beads in the deionizers are the only potential source of amines in the GE system. It was apparent through performance trends, substantiated by post-operative tests such as the one above, that amines from the main deionizer are eluting past the cation resin section in the downstream portion of the bed. Methyl amine degradation products in non-ionized form tend to ionize more fully when they reach the anode loop, which is at a higher temperature. At this point they can be readily absorbed by the membrane and catalyst, resulting in a performance degradation due to contamination.

Another section of an M&E from DOE-33 was cut out and run in 3" x 3" laboratory hardware. The cell demonstrated the poor performance typical of catalyst contamination; however, the performance improved after the cell was operated a few hours on the intrinsically purer water of the laboratory system. This performance improvement due to gradual decontamination of the cell is shown in Figure 48.
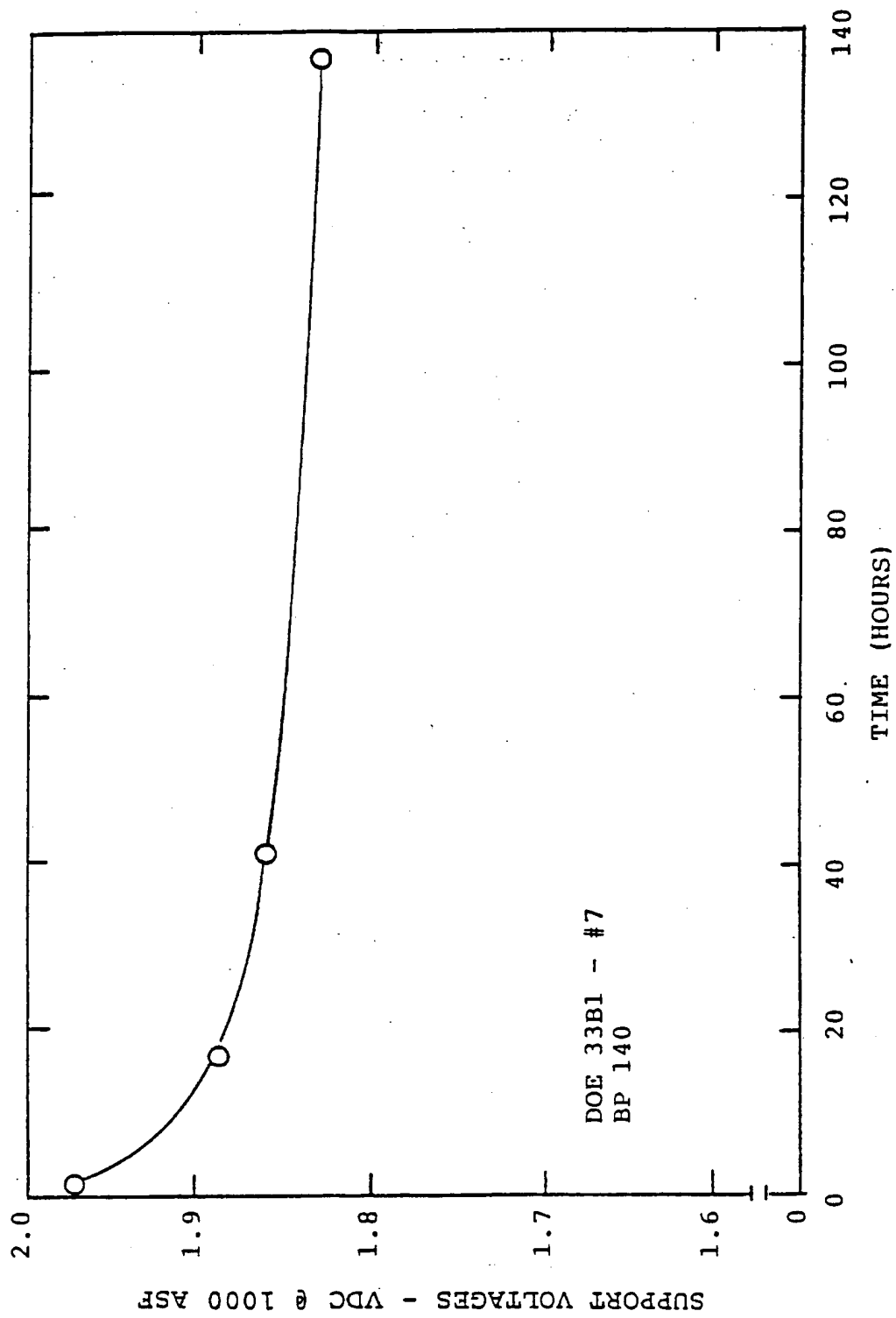
92

Figure 48. DOE-33 Performance vs. Time

DOE 33B1 - #7
BP 140

TIME (HOURS)

SUPPORT VOLTAGES - VDC @ 1000 ASF

93

DIRECT ENERGY CONVERSION PROGRAMS

The following system modifications decrease the possibility of amine contamination:

a) Operation of the deionizer at a lower temperature than the present 120°F maximum recommended by the resin bead vendors. This would reduce the degradation of the anion beads and reduce the release of amine.

b) An increase in the cation tail portion of the main deionizer, decreasing the space velocity to improve amine capture.

c) Installation of a high-temperature cation bed in the anode loop to scavenge amine at the point it is more highly ionized.

The results of these investigations are discussed in Section 4.6.24, Contamination Control.

4.6.23   DOE-34

Twelve-cell module DOE-34 had the following configuration:

● Kynar/carbon collectors with molded-in ridges.

● Silicone glue seals on the hydrogen side.

● One cell with low-loaded catalyst at 1 mg/cm^2.

● One cell with low-loaded catalyst at 2 mg/cm^2.

● One collector with Ti foil "spot"-adhered to the collector.

● One cell with presintered catalyst.

The stack was sealed to 125 psi using a 190°F heat-soak and subsequently operated for a total of 1014 hours. The performance exhibited by the stack during the test period is summarized in Figure 49.

The performance of a number of components in this stack relative to that of previous designs had important implications for the configurations used in future buildups. For example, it was determined that edge current collection is as successful as the original, more complicated and costly design. The voltage drop along the new bus plate (diaphragm) was .005V at 2440 amps, which does not produce a substantial current density maldistribution.

The end bus plates as well as the adjoining current collectors were of equal potential, indicating good current distribution to and from the stack. The other collectors within the stack exhibited voltage gradients along their edges. This may indicate current density gradients inside the cell.
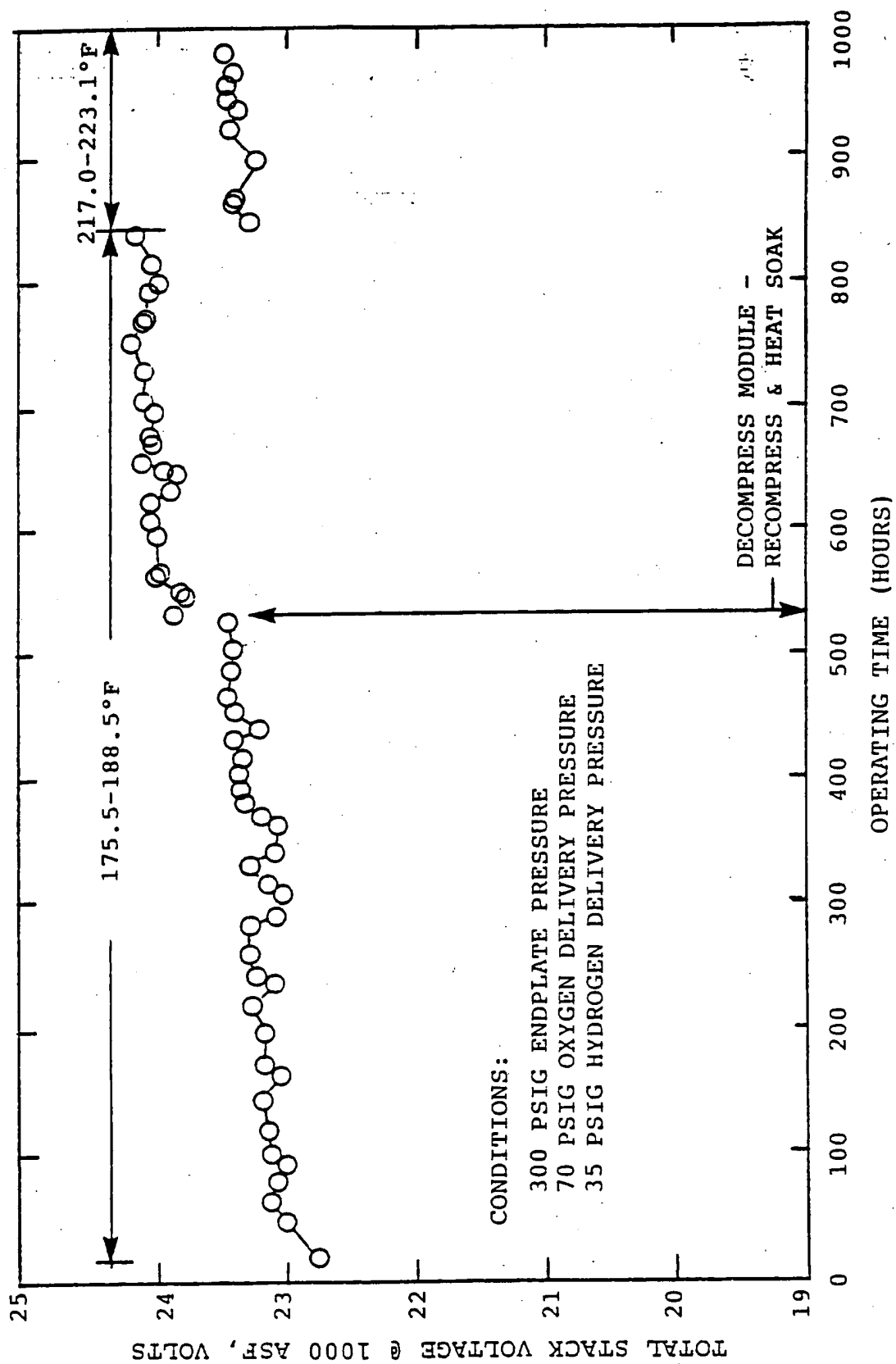
94

Figure 49. Performance History of (12) Cell Stack DOE-34

DIRECT ENERGY CONVERSION PROGRAMS

The natural tendency of a cell is to exhibit higher current density in the direction of the temperature rise across the face of the cells. Analysis has found that this effect is not detrimental to the overall power consumption of the stack. That is, the colder regions operate at lower current density and the hotter regions at higher current density, the voltage being determined by the local temperature. The integrated performance across the cell, however, is close to the average. For example, for a 2 1/2 ft^2 cell with a 50°F temperature rise, the current density ranges from 970 to 1030 ASF when the average is 1000 ASF.

However, current density gradients produced by regions of poor conductance are detrimental to overall power consumption because those regions can be virtually unused. The real average current density can, therefore, be higher than normal with attendant higher inherent voltage.

The pneumatic endplates were deliberately depressurized to simulate the procedure used in adding cells to the 200 kW unit, DOE-33. It was found that performance suffered by approximately 50 mV/cell when normal operation was resumed. This indicates that depressurization of the endplates does cause a voltage level increase similar to that seen in the 200 kW unit. The most probable cause of voltage increase, which is resistive in nature, is that the protective titanium collector foil detaches from the collector during depressurization and, when endplate compression is removed, allows disturbance of the contact point, resulting in an increased contact resistance.

The cell protected with spot-adhered foil, however, did not suffer a voltage rise after the endplate depressurization. This indicates that the contact resistance was unaffected by the depressurization.

The performance of the two cells with modified loadings was also a helpful indicator for future configurations. There was no variance in the performance of the two low-loaded cells from that of the standard cells, validating the potential use of low-loaded M&E's in full-scale hardware. In addition, those cells with pre-sintered catalyst performed as well as cells whose catalyst was prepared by previous processing methods.

The feedwater resistivity remained excellent at 180°F operation (20 mΩ-cm); at 218°F operation, it dropped slightly to 14 mΩ-cm. The anode loop water quality was good (2.8 mΩ-cm) at 180°F operation. It dropped to 2.2 mΩ-cm after endplate pressure excursions.

The 12-cell stack designated DOE-34 was operated for 1014 hours and voluntarily shut down. A post-test disassembly and analysis included resistance measurements taken on the collector, which had been configured with "spot-adhered" foil. It was found that the resistance of the foil and collector had increased from a normal value of 30 μohm ft^2 to as high as 400 μohm ft^2 at the center of the collector, primarily as a result of a drop in contact voltage at the surface of the foil facing the oxygen chamber. This was demonstrated by sanding the outer surface of the foil while it remained in place on the collector, and measuring the resistance again; it had decreased from 400 μ to 60 μ ohm ft^2. This indicated that improved platinization on the oxygen side of the foil will probably result in more uniform conductivity in this type of collector.

96

During the disassembly of DOE-34, it was found that membrane blistering had occurred in the active area in 7 of the 12 cells. The blistering was primarily in the anode exhaust region, the hottest portion of the cells. The membrane was cleaved (similar to a delamination) 2 mils from the cathode surface and 9.5 mils from the anode surface. The surfaces of the cleaved sections were chemically analyzed using SEM techniques which showed that the main chemical species present not indigenous to normal cell materials was iron - in large quantities (about 200 to 500 ppm). It is well-known that iron catalyzes peroxide degradation, even at a 50-ppm level, and it is most probable that the membrane degraded under the influence of iron in the higher-temperature regions.

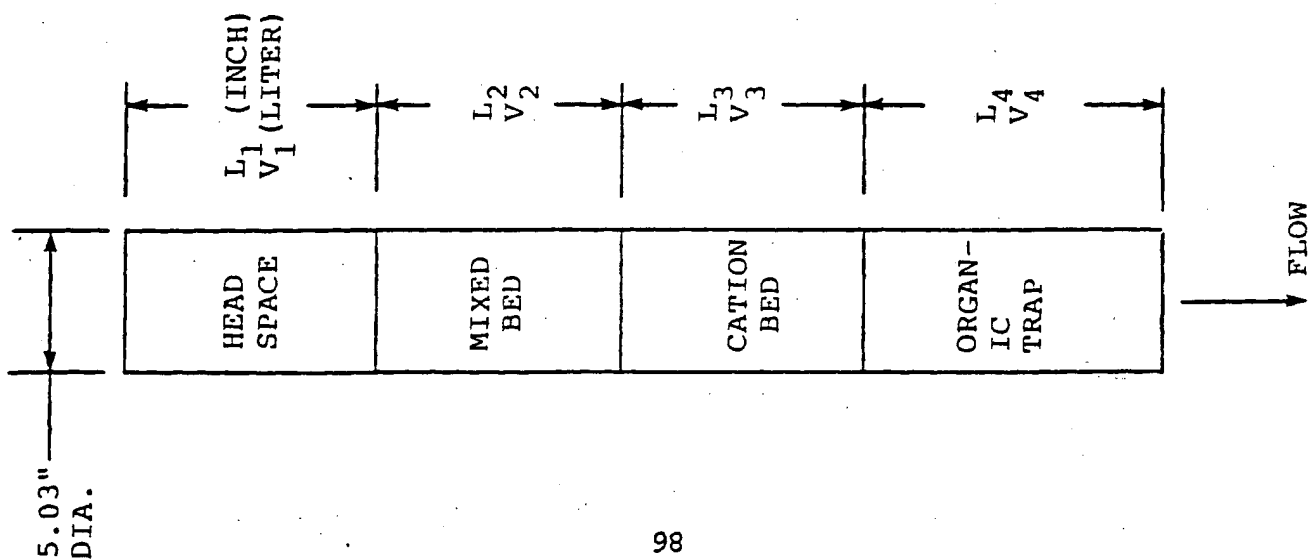## 4.6.24   DOE-41 - Contamination Control

A comparison of three systems was made in order to investigate the effect of deionizer configuration on electrochemical cell performance. The deionizers were configured as in Figure 50. Deionizer No. 5, representative of the standard deionizer design, was operated with the 12-cell stack DOE-34 for 1000 hours. After that test, the membranes were found to contain amine indicating that the standard cation tail was not fully effective in dropping amines emanating from the mixed bed.

Deionizer No. 7 was configured with a downstream bed of Rohm and Haas' Organic Trap XE-348, designed to remove any organics, specifically triethylamine, one of the degradation by-products from mixed beds. A cell was subjected to water from this deionizer, but not operated. A cutout from the cell showed impaired performance and current density limitations above 800 ASF. Table 5 shows the cation content of XE-348, which may have contributed to the problem. Similar results, i.e., contamination by the organic trap, were experienced on lab-sized cells. In view of this, the evaluation of organic traps was discontinued.

TABLE 5

CHEMICAL ANALYSIS OF XE-348 BY EMISSION SPECTROSCOPY

Element	ppm	ppm as $CaCO_3$
Na	150	327
Mg	80	328
Al	10	56
Si	10	143
K	20	26
Ca	150	374
Mn	3	5
Fe	30	81
Cu	5	8
Ag	1	2

97

Figure 50. Configuration of Deionizers in 50 kW Test Facility.

	DEIONIZER NO. 5	DEIONIZER NO. 7	DEIONIZER NO. 8
HEAD SPACE (L_1, V_1)	$L_1 = 7$ INCH	$L_1 = 4.5$ INCH	$L_1 = 7$ INCH
MIXED BED (L_2, V_2)	$L_2 = 35$ INCH $V_2 = 12$ LITER BIORAD RG-501-X8	$L_2 = 15$ INCH $V_2 = 5$ LITER ROHM & HAAS IRA900/IR200	$L_2 = 26$ INCH $V_2 = 9$ LITER BIORAD RG-501-X8
CATION BED (L_3, V_3)	$L_3 = 3$ INCH $V_3 = 1$ LITER ILLINOIS WATER TREATMENT TC-2	$L_3 = 13$ INCH $V_3 = 4$ LITER ROHM & HAAS IR-200	$L_3 = 13$ INCH $V_3 = 4$ LITER ILLINOIS WATER TREATMENT TC-2
ORGANIC TRAP (L_4, V_4)	$L_4 = 0$ $V_4 = 0$	$L_4 = 13$ INCH $V_4 = 4$ LITER ROHM & HAAS XE-348	$L_4 = 0$ $V_4 = 0$

5.03" DIA.

L_1 (INCH)
V_1 (LITER)

L_2
V_2

L_3
V_3

L_4
V_4

HEAD SPACE — MIXED BED — CATION BED — ORGANIC TRAP

FLOW

DIRECT ENERGY CONVERSION PROGRAMS

Deionizer No. 8, which contained an extended cation bed, ran with DOE-41 (single cell). No amine was found after 100 hours. The activity of deionizer No. 8 seemed to be adequate, at least for a single cell. Its adequacy for larger stacks was verified by subsequent test of a 12-cell module in the 200 kW system.

As a further extension of these investigations, the comparative effects on contamination of fully-deionized vs. partially deionized anode loops were evaluated through operation of single-cell module DOE-41. The module test took place in two modes: In the first mode, the cell was set up so that the entire anode flow stream was passed through the deionizer, forming a fully-deionized loop. During the 635 hours of the test, the performance (see Figure 51) remained invariant at the 1.91 V level (1000 ASF, 180°F) predicted from the resistance of the components.

During the second mode of the test - the final 365 hours, the piping of the module was rearranged to the traditional configuration. With this partially-deionized anode loop, the anode flow is continuously recycled, with only the makeup water being deionized as it is fed to the loop. It was found at the start of operation that the performance was 30 mV poorer than experienced during the first mode. The voltage remained invariant during the second-mode testing.

No amines were found in the membrane on disassembly indicating that the new deionizer, with its extended cation tail, had functioned effectively to trap amines in either mode.

Since incorporation of a fully-deionized anode loop represents serious ramifications for the system, this mode was not pursued further.

While no amines were found in the cell, there was evidence of extensive Fe contamination. This iron most probably entered the cell from corrosion of the Teflon-coated steel endplate in an area outside the cell where the edge of the SPE outside the cell and the endplate were inadvertantly in contact. To prevent such contamination in the future, a titanium sheet is being incorporated as a shield between the stack and the endplate/current bus bars.

Some membrane blistering was also found in DOE-41. Blistering of this nature is usually caused by the confluence of a number of factors on a localized area: insufficient water, elevated temperatures, and iron contamination.

4.6.25   DOE-43 & 45 - Improved Sealing

Two 12-cell modules (DOE-43 and DOE-45) were somewhat interrelated and will be discussed together. The configurations of the modules were:

DOE-43

Stack A (top stack) was composed of collectors with spot-adhered foils. The seals on the anode side of the collectors was taped with 3 mil TFE. A bead of silicone glue was placed on the hydrogen overboard seal to augment sealing.
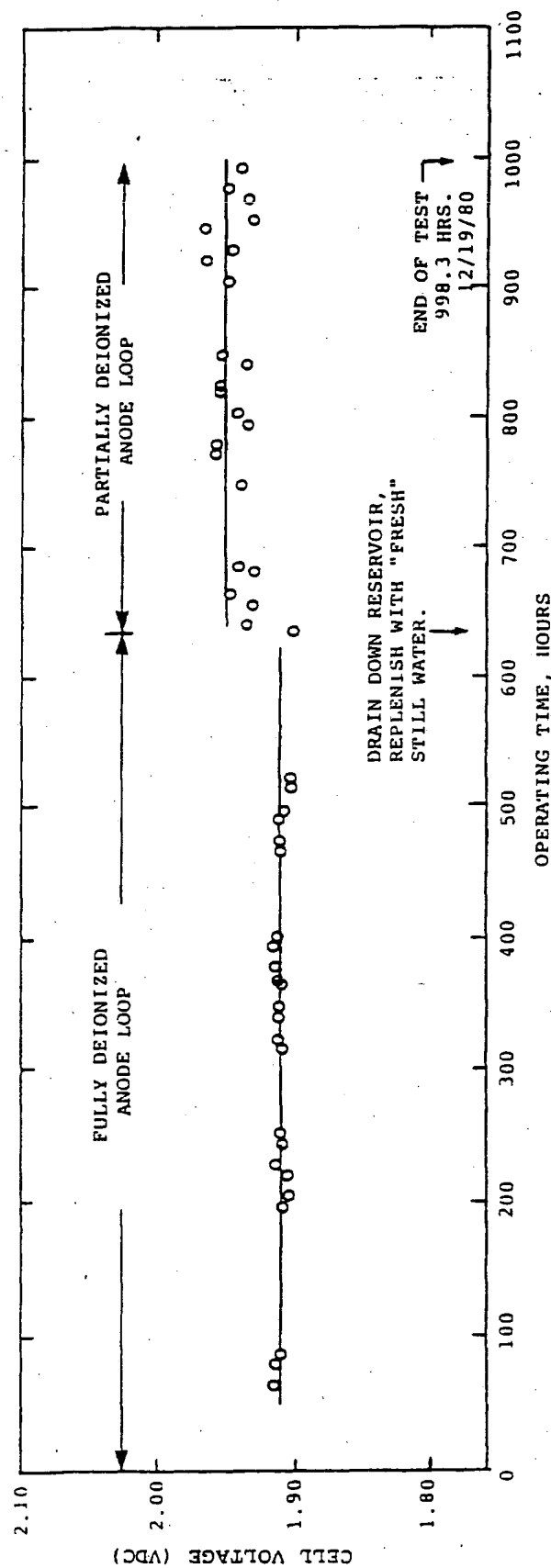
99

Figure 51. Performance History of DOE-41

Stack B (bottom stack) was composed of collectors with fully ad-
hered foils, anode side TFE taped, and no glue bead.

DOE-45

Stack A - same stack as DOE-43A.

Stack B was composed of the same collectors as DOE-43 Stack B,
except that the tape on the oxygen side was removed and the col-
lectors were taped on the hydrogen side seals.

Table 6 summarizes the configurational differences between the two
stacks.

DOE-43 was heat soaked in the separate heat soak fixture at 240°F
for about 16 hours. Sealing and operation were achieved.

No heat soak was required to achieve a seal at 125 psi on DOE-45.
It was, therefore, decided to continue the use of the TFE tape on the hydrogen
side of the collector rather than on the oxygen side. Subsequent stacks also
verified the efficacy of hydrogen side tape.

Figure 52 shows the performance history of the two modules. Sev-
eral points deserve further discussion:

1) In DOE-43, the average cell performance was the same for the
    stack with spot-adhered foils as for the stack with fully ad-
    hered foils. Since the method of attachment produces no sig-
    nificant performance effect, the foil configuration which of-
    fered the best reliability of manufacturing and cell assembly
    was chosen, that is, the fully adhered foil.

2) The subsequent module DOE-45 showed an increase in voltage of
    about 30 mV in steady state. This was accounted for by the
    increase in collector resistance which has usually accompanied
    the depressurization of the endplates.

3) The performance of DOE-45 was fairly invariant with time over
    a period of about 430 hours. Both stacks behaved similarly,
    1.96 v/cell at 1000 ASF, 180°F.

4) The feed water to the anodes was of high purity (15 megohm-cm)
    during the duration of testing (600 hrs). This verified the
    efficacy of the deionizer having the upstream bed of resin and
    an equal-sized bed downstream of strong cation resin.

5) The water in the circulating loop was of excellent quality (6
    megohm-cm) over the 600 hour test period.

The testing was suspended on 9 Mar 81 in response to a Stop-Work
order from DOE. DOE-45 was placed in a dormant condition with endplates
maintained at design pressure temporarily.

101

TABLE 6

CONFIGURATION OF 12-CELL MODULES DOE-43 AND DOE-45

MODULE & STACK DESIGNATION	UPPER STACK	LOWER STACK	O_2 SIDE TAPE	H_2 SIDE TAPE	H_2 SIDE SI GLUE	SPOT ADHERED FOIL	FULLY ADHERED FOIL	NO. OF CELLS
DOE-43 STACK A	X		X		X	X		6
DOE-43 STACK B		X	X				X	6
DOE-45 STACK A			REUSED DOE-43 STACK A					
DOE-45 STACK B		X		X			X	6

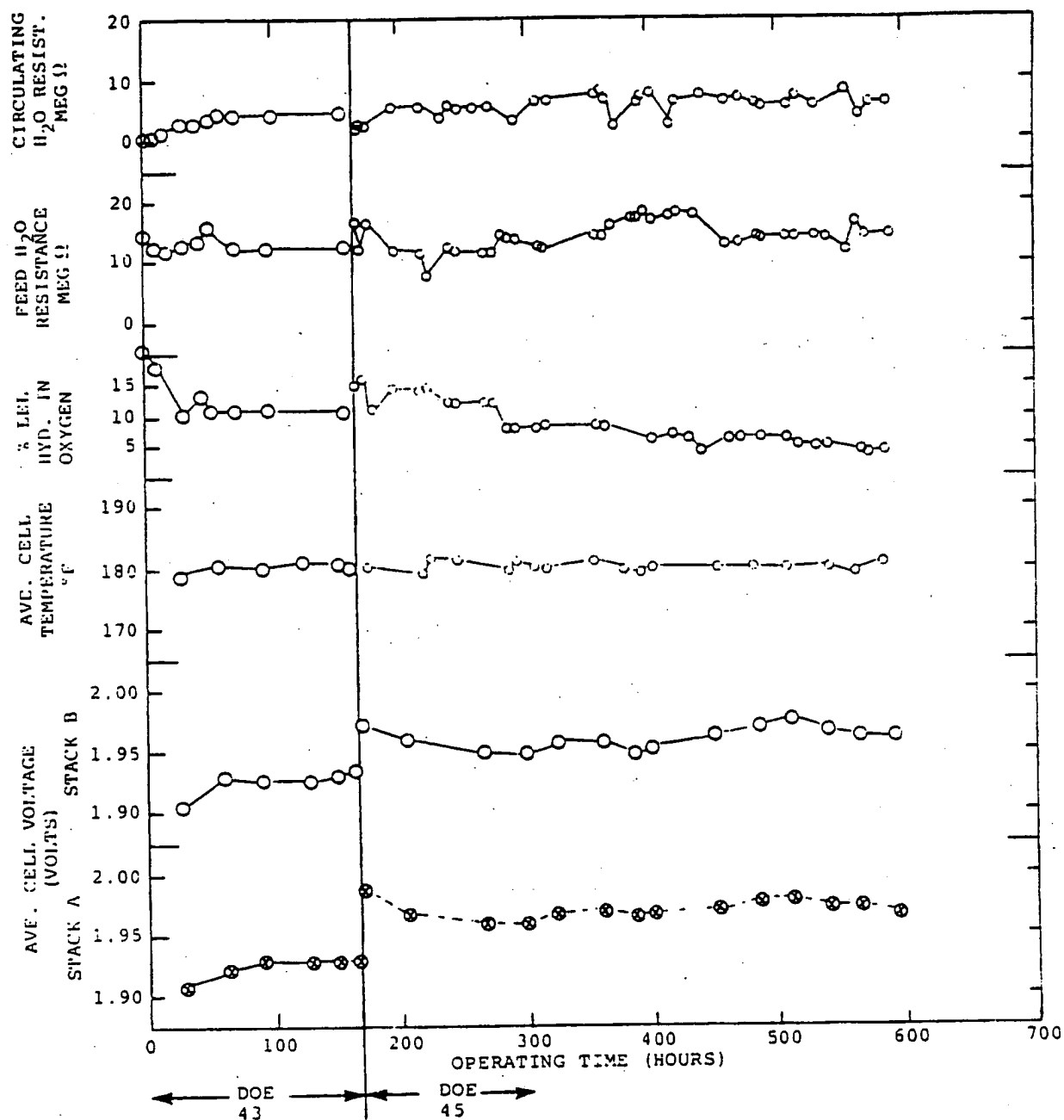NOTE: All Collectors were reused from DOE-42 in the same location in the stacks.

Figure 52.   History of Modules DOE-43 and DOE-45

4.6.26   DOE-44 - Low Catalyst Loaded 2.5 Ft^2 Module

Module DOE-44 was a 3-cell stack of M&E's having low catalyst loading ($15/ft^2 total). It contained collectors with Teflon tape on the oxygen seal area and a bead of silicone glue on the hydrogen side overboard seal.

The cell was sealed without a heat soak, and operation was initiated. At the outset, at 1000 ASF, the amount of hydrogen in the oxygen was above the shutdown limit of 1.6%, and the stack current had to be increased to 1500 ASF to dilute the anode gas. After about 60 hours, the stack could be run at design current density of 1000 ASF. Over the 600 hour test, the cell voltage rose from about 2 v/cell to 2.03 v/cell (see Figure 53). The higher-than-normal hydrogen in oxygen, as well as the voltage degradation, was attributed to the low catalyst loading.

Feed water quality (Figure 54) tended to fall with time, indicating that some ionic species was not being removed from the recycled water. In order to determine the source of the ionic species, the hydrogen side water was dumped overboard at the 230 hour point in the test. For the remainder of the test, the feed water improved quickly to 18 megohm-cm and higher (ultra pure). It can be concluded, therefore, that an ionic species was coming from the hydrogen side of the module. Measurements on the hydrogen water effluent showed the presence of fluoride. Since fluoride is only removed with difficulty in demineralizers, it was concluded that fluoride from the hydrogen side was the cause of earlier feed water quality problems.

Disassembly of this module showed that two of the three M&E's exhibited several small blisters in the oxygen exhaust regions, customarily the hottest regions. The presence of fluoride in the hydrogen exhaust was undoubtedly resulted from this membrane degradation.

Membrane degradation of this type is typically caused by poor water transport. A program to determine the causes of poor water transport was implemented under the technology development program funded by others.

4.6.27   DOE-46 - Thinner Membrane Module

A three-cell stack (DOE-46) was constructed using:

● Thinner SPE (9 mils wet vs. 12 mils) to verify the performance improvement associated with lower cell resistance and to demonstrate the sealing capability of thin membrane.

● Solid polymer electrolyte containing the degradation inhibitor used on other programs to eliminate membrane blistering and to lower the permeation of hydrogen through the membrane. Two of the M&E's were treated. The results of this testing showed:

   ● Sealing was satisfactory and without the need of a heat soak. This indicates that there is no fundamental problem sealing the thinner membrane.

0.5 mg/cm^2 catalyst
2.25 ft^2 active area
12 mil (wet) membrane
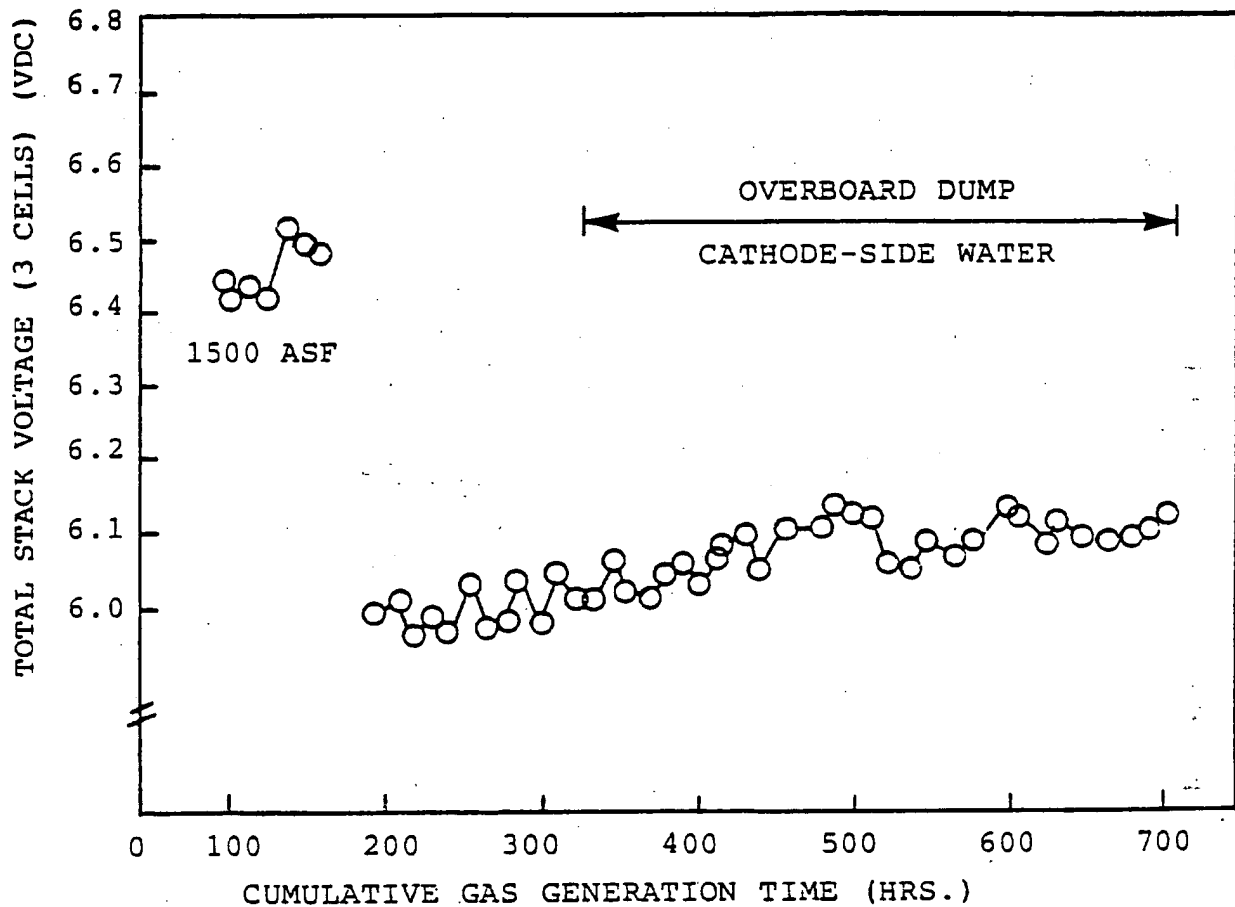Oxygen pressure = 100 psig
Hydrogen pressure = 50 psig
Temperature = 180°F

Figure 53. History of 3-Cell DOE-44 (Low Catalyst Loading)
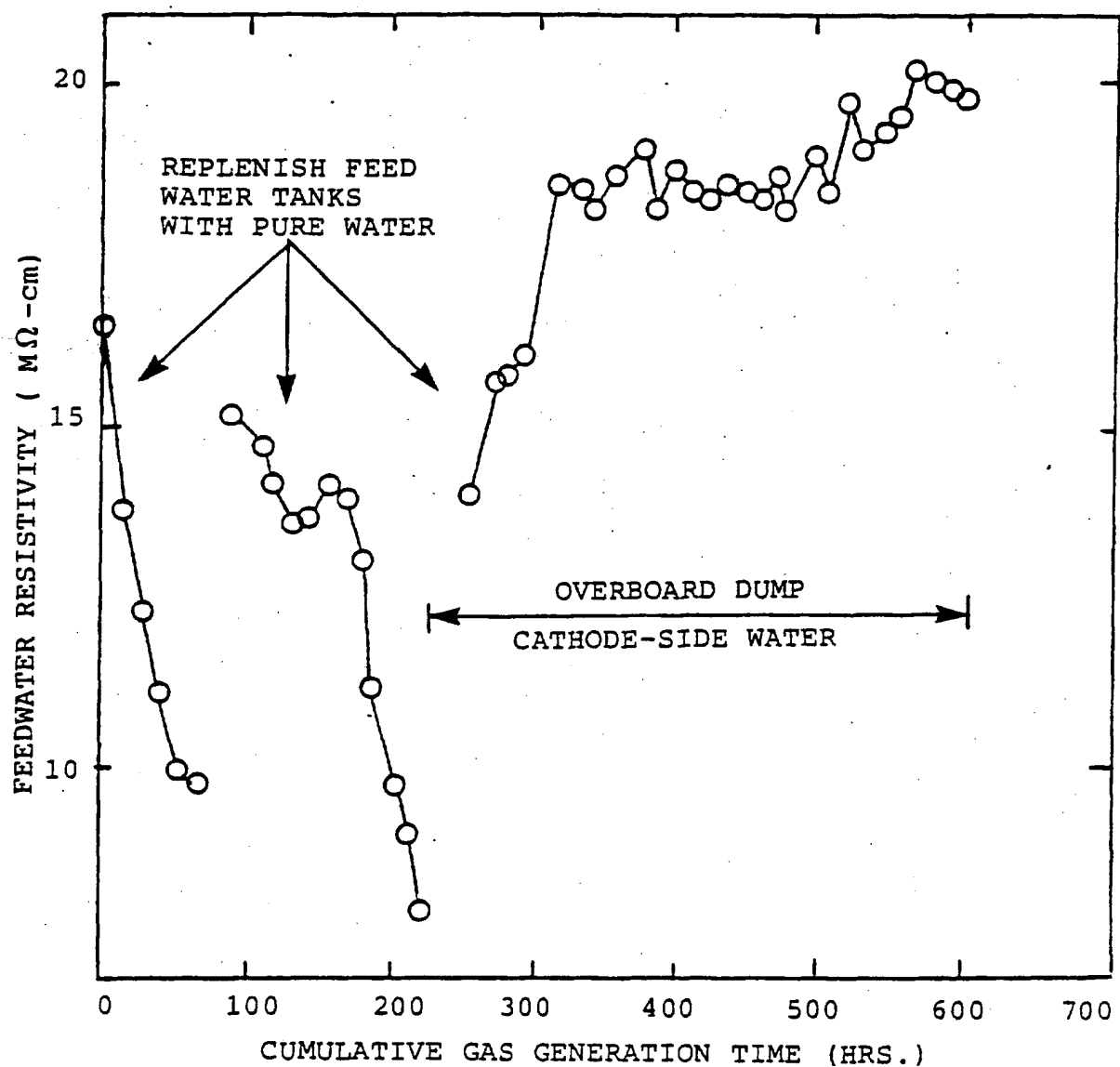
DIRECT ENERGY CONVERSION PROGRAMS

Figure 54. Feed Water Quality During DOE-44 Testing.

- The voltage at 1000 ASF, 180°F was 1.82 volts per cell versus about 1.90 for standard cells. This indicates that all the conductive benefits of the thinner membrane were realized.

  The amount of hydrogen in the product oxygen was 0.6% versus previous standard cells of 1.2%. This, coupled with the facts that these membranes are thinner, and only 2 were treated, indicates the effectiveness of the membrane treatment.

- The polarization curve (Figure 55) showed a tendency to "tail" upwards when run at high current density (above 1700 ASF). This is indicative of lower than design water flow, similar to the effects in other recent modules.

Testing of DOE-46 was suspended on 9 Mar 81 in response to a Stop-Work directive from DOE. The facility has been secured.

4.6.28   Performance Improvement Analysis

The testing of full-scale modules has generally shown that the average cell voltage will be approximately 90 mV higher than demonstrated by small laboratory-size cells at similar conditions of 180°F and 1000 ASF. Much of the difference arises from penalties incurred in the scaled-up cells due to use of a slightly thicker membrane with a slightly lower ion exchange capacity, slightly thicker collectors, and operation at a higher pressure.

The data in Table 7 are useful in illustrating these conclusions. This table compares actual and predicted (calculated) voltages for various cell configurations, both lab-sized and full-scale. The calculated value is made up of resistive elements added to the initial IR-free voltages for appropriate elements within each cell configuration. Total calculated voltage can be compared to the actual voltage demonstrated by the respective configurations while under test. It can be seen that the calculated values agree closely with the experimental results.

For instance, in the case of the 2.5 ft^2 cells tested (columns 3 & 4), the membrane used was 3 mils thick (wet) with an ion exchange capacity (IEC) of .83. The membrane used for the 1/20 ft^2 cells tested was 12 mils thick, with an IEC of .86. The table shows a difference in voltage of 54 μohm ft^2 due to these factors. In addition, the thickness of the two types of collectors differed: .205 vs. .165 inch for the 2.5 ft^2 and lab-sized collectors, respectively. This difference is felt to be primarily responsible for the range in collector resistance from 42 μohm ft^2 for the laboratory hardware, to 57 to 100 μohm ft^2 for the larger collectors.

Finally, the large cells operate at 100 psi, incurring a 20 mV penalty over laboratory-size cells, which operate at ambient pressure.

It can be seen that the calculated cell voltage for 2 1/2 ft^2 cells is 1.836 to 1.904 volts at 1000 ASF, 180°F. The test results for the 12-, 30-, and 60-cell modules (DOE's 31, 32 and 33, respectively) range within this band.

3-CELL MODULE
180°F OPERATION
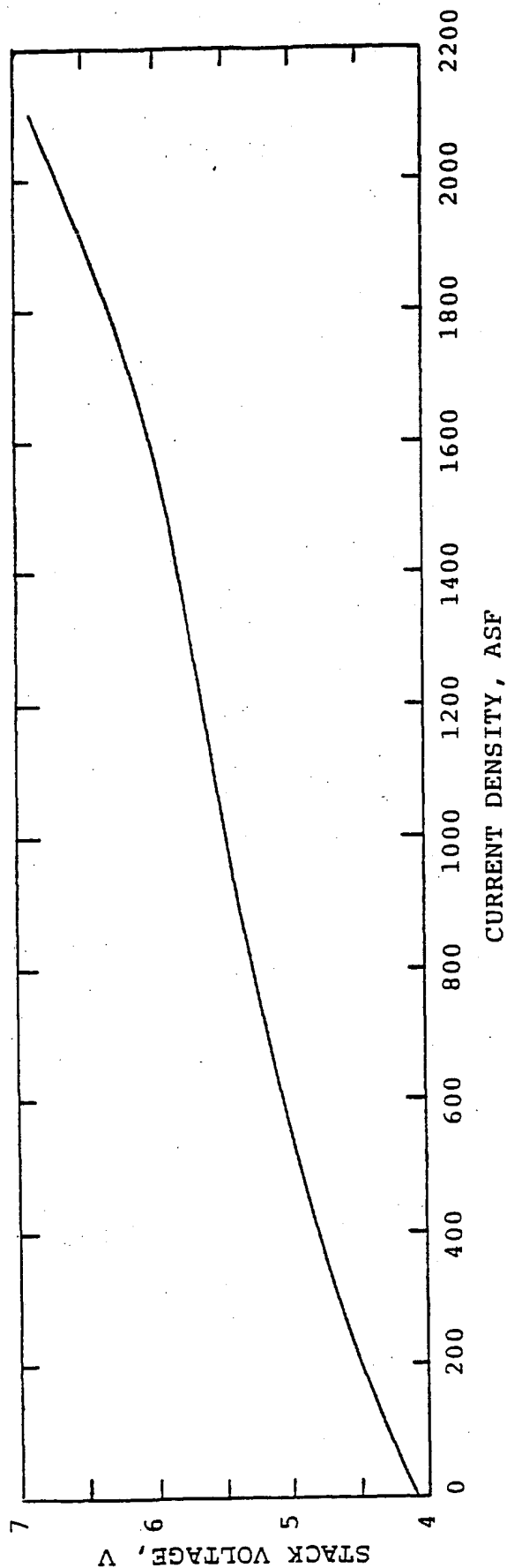HYDROGEN PRESSURE = 100 psig
OXYGEN PRESSURE = 150 psig

Figure 55.   Performance of DOE-46

DIRECT ENERGY CONVERSION PROGRAMS

TABLE 7

INITIAL VOLTAGE OF ELECTROLYZERS @ 1000 ASF, 180°F

	(1)	(2)	(3)	(4)	(5)	(6)	(7)
		2½ Ft³ Cells				3 x 3 Cells	Possible 2½ Ft² Stack
VOLTAGE ELEMENT						3x3 Cut Outs	
			Hi	Lo			
IR Free Voltage		1.485	1.485	1.485	1.485	1.485	1.485
ΔV SPE for Wet Thickness:							
9 mil 1150 EW = .87 IEC		.165					.165
10 mil 1150		.183					
11 mil 1150		.202					
12 mil 1150		.220				.220	
12 mil 1200 EW = .83 IEC		.253					
13 mil 1200		.274		.274	.274		
13 mil 1250 EW = .80 IEC		.299	.299				
100 psi H₂ Pressure		.020	.020	.020	–		.020
Collector ΔV			.100	.057	.042	.042	.079
CALCULATED CELL VOLTAGE			1.904	1.836	1.801	1.747	1.749

TEST	DOE-31	1.852	
	DOE-32	1.865	
	DOE-33	1.893	
	Average of (9) 3 x 3's	1.816±.014 (1.802 to 1.83)	
TEST	Average of (33) Cells	1.740±.026 (1.714 to 1.773)	

109

DIRECT ENERGY CONVERSION PROGRAMS

Also, when run in laboratory hardware, the performance of 1/20 ft^2 cutouts from 2 1/2 ft^2 cells falls near the calculated value of 1.801 volts.

Laboratory-size cells were calculated to run at 1.747 V, while actual performance measured 1.740 V.

Column 7 shows that a performance of 1.749 V has been calculated for a hypothetical 2.5 ft^2 stack configured with a) thinner (9-mil, wet) membrane with an IEC of .87, and b) scaled-up collectors of an average resistivity. Thus the goal of 1.80V should be achievable, even at moderate temperatures. The procurement of a thinner membrane with an increased IEC, held to closer tolerances, is being negotiated with the manufacturer.

The data used to predict the cell voltage are presented in Table 8, which lists the component resistances measured in small stacks. The numbers agree with previous resistance measurements.

TABLE 8

COLLECTOR VOLTAGE DROPS AT 1000 ASF, mV

From 2.68 x 2.68 in^2 cutouts stacked in a 3 collector series array with supports.

Contact - Carbon paper to H$_2$ collector	20.7 ± 10.1
Carbon paper bulk	2.0
Porous Ti bulk	1.0
Contact - Porous Ti to collector foil	8.0 ± 2.4
Collector foil bulk	0
Contact - Collector foil to collector	10.8 ± 0.9
Center collector bulk (.205 thick)	36.0 ± 7.8
	78.5 ± 21.2
	(57.3 to 99.7)

4.7   Fabrication of 2.5 ft² Cells with Updated Technology

4.7.1   Collectors

4.7.1.1   Increased Sealing Ridges

In stacks containing collectors with the 4-mil, molded-in sealing ridges (see Figure 56), it has been found that cross-cell sealing has been excellent, but overboard seals have been marginal.

In order to improve the sealing, the height of the sealing ridges was increased. Considering the stack-up of parts, it was determined that the ridge height should have been 7 mils rather than 4 mils.

The mold was modified to change the ridge configuration to that shown in Figure 57. The radius at the top of the ridge was also increased to 3 mils to allow for better separation from the mold.

A collector molding run was made at Premix Corp., where 143 collectors were manufactured. Only 15 of these collectors were judged acceptable enough to go through final machining. Most of the collectors showed excessive run-out due to the fact that the pre-form mold had become worn. The worn pre-form mold was remachined. In addition, a new mold was designed which hydraulically positions the edge members to control mold clearance. The new mold also allows controlled opening and venting of the preformed part during the preforming cycle.

4.7.1.2   Collector Resistance

Figure 58 depicts a resistance fixture which was built to facilitate development of resistance profiles. The fixture consists of two square, 0.5 inch-thick, copper electrodes, each 0.05 ft² in area, configured in the direction of flow. The voltage probes are introduced at the center of the electrodes so that they touch the specimen to be measured and are insulated from the electrodes. To provide uniform pressure against the specimen, standard porous "carbon paper" is used as a cushion. The carbon papers are provided with holes through which the voltage probes pass. The fixture is loaded by using a hydraulic cylinder.

Several component resistivities were measured. The results in Table 9 show that collectors being molded at the new vendor, Premix Corporation, have about the same resistivity as those molded earlier at the original vendor, Brush-Wellman Inc.

In addition, it can be seen that if one adds the component hardware resistances for a single cell with new parts, the results indicate a drop in hardware resistance of about 70 mV at 1000 ASF. The same value was measured by stacking all parts of a cell and measuring the entire package.
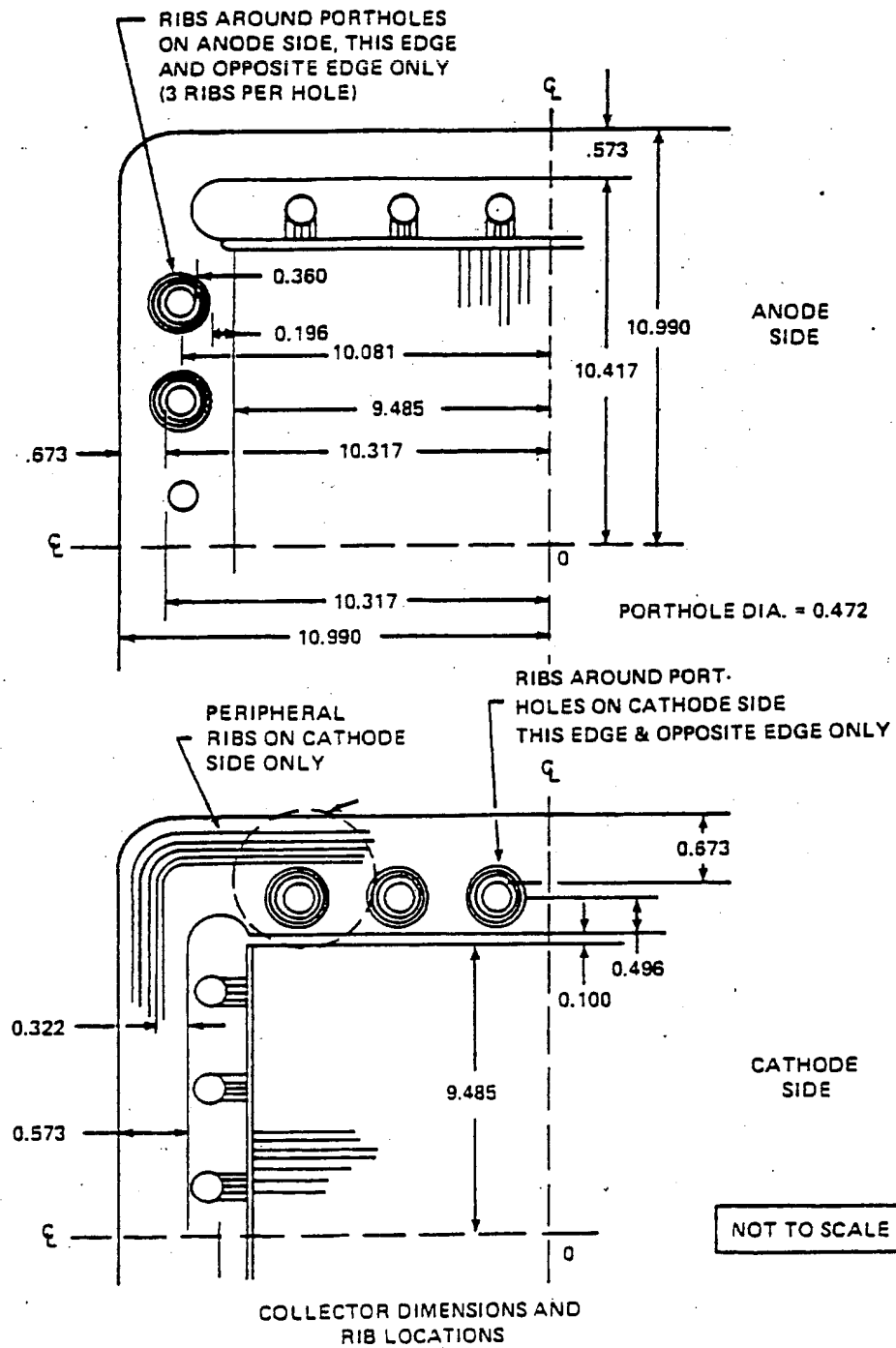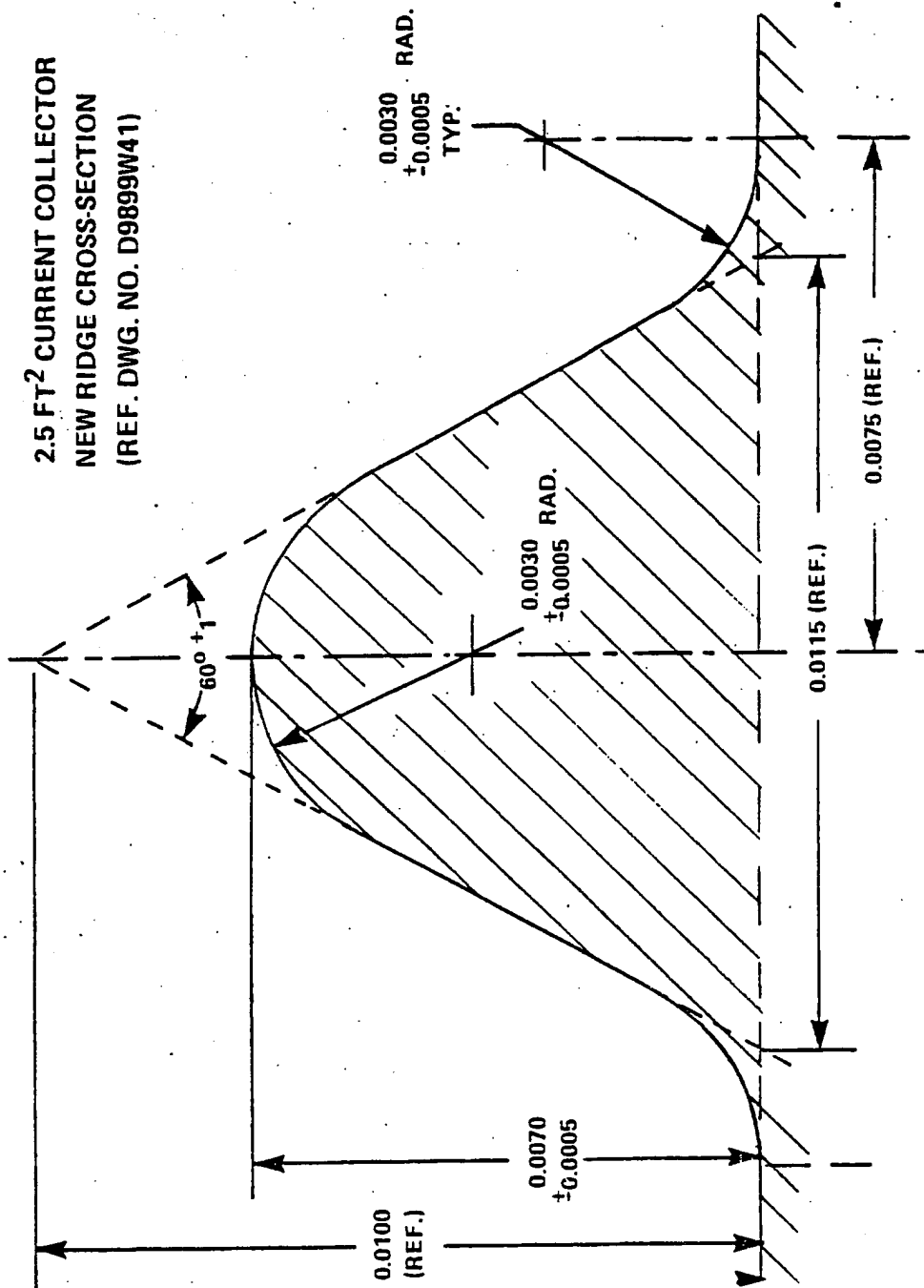
111

RIBS AROUND PORTHOLES ON ANODE SIDE, THIS EDGE AND OPPOSITE EDGE ONLY (3 RIBS PER HOLE)

0.360

0.196

10.081

9.485

.673

10.317

10.317

10.990

.573

10.990

10.417

ANODE SIDE

PORTHOLE DIA. = 0.472

RIBS AROUND PORT· HOLES ON CATHODE SIDE THIS EDGE & OPPOSITE EDGE ONLY

PERIPHERAL RIBS ON CATHODE SIDE ONLY

0.673

0.496

0.100

0.322

9.485

0.573

CATHODE SIDE

NOT TO SCALE

COLLECTOR DIMENSIONS AND RIB LOCATIONS

Figure 56. Collector Dimensions and Rib Locations

112

2.5 FT² CURRENT COLLECTOR
NEW RIDGE CROSS-SECTION
(REF. DWG. NO. D9899W41)

SCALE: 500X

0.0030 RAD.
±0.0005
TYP.

0.0030 RAD.
±0.0005

0.0075 (REF.)

0.0115 (REF.)

60° +1

0.0100 (REF.)

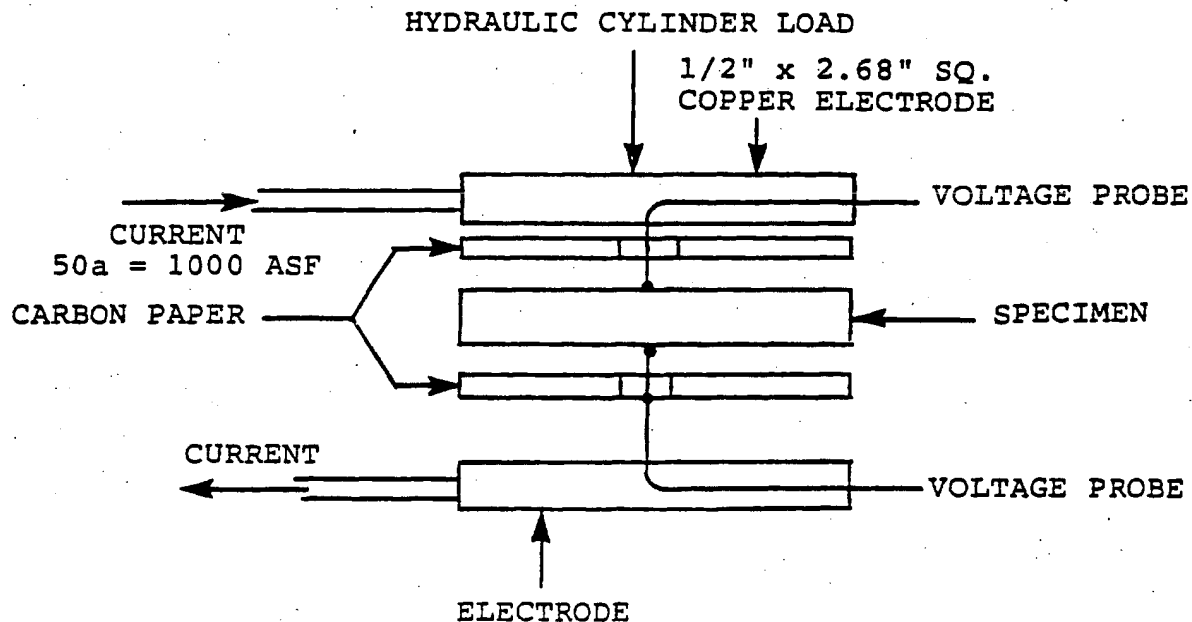0.0070 ±0.0005

Figure 57. New Sealing Ridge Design

113

Figure 58. Resistance Fixture

TABLE 9

RESISTIVITIES OF CELL COMPONENTS

(pl) are Resistivities in (micro ohm ft^2) = $\dfrac{mV}{1000\ ASF}$

Contact Pressure = 300 psi $\dfrac{pl}{\mu ohm\ ft^2}$ = $\dfrac{mV}{1000\ ASF}$

Component & Resistive Description	New	Used
Phenolic Collector with Ti Foil	12	
Phenolic Collector without Ti Foil	8	
Machined Kynar/Carbon Sheet (Flat), Platinized	14	
BWI Center Collector with Ti Foil	30-35	41-295
BWI Center Collector without Ti Foil	20	21
BWI Hydrogen End Collector	8-14	
BWI Oxygen End Collector without Foil	16	
Premix Center Collector with Ti Foil	35	
Premix Center Collector without Ti Foil	20	
(2) Sheets of Carbon Paper	2	
Porous Ti Support	1.3	
Contact Carbon Paper to Cathode of Collector	17-23	
Kynar/Carbon Bulk	20	
Contact Collector to Ti Foil	10	
Contact Porous Ti to Ti Foil	20	
Adding	70-76	
Measured Total Cell Including Supports, Excluding M&E	68	

114

When measurements are made on a previously operated collector, the resistance significantly increases between the collector and the foil. The resistance increases more in the region where the cell is hottest (anode exhaust), as might be expected. The resistance of the bare carbon collector, however, is not affected by operation. These data re-emphasize the need for a better foil-to-collector interface.

4.7.1.3 Molding Development

The second molding run at Premix Corp. resulted in poor sealing ridge formation on the collectors. Investigations were conducted to define the malformations, determine the reasons for the imperfections, and define corrective actions.

The problem can be described as follows: The sealing ridges in the collector edges which run perpendicular to the H_2 field ribs were displaced laterally 5 to 10 mils from the position in which they were formed. Evidently the ridges were formed under heat and pressure, but when the mold was released, the collector and mold punch moved relative to one another, causing the two parallel sets of ridges to be shifted in the same direction. Since the ridges parallel to the H_2 field ribs were not affected, it seems that the ribs prevented the collector from moving sideways, but rather guided the motion along the grooves, acting as rails.

Measurements of the mold made by Premix personnel showed that all the mold dimensions were within specified limits and that the mold guide pins and bushings were true.

There were two major differences in equipment used in the first and in the second, less successful molding run that are believed to have affected the collectors produced. A different press was used in the second run which is larger and faster than used in the first. The second press also has three rams instead of one which could cause platen bending and spring-loading of the mold. The much higher speed of opening could cause the collector to be sucked up by the punch with relative sideways motion. While the press construction will not be modified, the opening speed will be slowed to avoid sudden accelerations of the collector on punch disengagement.

In addition, new transite thermal insulators were used in the second run along with 1/16-inch lead sheets to take up misalignment.

A third molding run was made to resolve the ridge breakout problem and produce collectors for operational evaluation.

The explanation for this phenomenon was that the platen was shifting slightly during the degas cycle, when the press pressure was being automatically reduced, causing the ridges to shear. This action was corrected by increasing the pressure slightly during the degas cycle. Thereafter, the collector ridges have emerged from the molding cycle undamaged.

DIRECT ENERGY CONVERSION PROGRAMS

During this molding run, preforms prepared in the standard manner exhibited a lower-than-normal thermal expansion. With a pre-heat temperature of 480°F, the preforms did not expand enough to completely fill the mold. This resulted in parts with unacceptable edge porosity. The problem was corrected by increasing the molding pressure from 3000 to 3500 psi, and the preform temperature from 480 to 535°F. This resulted in parts of good density. The electrical resistivity was, however, slightly increased.

Discussions were conducted with the resin manufacturer to define quality control provisions which might result in more uniform expansion characteristics.

During the latest molding run in January 1981 a more uniform blended molding material was used and 92 collectors were molded with an 83% yield. Improvements in collector porosity, resistance, and density were realized.

A new hydraulically operated preform mold, designed to improve preform uniformity, was delivered to Premix Inc. from the mold maker. The electrical and hydraulic control systems have been installed and system is ready for checkout. This checkout was held up as a result of the DOE Stop-Work order. Completion of this work is planned under the continuing program during 1982.

4.7.1.4   Collector Porosity Effects

An extensive investigation of sealing was conducted on 12-cell module DOE-43. As shown in Figure 59 the sealing of this module was a function of time at pressure. In one case, the leakage rate increased after a considerable time from essentially membrane diffusion only to 5 times membrane diffusion. The leakage could be stopped by filling the stack with water and then immediately blowing the water out with gas. Thereafter, a seal could be achieved for a relatively long time.

This behavior was indicative of the effects of collector porosity. That is, pores in the collector could be sealed with water which then could be blown out or evaporated as a function of time and pressure if no more water was added to the system. Since, in operation, water is continually supplied to both sides of the collector, it is reasonable to conclude that if a water seal can be achieved for 1/2 to 1 hour in a static condition, it can be achieved indefinitely when water is continually supplied. Therefore, leak-test procedures were modified to insure that the proper water content of the system is maintained. This reduced the time expended in preliminary testing and provided more consistent and meaningful results.

The validity of this hypothesis and the proposed corrective actions were then tested. Collectors were selected from the production runs and tested for permeability. The setup was arranged so that any measured leakage had to be through the collector material, not through the portholes. This was insured by not drilling the portholes.

The results are shown in Figure 60, the bar graphs indicating permeability in cc/hr-psi. (For comparison, the normal permeability of membrane at 70°F is approximately 1-2 cc/hr-psi.)
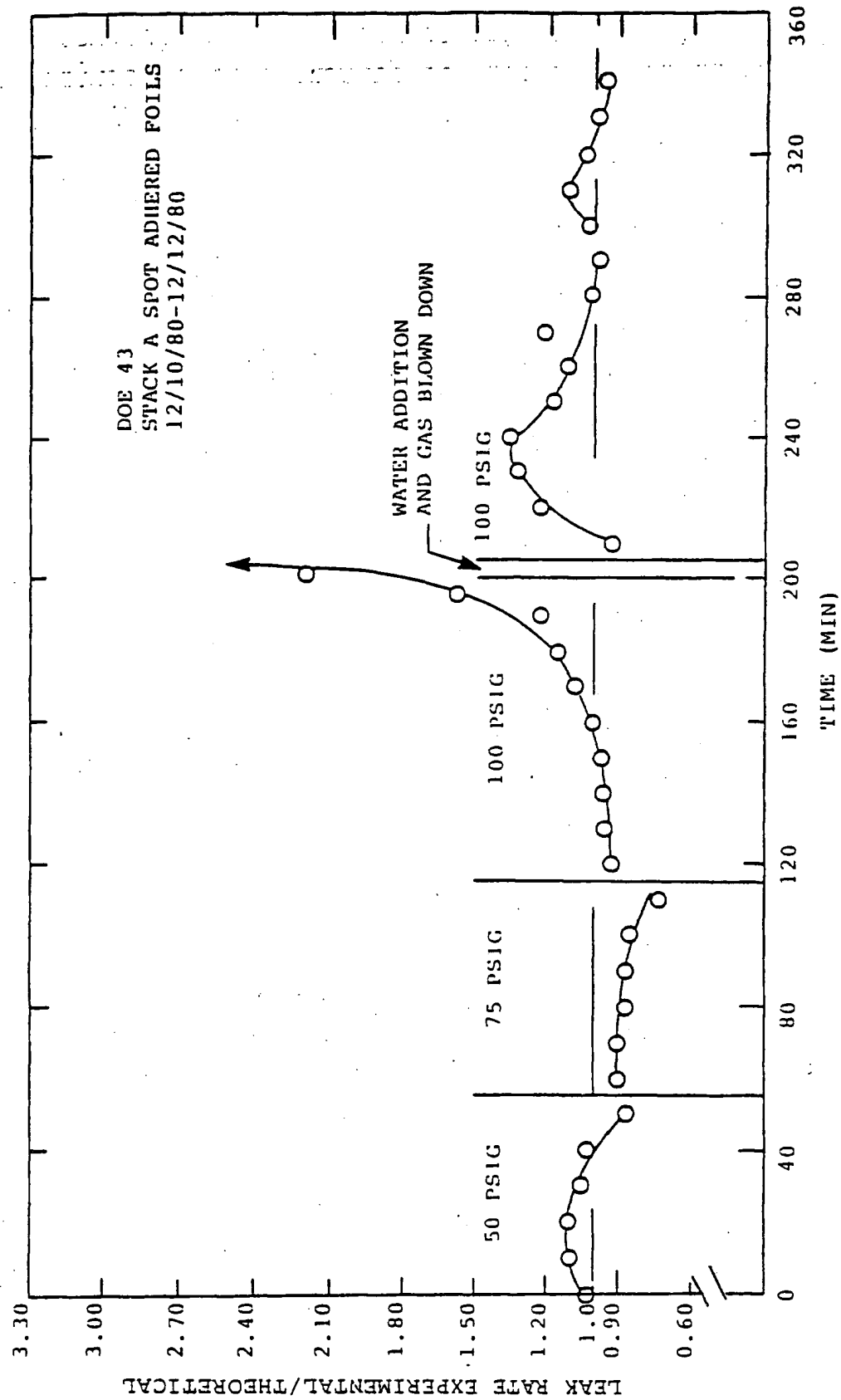
Figure 59. Leakage History of Module DOE-43

117

Pa = PRESSURE APPLIED TO ANODE SIDE OF COLLECTOR (FOIL SIDE)
Pc = PRESSURE APPLIED TO CATHODE SIDE OF COLLECTOR (FOIL SIDE)

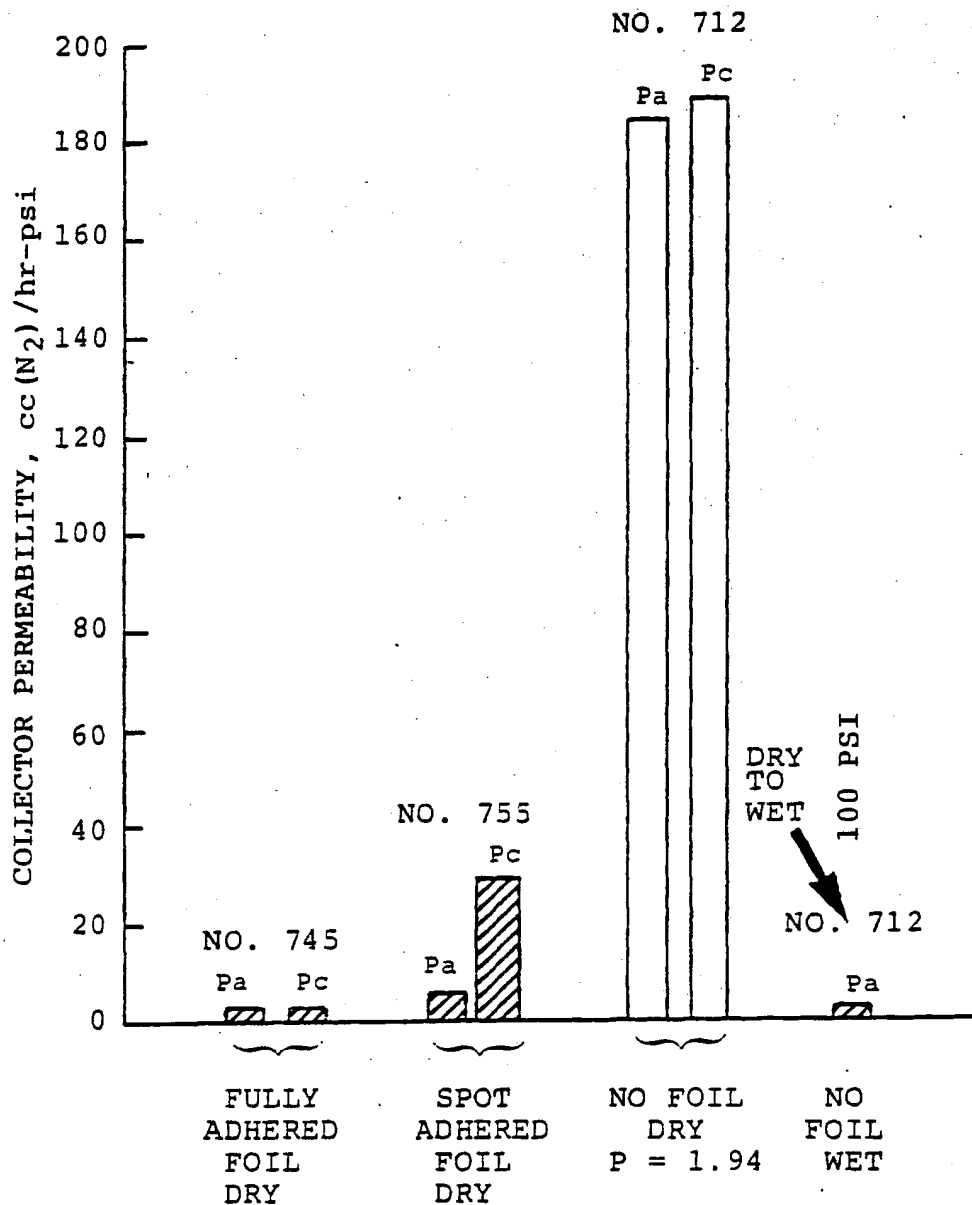TESTS RUN AT 25 TO 50 PSIG NITROGEN PRESSURE EXCEPT AS NOTED

Figure 60. Bar Graph Showing 2 1/2 Ft^2 Collector
Permeability for Various Configurations
Premix Run 11

The results showed that the collectors are indeed permeable. A collector with fully-adhered foil has a low, although measurable, permeability, about 1 to 3 cc/hr psi. The results are approximately the same when the collector is pressurized from either side. This indicated that the foil forms a tight barrier to gas. The spot-adhered foil shows a higher permeability when pressurized from the carbon side of the collector. This was the result of a "check valve" effect of the foil on the collector surface.

The data derived from collector No. 712 were even more interesting. This collector had no foil and a rather low density. When the collector was dry, its permeability was two orders of magnitude greater than the normal permeability of membrane, and was the same in either direction. However, when the collector was wetted, the permeability decreased nearly to zero for a period of greater than one hour at 100 psi, a dramatic demonstration of a water seal.

It was concluded from these seal investigations that:

- It is necessary to use flexible (highly-conforming) endplates.

- Long-term sealing is achieved by liquid water which fills the porous areas of collectors.

- Reduced collector permeability will be beneficial to sealing.

4.7.2   Cell and Stack Sealing

During the development of the SPE electrolyzer, it has been determined that sealing is strongly related to the compression diaphragm configuration. Two configurations tested include:

- Edge-collection diaphragm

- Flexible-type diaphragm

The differences between these types of configurations are shown in Figure 61.

Figure 61a shows the flexible diaphragm originally designed and used during most of the program. This provides the ultimate in compliance to the stack, commensurate with the thickness needed to transmit electricity at minimal voltage loss. However, it is somewhat complicated to manufacture and allows water to fall into the space between endplate and diaphragm.

A simpler system is shown in Figure 61b, which allows the conducting diaphragm to be outside the endplate protecting it from water. To provide the seal, an integral ring was fit into the endplate cavity.

It was found that the edge-collection diaphragm consistently produced inferior seals compared to the flexible plate. The integral ring was too stiff to conform to stack-up tolerances in the collectors. To provide proper sealing, a flexible diaphragm must be used.
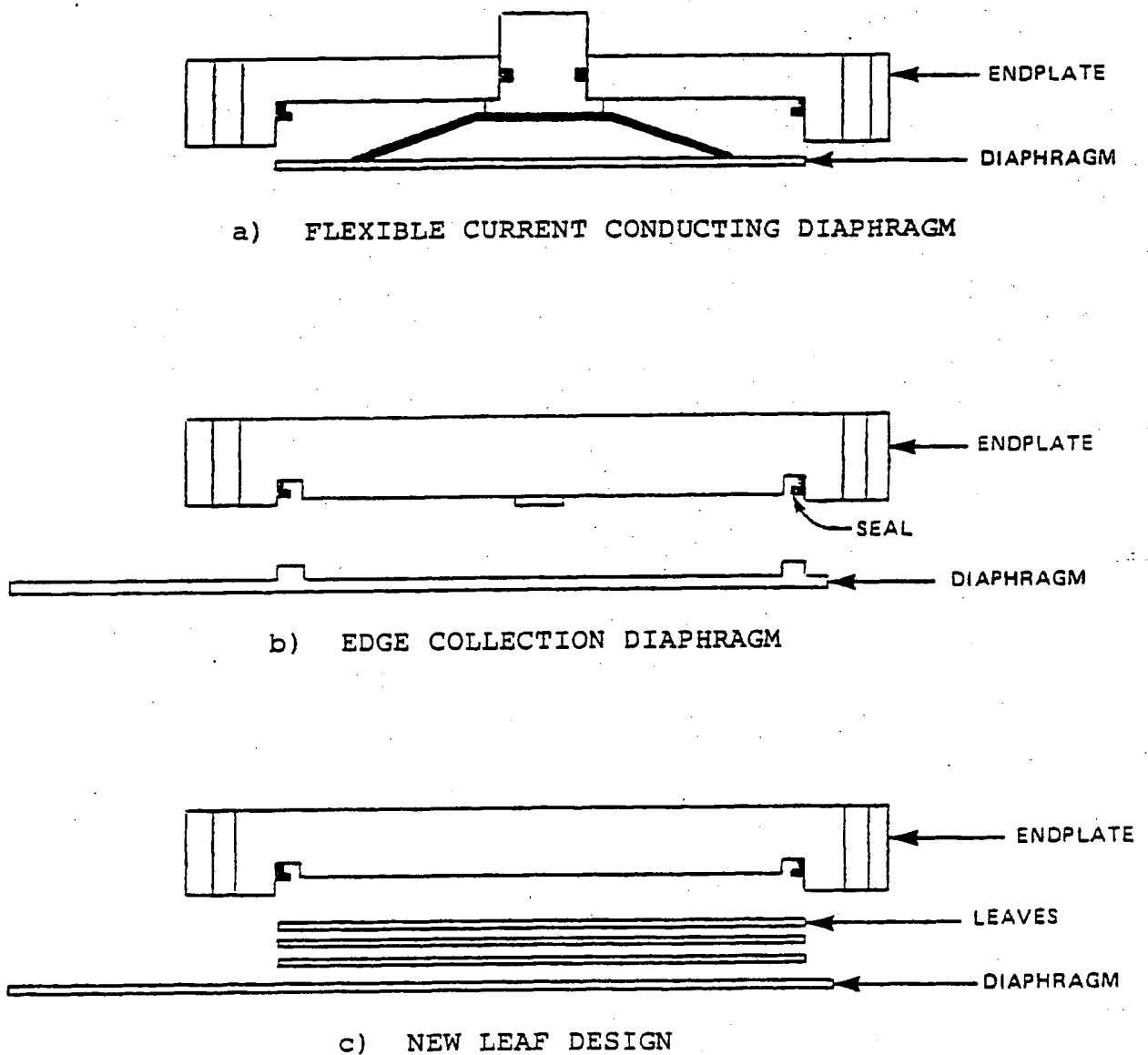
a)   FLEXIBLE CURRENT CONDUCTING DIAPHRAGM

b)   EDGE COLLECTION DIAPHRAGM

c)   NEW LEAF DESIGN

Figure 61. Three Types of End Plate/Diaphragm Configurations

120

A third variation being implemented consists of the leaf design shown in Figure 61c. This flexible configuration with edge current collection provides effective sealing while isolating water from the endplates. The concept has worked well in 1 ft^2 modules. Implementation in 2.5 ft^2 modules was delayed due to the DOE Stop-Work order.

4.7.3 Membrane & Electrode Assembly

In the area of membrane and electrode assembly fabrication, improved resistance has resulted from an optimization of the water content during the press cycle. In addition, the resistance of M&E's fabricated prior to the process optimization were improved by reprocessing.

This reprocessing procedure consists of re-equilibration in water and a repressing operation using the optimized water. Figure 62 shows typical results of the reprocessing steps, wherein M&E resistance is plotted against time in the resistance fixture. The level of resistance is clearly enhanced by the reprocessing steps. The decreases with time in the fixture are due to excess water exerting a transient hydrodynamic pressure which "floats" the flat surface of the resistance fixture above the electrode surface. With time, the water squeezes out, allowing the fixture to contact the electrode more closely. It is important, therefore, in measuring resistance, to allow sufficient time to reach steady-state resistance, otherwise discrepancies in contact pressure can yield unreproducible results.

The M&E manufacturing process was modified to reflect the improvement previously achieved with re-pressing. The M&E's are now made with controlled water content and show good reproducibility, eliminating the need for the extra re-pressing step.

4.8 Process Development of 10 Ft^2 Cell

In 1979, the design of a 10 ft^2 cell and module was accomplished under Gas Research Institute (GRI) sponsorship. During 1980, GRI sponsorship covered the labor and DOE sponsored the material associated with the process development of the 10 ft^2 cell. The DOE effort primarily entailed procurement of:

a) The power supplies, several major components and some electronic controls for a 200 kW system to serve as a test bed for 10 ft^2 cells.

b) Procurement of 10 ft^2 M&E tooling such as catalyst spreading molds.

The 10 ft^2 process development effort was terminated upon receipt of the DOE Stop-Work order in late February 1981. Further 10 ft^2 development will await a focused program which would justify the large collector tooling cost which would be required.
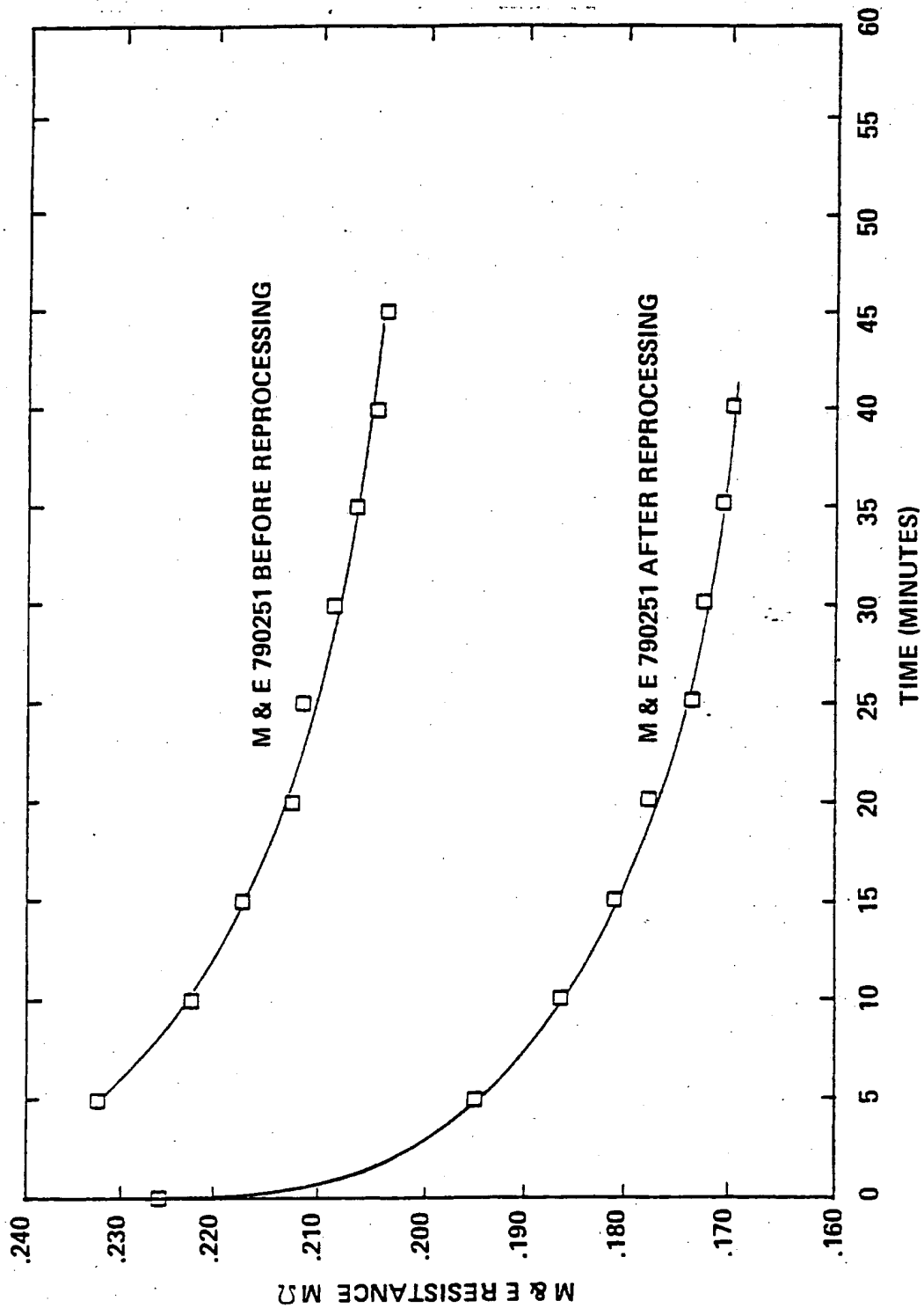
121

Figure 62.   Resistance of M&E's

5.0 TECHNO-ECONOMIC STUDY

During the latter part of GFY 81, a techno-economic analysis was performed to quantify the cost of hydrogen as a function of operational parameters (such as current density, operating temperature, and gas generation pressure) and design parameters (such as module cost and module performance capability). In addition, the sensitivity of the cost of gas to the various parameters was established.

Under this analysis a detailed cost estimate of an installed 2 MW SPE water electrolysis plant (battery limits) was completed based on current technology and a mature production level. Figure 63 shows, schematically, the system studied. A separate estimate was made for plants utilizing a single 10 ft^2 module and 4-2.5 ft^2 modules. The results of this cost study are shown in Table 10.

In addition, costs were estimated at 3 catalyst loadings: the standard catalyst loading of 4 gms/ft^2 which represents the bulk of our 2.5 ft^2 test experience and produces the best cell performance and module efficiency, a reduced loading of 1 gm/ft^2 which preliminary 2.5 ft^2 test data indicates will introduce little if any performance loss, and a low catalyst loading of 0.25 gms/ft^2. The latter, while having demonstrated baseline performance in laboratory-size cells, has to date introduced some performance loss in 2.5 ft^2 hardware. It is expected that this performance loss with low catalyst loading can be eliminated with continued development. A breakdown of the mature production costs of a 20 MW electrolyzer, assuming achievement of the low catalyst loading goals, is shown in Figure 64, compared against the cost goals established in 1975. Shown in Figure 65 is a chronological history of module cost reduction as the program has progressed since 1975. It can be seen that 87% of the cost reduction goal has been demonstrated in laboratory sized hardware.

As discussed previously, demonstrated technology is showing efficiency of approximately 87% at beginning of life. Experience has shown, however, that there will be some performance degradation with life. Based on analysis of the long life cell performance data accumulated to date, the estimated overall system efficiency characteristics with time, shown in Figure 66, has been generated for use in the techno-economic study. This performance results in an average module efficiency over the 5-year (40,000 hour) period of 80.1% at 100 psi, H$_2$ generation pressure. When coupled with a minimum power supply efficiency of 95% and 20 kW ancillary power loss, this gives a 75.5% average overall plant efficiency. At the 350 psi generation pressure desired for injection into high pressure gas lines the module efficiency would be 77.1% with a corresponding overall system efficiency of 72.7%.

As part of the techno-economic study, a methodology to calculate a cost of generated gas has been developed in conjunction with Arthur D. Little who is performing a comparative cost study of advanced electrolyzers under DOE sponsorship. This methodology leads to a cost of hydrogen expressed in 1981 dollars per million BTU and is based on the following assumptions:

123

Figure 63. SPE Water Electrolysis System Flow Schematic – 2 MW (HHV H₂) Plant

TABLE 10

MATURE PRODUCTION ELECTROLYZER COST ESTIMATE FOR COMMERCIAL SCALE HARDWARE

1981 Dollars
2 MW Plant Capacity
Cell Size and Catalyst Loading as Shown

	Catalyst Loading		
	Low ($.25$ gms/ft^2)	Reduced (1 gm/ft^2)	Standard (4 gms/ft^2)
10 Ft^2			
Single 10 ft^2 Module	88.5 $/kW	103.4 $/kW	163.0 $/kW
Supporting System	147.4 $/kW	147.4 $/kW	147.4 $/kW
Installed Plant (Battery Limits)	235.9 $/kW	250.8 $/kW	310.4 $/kW
2.5 Ft^2			
4-2.5 Ft^2 Modules	107.0 $/kW	121.9 $/kW	181.5 $/kW
Supporting System	171.6 $/kW	171.6 $/kW	171.6 $/kW
Installed Plant (Battery Limits)	278.6 $/kW	293.5 $/kW	353.1 $/kW

	GOAL (1975 Study) $/ft²	Present Technology $/ft²	Basis (Present Technology)
Cathode Catalyst	3.50	4.22	.25 gm/ft² Pt @ $16.86/gm
SPE	4.59	35.11	$33.44/ft²
Anode Catalyst	3.54	1.80	0.25 gm/ft² WE-3 @ $7.20/gm
Anode Support	11.63	21.04	Porous Ti Plate @ $15.00/ft² + Pt + Labor
Collector		16.06	Molded Carbon/Fluoropolymer Materials + Molding + Pt + Labor
Cathode Support		6.19	Carbon Fiber Paper + Nb Covers + Labor
Cell Labor	9.97	6.14	3.07 Man-hours/M&E
Compression Hardware		1.60	20 mW Module, Double-Sided, ASME Code, 300 psig
Module Labor		0.53	1350-Cell Module Assembly & Non-operating Test, 361 Man-hours Total
Total	33.23	92.69	1981 $
On 1975 Basis (For Reference)	18.00	50.21	1975 $

Figure 64. Projected Electrolyzer Production Costs
10 Ft² Cell, 20 MW Module, Mature Production, 1981 Dollars
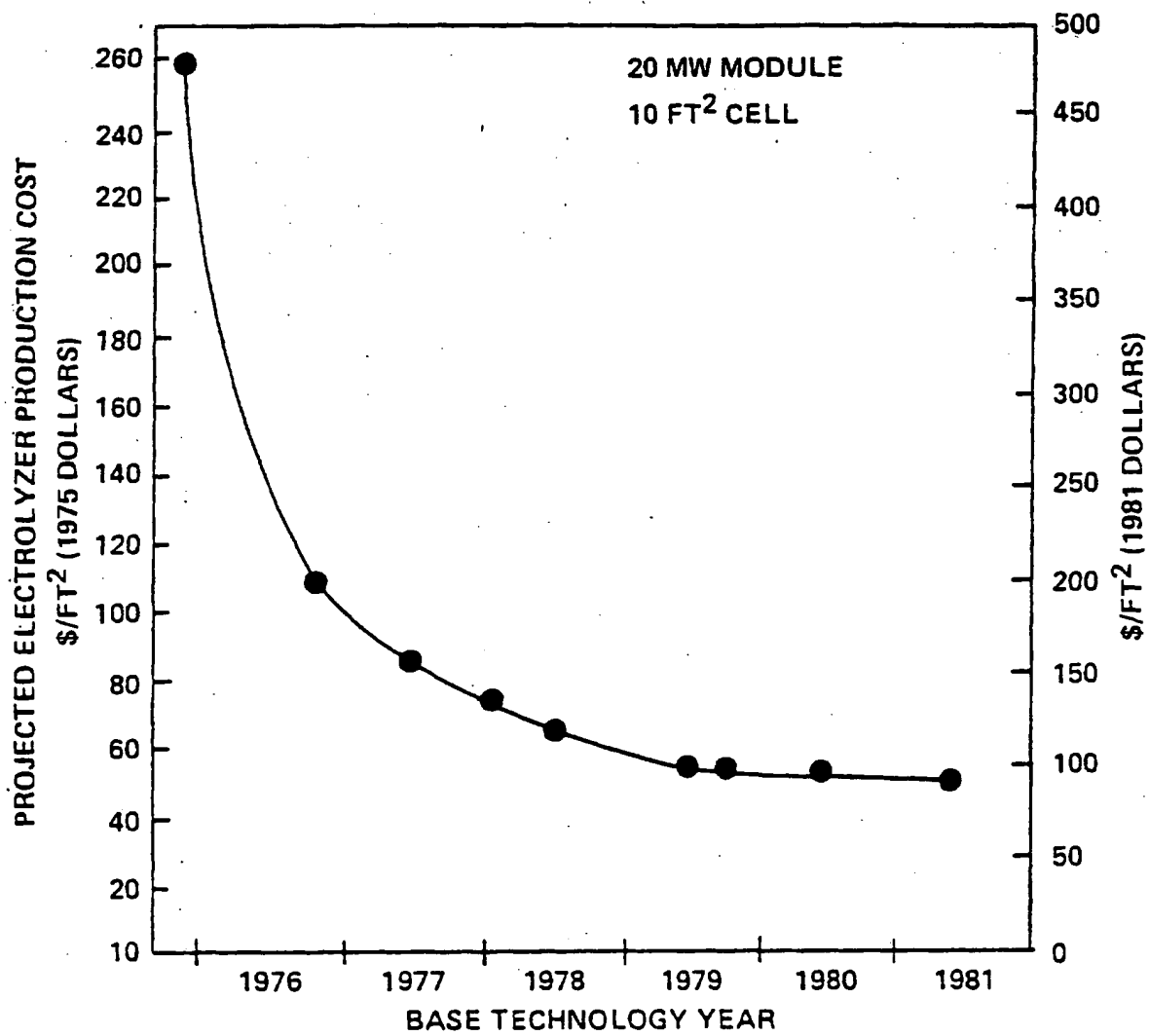
Figure 65. Chronological History of Module Cost Reduction

127
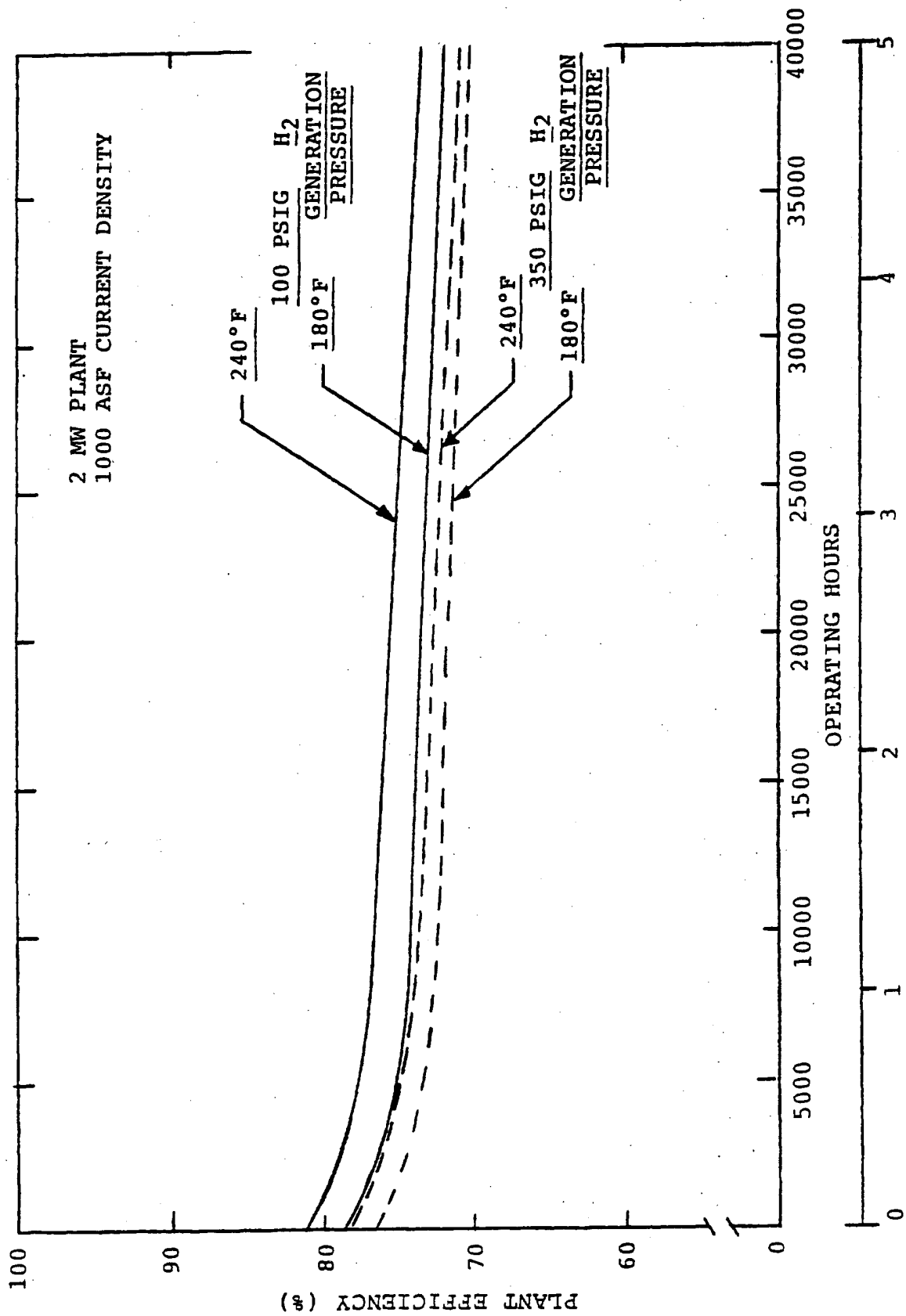
Figure 66. Overall Electrolyzer Plant Efficiency Versus Operating Time

- A 20 year plant life

- A 5 year (40,000 hr.) module life with precious metal credit on
  replacement modules

- A 16% fixed charge rate

- A 10% inflation rate

- A 12.14% discount rate

- A direct labor rate of $8/hour

- A labor overhead rate of 150%

- A General and Administration rate of 12% and 1% insurance and
  taxes

- A stream factor of 90% appropriate for generation of hydrogen as
  a fuel

A map of hydrogen cost vs. installed plant initial cost for elec-
tricity costs and plant efficiencies of interest is shown in Figure 67. A
similar map is shown in Figure 68 for a 40% stream factor appropriate for util-
ization of hydrogen for peak load shaving and cyclic energy storage. Shown
on these maps is the projected cost of gas associated with the capital cost
estimates and projected average performance over the plant life.

5.1 The Effect of Cell Size

For a 2 MW plant, the use of four 500 kW 2.5 ft^2 modules instead
of a single 2 MW 10 ft^2 module increases the electrolyzer cost by 21%. Since
a separate power supply would probably be used by each of the smaller modules,
the cost of the supporting system is also increased by approximately 16%.
The overall 2 MW plant cost thus would increase by approximately 18%.

However, at a 40 mil/kWH electricity cost and a 90% stream factor,
this only increases the cost of hydrogen by 18¢/MBTU - an increase of only 1
to 1.5%.

Thus, demonstration of a 1 to 2 MW plant using 500 kW 2.5 ft^2 mod-
ules would be representative of SPE capability while avoiding the high cost
of development of the larger 10 ft^2 module.

5.2 Effect of Temperature

A major goal of the bulk hydrogen program to date has been to oper-
ate at elevated temperature in order to improve efficiency and reduce cost of
gas. At high temperatures, however, both mechanical and chemical stresses
are more severe and reliability is generally reduced. For temperatures above
approximately 200°F, system complications are introduced to prevent drying of
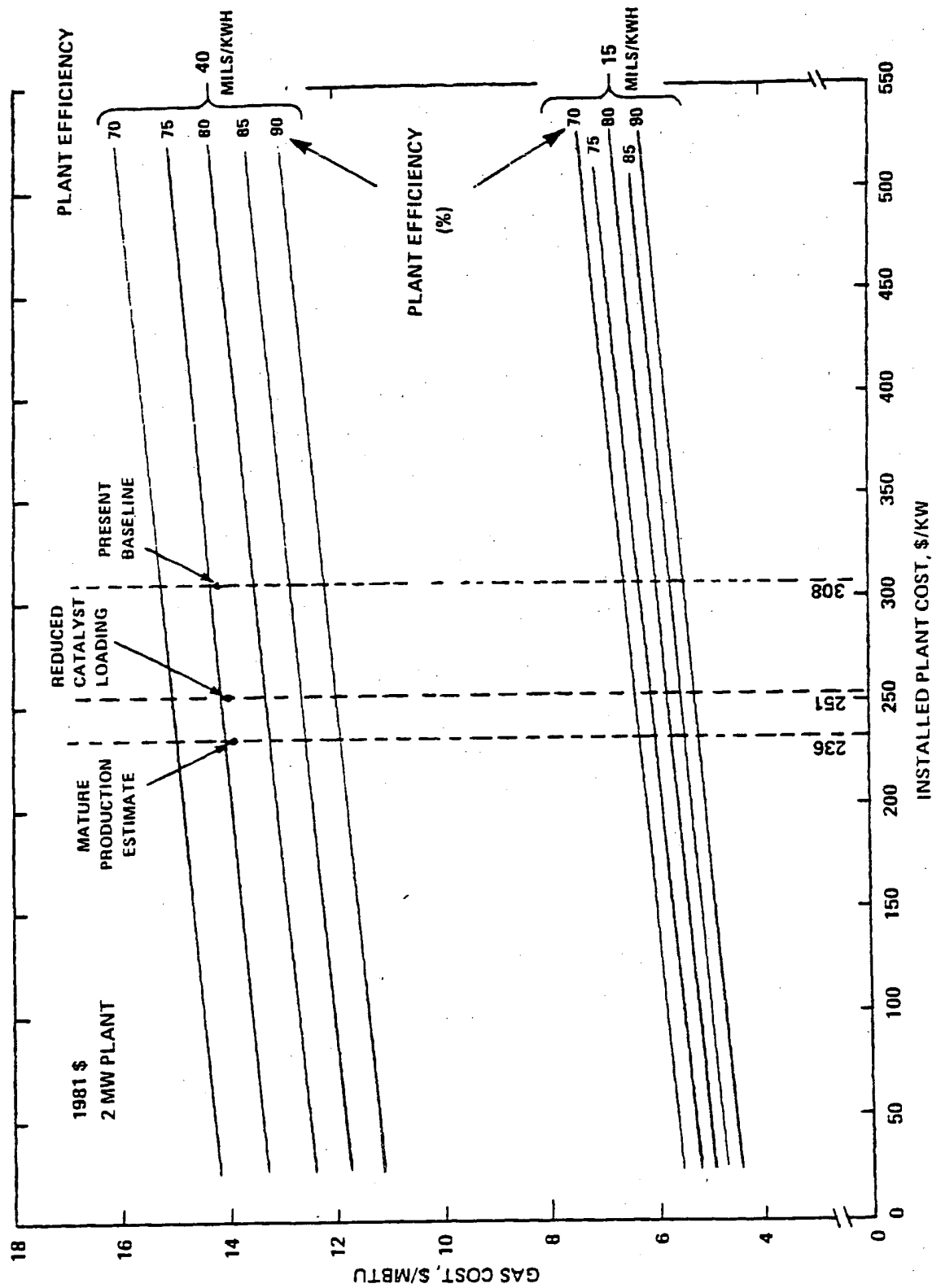the cell during a high temperature shutdown.

DIRECT ENERGY CONVERSION PROGRAMS

Figure 67. Gas Cost vs. Installed Plant Cost @ 90% Stream Factor
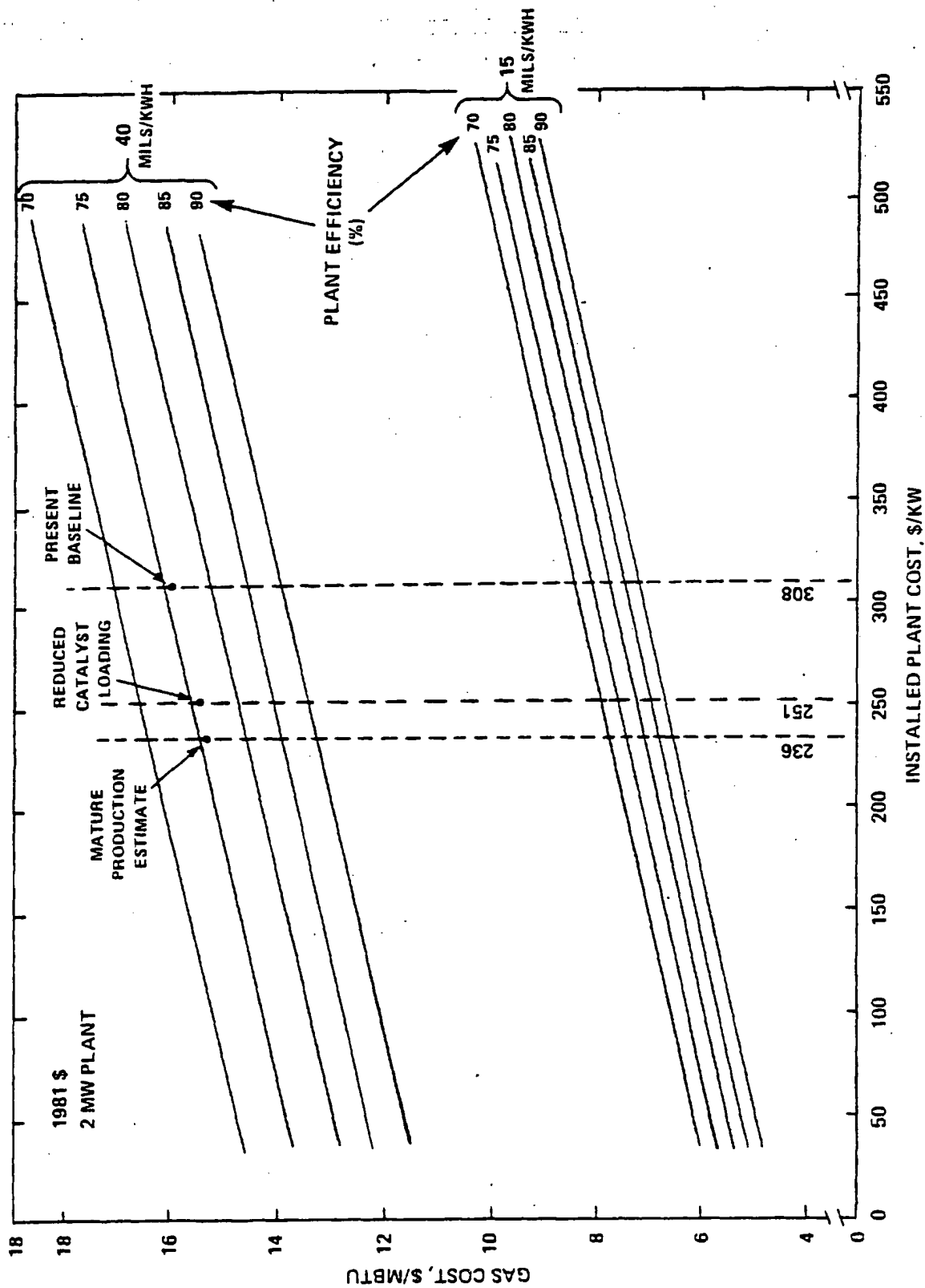
130

Figure 68. Gas Cost vs. Installed Plant Cost @ 40% Stream Factor

131

One aspect of the techno-economic study is, therefore, to quantify the impact of reducing the current 240°F goal to a lower temperature where increased reliability can be attained and system complication avoided.

To date, the reduction of temperature from 240°F to 180°F has been quantified. This reduction would have about a $0.22/MBTU increase in the cost of hydrogen and a 1.6% drop in efficiency at 350 psig. At 100 psig, the cost of gas increases by approximately $0.43/MBTU and the efficiency is reduced by about 3%.

5.3 The Effect of Current Density

Figures 69 and 70 show the variation in generated hydrogen cost, system efficiency and plant cost as current density is varied. It can be seen that reduction in current density below the "standard" 1000 ASF has very little effect on the cost of hydrogen since the increase in plant efficiency is largely offset by increase in plant cost. Thus, for general applications, where the cost of hydrogen is a prime long range criteria and the initial capital outlay a prime short range criteria, operation at 1000 ASF is preferable. In applications where system size is a consideration (such as OTEC), operation at as high a current density as possible is desirable.

For applications requiring high efficiency, operation at reduced current density (in the 500 ASF range) will result in plant efficiencies of ~85% at 100 psi or ~81% at 350 psi generation pressure.

5.4 Effect of Membrane Thickness

The techno-economic study was based on the use of 7 mil membrane. This results in a $0.50-0.60/MBTU reduction in the cost of hydrogen and a 3 to 3.5% increase in plant efficiency over the use of standard 10 mil thick membrane. Thus, continued evaluation of reduced thickness membrane is warranted and is planned.

5.5 Effect of Pressure

Increasing the hydrogen generation pressure from 100 psig to 350 psi (240°F) introduces a $0.50/MBTU increase in the cost of generated hydrogen and a 2.8% decrease in the overall plant efficiency. However, based on preliminary estimates, use of a separate compressor to achieve 350 psi would result in an increase of approximately a $1.17/MBTU increase in gas cost and a reduction in overall plant efficiency of about 2.7%.

Generation of hydrogen at the higher pressure is advantageous from a cost of gas (with comparable efficiency impact), assuming no adverse effect on reliability. It is thus desirable to develop and prove sealing capability in the 350-400 psi pressure range.

5.6 Summary of Conclusions to Date from the Techno-Economic Study

A summary of the results to date from the techno-economic study is shown in Table 11. Explanatory comments and planned actions relative to each of the parameters are shown.
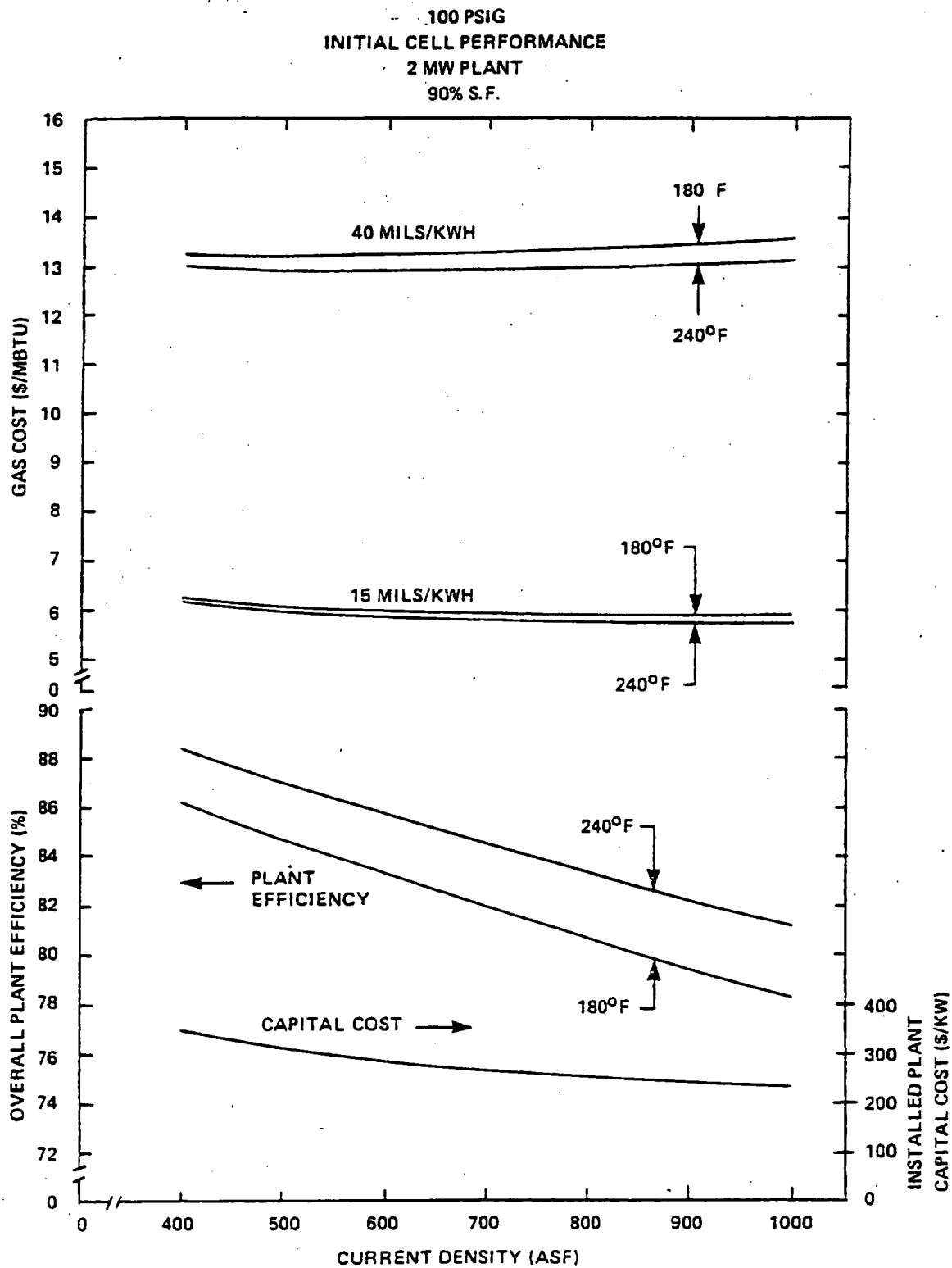
132

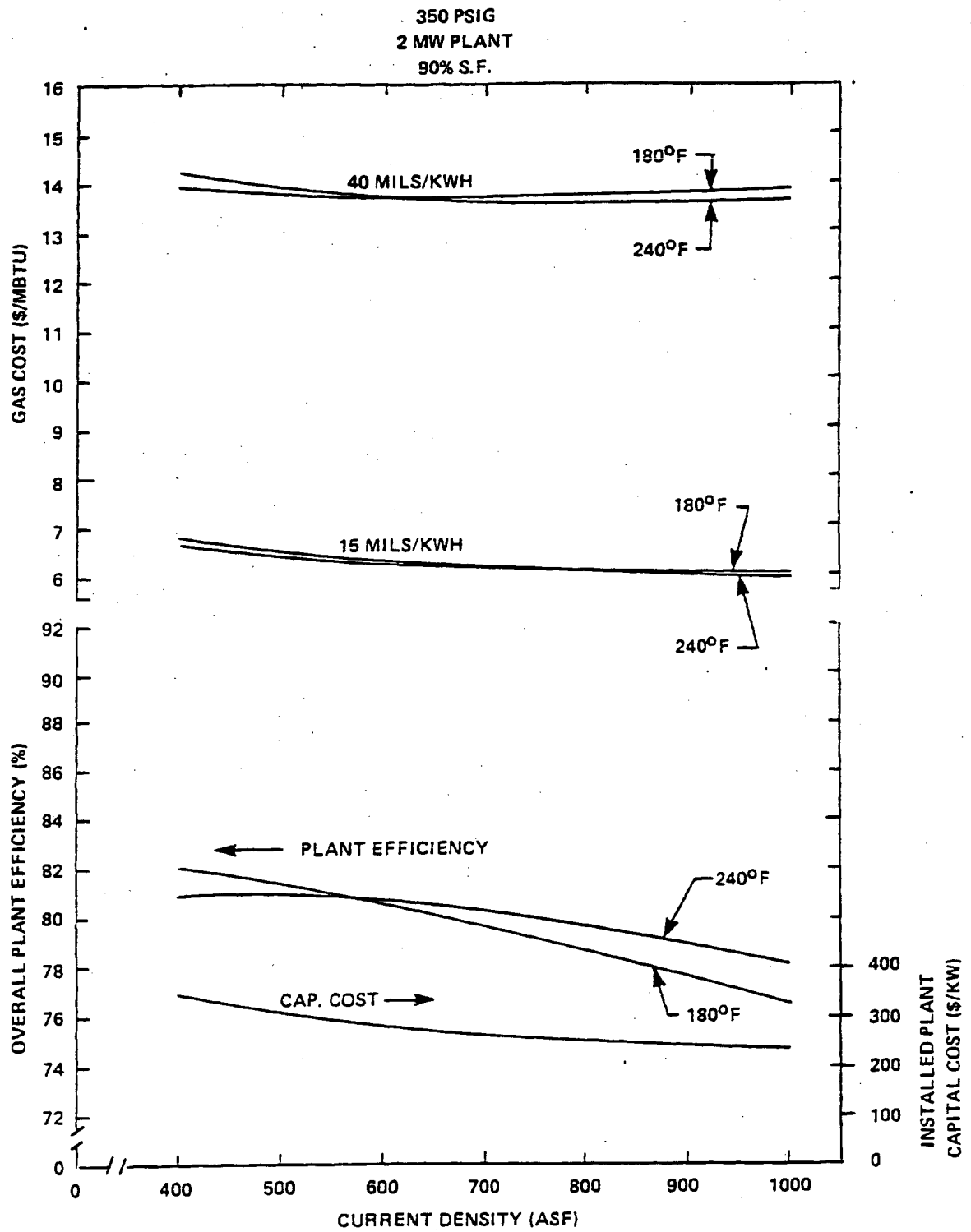Figure 69.   Effect of Reducing Current Density – 100 psig

DIRECT ENERGY CONVERSION PROGRAMS

Figure 70.   Effect of Reducing Current Density - 350 psig

134

TABLE 11

SUMMARY OF RESULTS TO DATE FROM TECHNO-ECONOMIC STUDY

	Cost of Hydrogen $/MBTU	Overall Plant Efficiency	Comments	Action
Base Line:	14.30	75.5%		
100 psi. 240°F 7 mil membrane 1000 ASF 40 mils/KWH Electricity 308 $/KW System Cost (2 MW, Std Catalyst Loading)				
Change of Baseline	Δ$/MBTU	Δ% Efficiency		
1. Reduction to 180°F	+ .43	-2.9%	Limited development funding precludes achievement of high reliability at 240°F.	Limit to 180°F operation near term. Keep 240°F as long range goal.
2. Reduced Current Density (500 ASF)	- .20	+5.8	Good for applications where efficiency is paramount.	Keep 1000 ASF as standard.
3. Use of 10 mil membrane	+ .47	-3.0	Use of thinner membrane is technically achievable within scope of proposed program.	Continue to pursue reduced thickness membrane.
4. 350 psi Hydrogen Delivery				
By Electrolyzer	+ .50	-2.8	350 psi electrolytic generation shows significant cost of gas advantage over use of separate compressor.	Develop and prove 350 psi capability.
By Compressor	+1.17	-2.7		
5. Reduced Catalyst loading				
• Present Experience (.25 gm/ft²)	+ .80	-5%	Performance loss of present experience over-shadows advantage of hardware cost reduction.	Evaluate intermediate loadings (1-2 gm/ft²)
• Intermediate Catalyst Loading (1 gm/ft²)	- .22	0	Can be achieved with reasonable development cost.	Pursue as funding permits.
• Goal: Base Line Performance Achieved with .25 gm/ft² catalyst loading	- .2	0	Small cost of gas impact but significant capital cost reduction.	Keep as long term goal.

135

Each of the parameters studied (temperature, current density, membrane thickness, pressure and catalyst loadings) had a relatively small impact on the cost of hydrogen.

In view of this limited impact on hydrogen cost and the severe limitation on developmental funding, near term funding should be focused on demonstrating the basic stability, longevity and reliability of the scaled up hardware. Only those technology advances which are readily achievable within the program resources should be pursued.

In summary it is planned to:

● Limit operation temperature to 180°F since the resources required to achieve high reliability at 240°F are not available in the near term.

● Maintain 1000 ASF as the design standard recognizing that operation at lower current densities can always be utilized for application which are sensitive to efficiency rather than capital cost or cost of hydrogen.

● Continue to pursue reduced thickness membrane since it is technically achievable with minimal development.

● Develop and prove 350 psi gas generation capability. High pressure generation shows significant cost of gas advantage over the use of a separate compressor in the 350 psig delivery pressure range.

● Pursue reduced catalyst loading as funding permits. Intermediate loadings in the range of 1 gm/ft^2 could be achieved with reasonable development costs.

● Keep 240°F operation and low (.25 gm/ft^2) catalyst loading as long term goals. The development cost for each of these parameters is relatively high compared to the cost of gas advantage they offer. These will be pursued only if the specific advantages they offer warrant the development investment.

136

6.0   CONCLUSIONS AND RECOMMENDATIONS

6.1   Conclusions

As a result of the effort reported on herein, it is concluded that:

• The large scale generation of hydrogen by solid polymer electro-
  lyte water electrolysis utilizing cells of 2.5 ft^2 active area is
  feasible.

• Further development in the 2.5 ft^2 cell size is warranted, par-
  ticularly in the area of reduction of collector resistance and
  the use of thinner SPE, to achieve performance at 1000 ASF in the
  range of 1.7V (87% voltage efficiency) at 240°F average operat-
  ing temperature.

• Based on the 2.5 ft^2 experience to date, further scale-up to 10
  ft^2 cell area (or larger) is also feasible.

6.2   Recommendations

• It is recommended that government support for solid polymer
  electrolyte water electrolysis development program continue; at
  least through the rent-free use of existing system hardware and
  tooling in the on-going utility/company-sponsored program.
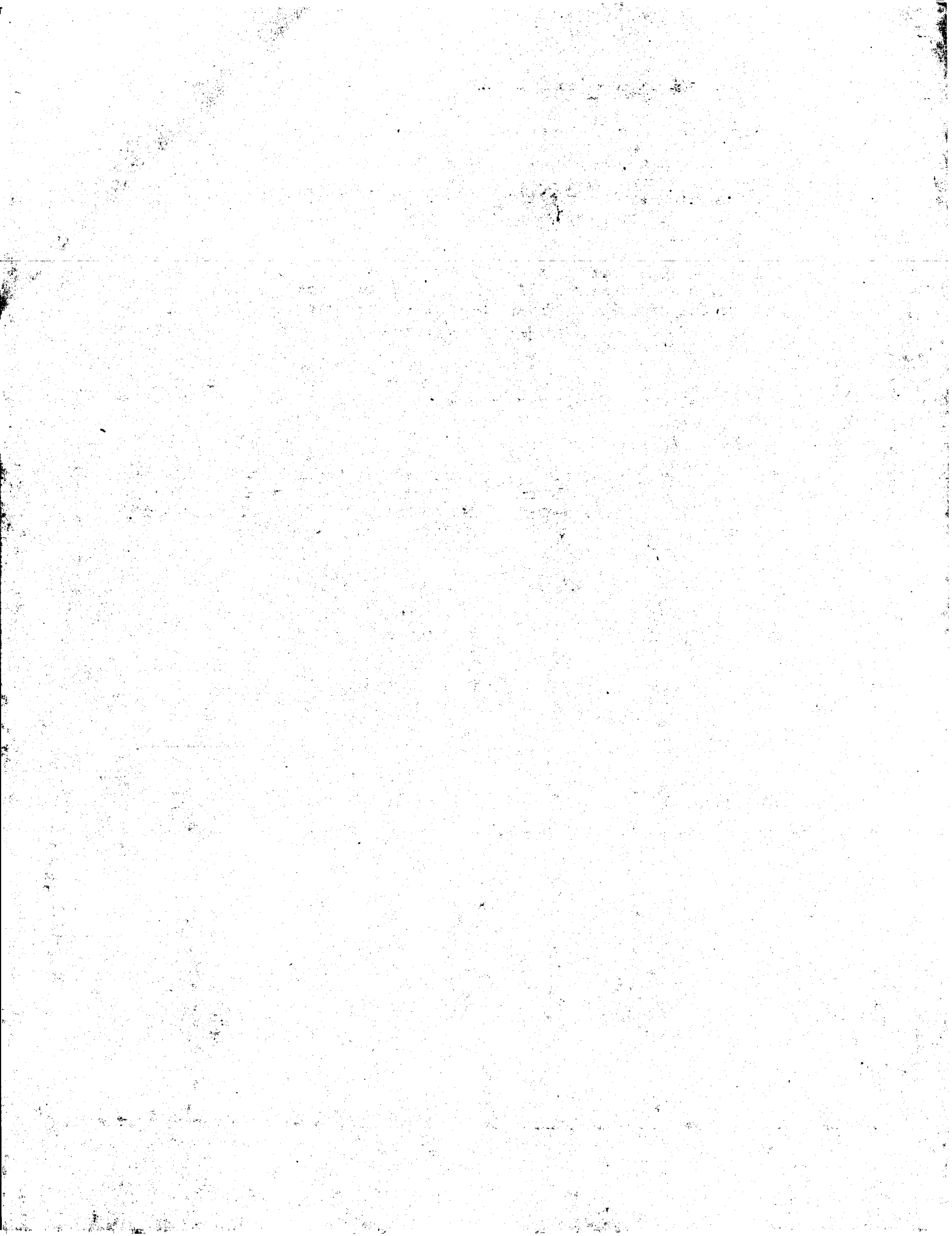
U.S. DEPARTMENT OF COMMERCE
Technology Administration
National Technical Information Service
Springfield, VA 22161   (703) 605-6000